(12)

VSC-TR-81-10

IMPROVED LOCATION WITH REGIONAL EVENTS

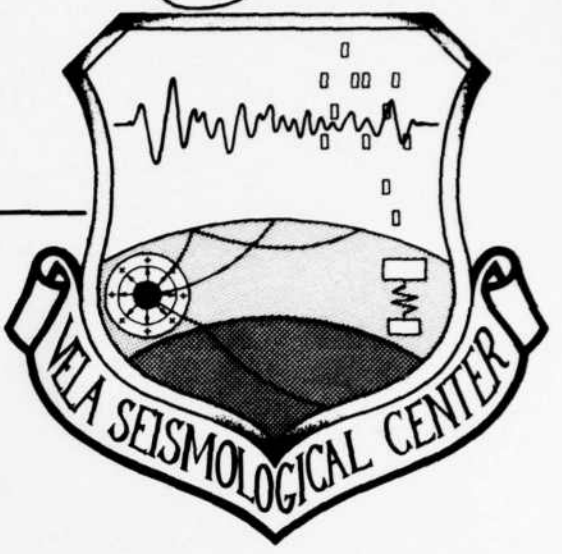

A.C. Chang, D.W. Rivers, J.A. Burnetti

Seismic Data Analysis Center
Teledyne Geotech
314 Montgomery Street
Alexandria Virginia 22314

15 JUL 1981

APPROVED FOR PUBLIC RELEASE; DISTRIBUTION UNLIMITED.

Monitored By:
VELA Seismological Center
312 Montgomery Street
Alexandria, VA 22314

Sponsored by

The Defense Advanced Research Projects Agency (DARPA)

DARPA Order No. 2551

Unclassifed

SECURITY CLASSIFICATION OF THIS PAGE (When Date Entered)

(19) REPORT DOCUMENTATION PAGE		READ INSTRUCTIONS BEFORE COMPLETING FORM
(18) 1. REPORT NUMBER VSC-TR-81-10	2. GOVT ACCESSION NO. AD-A105	3. RECIPIENT'S CATALOG NUMBER 486
(6) 4. TITLE (and Subtitle) IMPROVED LOCATION WITH REGIONAL EVENTS,		(9) 5. TYPE OF REPORT & PERIOD COVERED Technical Rept.
		(14) 6. PERFORMING ORG. REPORT NUMBER SDAC-TR-81-2
(10) 7. AUTHOR(s) A. C. Chang, D. W. Rivers, J. A. Burnetti		(15) 8. CONTRACT OR GRANT NUMBER(s) F08606-79-C-0007 DARPA Order-2551
9. PERFORMING ORGANIZATION NAME AND ADDRESS Teledyne Geotech, 314 Montgomery Street, Alexandria, Virginia 22314		10. PROGRAM ELEMENT, PROJECT, TASK AREA & WORK UNIT NUMBERS VT/0709/B/PMP
11. CONTROLLING OFFICE NAME AND ADDRESS Defense Advanced Research Projects Agency, 1400 Wilson Boulevard, Arlington, Virginia 22209		(11) 12. REPORT DATE December 1980
		13. NUMBER OF PAGES 92
14. MONITORING AGENCY NAME & ADDRESS (if different from Controlling Office) VELA Seismological Center, 312 Montgomery Street, Alexandria, Virginia 22314		(12) 94 15. SECURITY CLASS. (of this report) Unclassified
		15a. DECLASSIFICATION/DOWNGRADING SCHEDULE

16. DISTRIBUTION STATEMENT (of this Report)

APPROVED FOR PUBLIC RELEASE; DISTRIBUTION UNLIMITED.

17. DISTRIBUTION STATEMENT (of the abstract entered in Block 20, if different from Report)

18. SUPPLEMENTARY NOTES

19. KEY WORDS (Continue on reverse side if necessary and identify by block number)

Seismic locations with P_n, P_g

Successive determination of event locations
Simultaneous inversion method

20. ABSTRACT (Continue on reverse side if necessary and identify by block number)

Three methods of locating events with regional phases were tested and compared for accuracy of hypocenter determination. A modified HYLO method was found to be slightly less accurate than a standard location algorithm using a Herrin 68 earth model. In addition, we found that the modified HYLO method requires a much more detailed knowledge of the earth's crust and upper mantle than is generally available. Two methods which do not require any previous knowledge of the crust in the area of interest, the methods of successive determinations and simultaneous inversions, were found to reduce location errors

DD FORM 1 JAN 73 1473 EDITION OF 1 NOV 65 IS OBSOLETE

Unclassified

SECURITY CLASSIFICATION OF THIS PAGE (When Date Entered)

408 258

about 50%, as compared to the standard location algorithm with a Herrin 68 earth model.

IMPROVED LOCATION WITH REGIONAL EVENTS

SEISMIC DATA ANALYSIS CENTER REPORT NO.: SDAC-TR-81-2

AFTAC Project Authorization No.:	VELA /0709/B/PMP
Project Title:	Seismic Data Analysis Center
ARPA Order No.:	2551
Name of Contractor:	TELEDYNE GEOTECH
Contract No.:	F08606-79-C-0007
Date of Contract:	1 October 1980
Amount of Contract:	$1,493,393
Contract Expiration Date:	30 September 1981
Project Manager:	Robert R. Blandford (703) 836-3882

P. O. Box 334, Alexandria, Virginia 22313

APPROVED FOR PUBLIC RELEASE; DISTRIBUTION UNLIMITED.

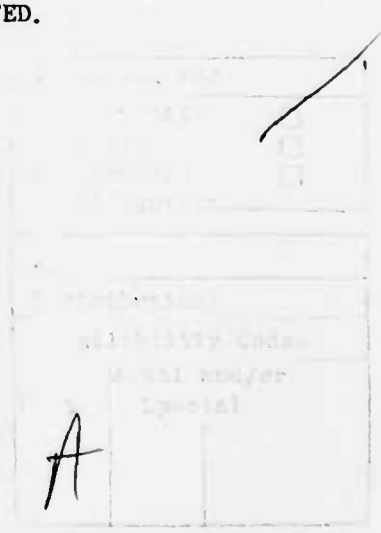

ABSTRACT

Three methods of locating events with regional phases were tested and compared for accuracy of hypocenter determination. A modified HYLO method was found to be slightly less accurate than a standard location algorithm using a Herrin 68 earth model. In addition, we found that the modified HYLO method requires a much more detailed knowledge of the earth's crust and upper mantle than is generally available. Two methods which do not require any previous knowledge of the crust in the area of interest, the methods of successive determinations and simultaneous inversions, were found to reduce location errors about 50%, as compared to the standard location algorithm with a Herrin 68 earth model.

TABLE OF CONTENTS

LIST OF FIGURES

LIST OF TABLES

1. INTRODUCTION

The accuracy of location of events located with regional phases (P_n, P*, P_g, S_n, S*, S_g) is affected strongly by lateral variations in crustal and upper mantle structures.

Herrin and Taggart (1962) demonstrated that the velocity of the regional phase P_n varies significantly across the United States. Figure 1 shows their revised map of apparent P_n velocities across the United States. Herrin and Taggart (1962) introduced a method known as HYLO, which applies corrections to the travel time tables of phase P_n, based on the velocity model shown in Figure 1. They were able to improve significantly hypocenter and origin time estimates for the nuclear explosion GNOME and the Hebgen Lake earthquake of 18 August 1959. In addition, they were able to eliminate the bias in travel time residuals resulting from the general pattern of faster P_n velocities in the Eastern United States (EUS), as opposed to the Western United States (WUS). Subsequently, Herrin and Taggart (1966) reported similar success in locating the nuclear explosion SALMON. The method, however, has several drawbacks. Only the phase P_n, which, in many regions of the world, is the lowest amplitude phase on the record, may be used. In addition, HYLO makes no correction for variation in crustal thickness between source and receiver, which as Chang and Racine (1979) have shown, may contribute more to travel time residuals than does lateral variation in the phase velocity.

Chang and Racine (1979) relocated twelve nuclear explosions, utilizing data for the phases P_n and P_g. They used Julian's (1974) location program as modified by McCowan (1978) to accept crustal phases P_n, P*, P_g, S_n, S* and S_g. They further modified the program to allow an option for selecting up to fifty local crustal models, such that the analyst may utilize an independent model for each epicenter to station path. Figure 2 shows the boundaries of the regional crustal models they used, first published by Pakiser and Robinson (1966). Figure 3 shows the boundaries and codes for fifteen more localized models developed by Racine (1979). In addition, two generalized models, Herrin 68 (1968) and Jeffreys-Bullen (1958) were also used.

Table I is a comparative listing of the general, regional, and localized models. Chang and Racine (1979) were marginally successful in improving the location estimates of the twelve explosions, as compared to a standard location algorithm with a Herrin 68 model.

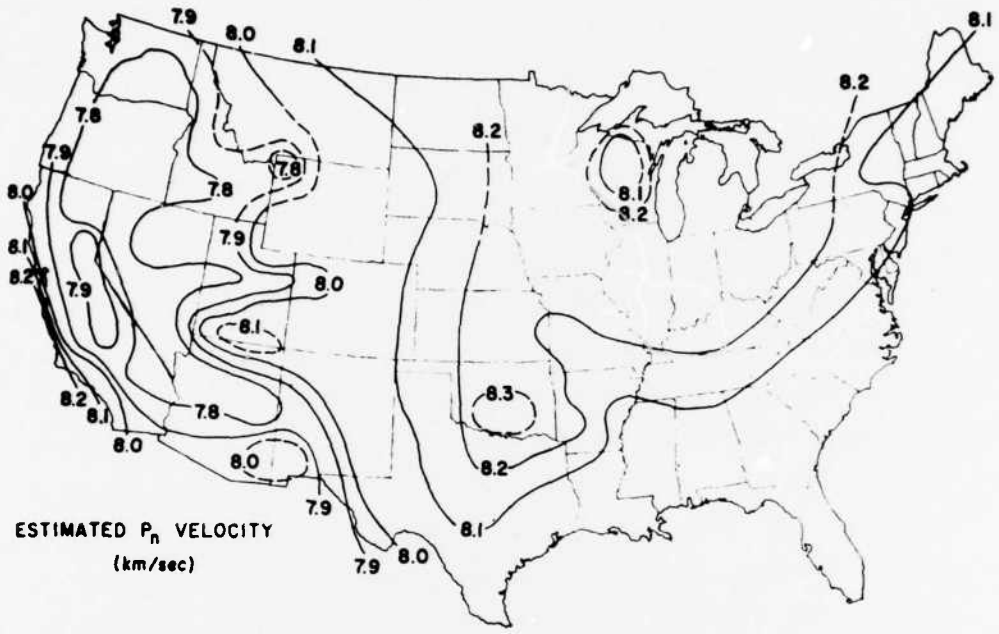

Figure 1 Map of P_n velocities, after Herrin and Taggart (1966).

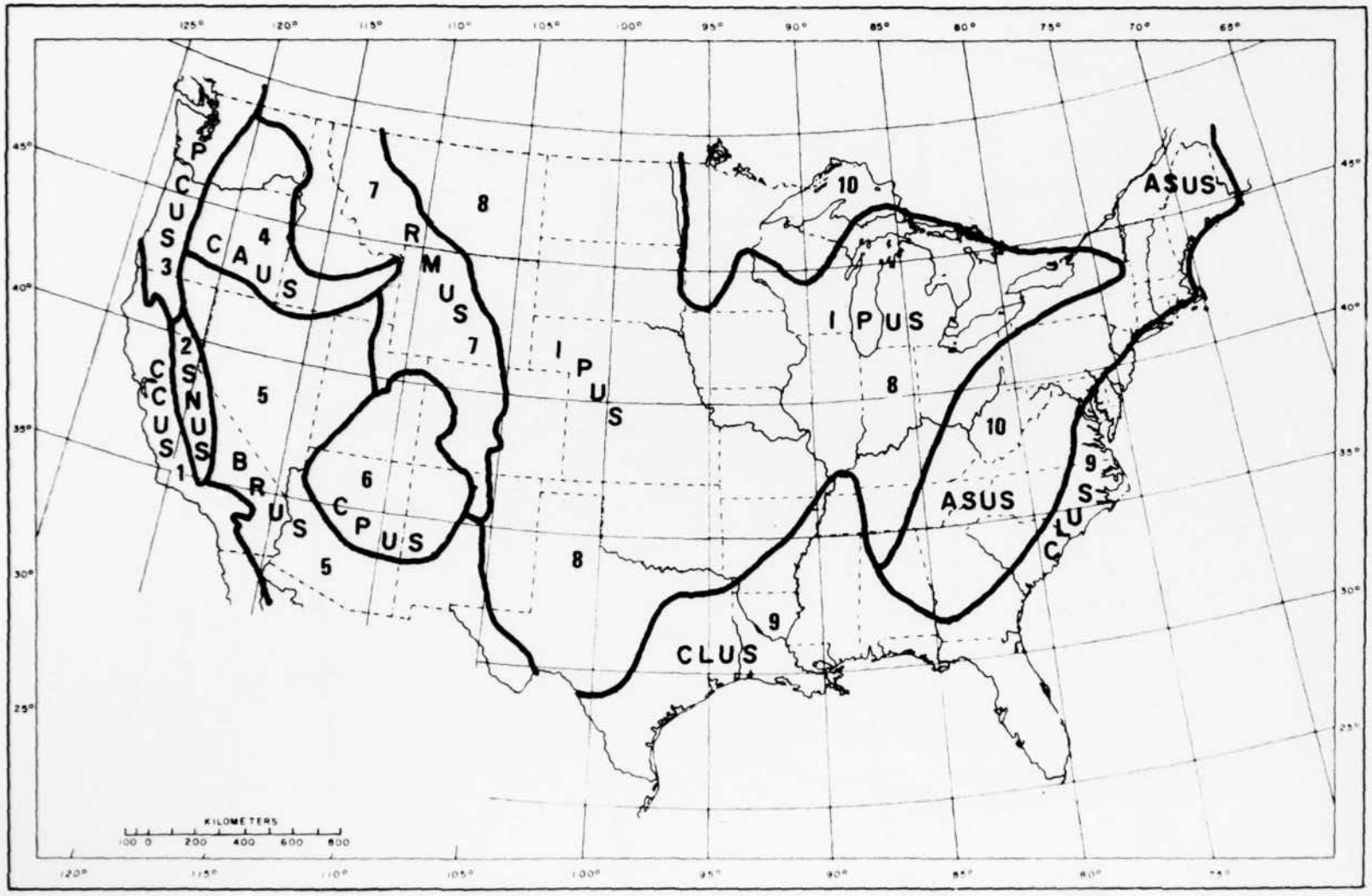

Figure 2 Boundaries of regional crustal models of Pakiser and Robinsion (1966).

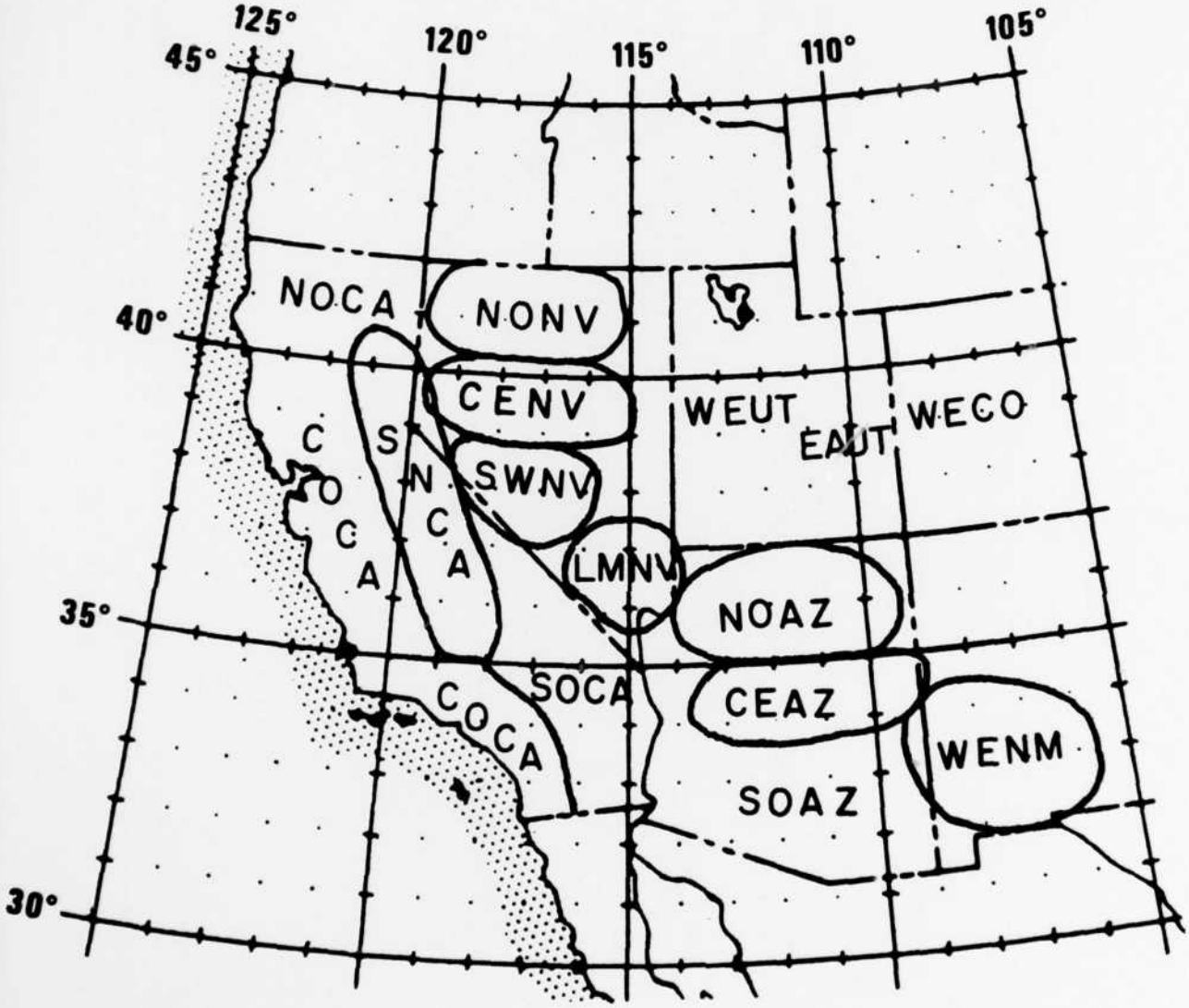

Figure 3 Boundaries of local crustal models of Racine (1979).

TABLE I

General, regional and local crustal models.

Model		1st Layer		2nd Layer		Mantle
Area	Designator	Thickness	Velocity	Thickness	Velocity	Velocity
General:						
Jeffrey-Bullen	J-B	15.00	5.57	18.00	6.50	7.80
Herrin 68	HE	15.00	6.00	25.00	6.75	8.05
Regional:						
Calif. Coast	CCUS	15.00	6.20	5.00	7.00	8.10
Sierra Nevada	SNUS	25.00	6.20	25.00	7.00	7.90
Pac. NW Coast	PCUS	10.00	6.20	25.00	7.00	7.70
Columbia Plat.	CAUS	10.00	6.20	35.00	7.00	7.90
Basin & Range	BRUS	20.00	6.20	10.00	7.00	7.90
Colorado Plat.	CPUS	25.00	6.20	15.00	7.00	7.80
Rocky Mtns.	RMUS	25.00	6.20	15.00	7.00	8.00
Int. Plains	IPUS	20.00	6.20	30.00	7.00	8.20
Coastal Plain	CLUS	20.00	6.20	15.00	7.00	8.10
App. Highland & Sup. Upland	ASUS	15.00	6.20	25.00	7.00	8.10
Local:						
N. Calif.	NOCA	12.00	5.60	18.00	6.70	8.00
Coast Calif.	COCA	10.00	5.60	10.00	6.70	8.00
Sierra Nevada	SNCA	15.00	6.00	20.00	6.50	7.60
S. Calif.	SOCA	20.00	6.20	10.00	6.90	7.80
N. Nevada	NONV	20.00	6.00	10.00	6.70	7.90
Cent. Nevada	CENV	20.00	6.00	10.00	6.60	7.80
SW Nevdad	SWNV	27.00	6.20	9.00	7.10	7.80
Lake Mead Nev.	LMNV	15.00	6.00	15.00	6.50	7.90
W. Utah	WEUT	15.00	5.90	10.00	6.40	7.40
E. Utah	EAUT	27.00	6.20	13.00	6.80	7.80
N. Arizona	NOAZ	26.00	6.00	12.00	6.80	7.80
Cent. Arizona	SOAZ	15.00	6.00	7.00	7.00	7.80
W. Colorado	WECO	9.00	6.10	31.00	6.60	7.80
W. New Mexico	WENM	19.00	6.20	21.00	6.50	7.90

Their results indicated that several models were needed for each event-station path: a source model for the downgoing ray, a path model to give the average propagation velocity, and a receiver model for the upcoming ray. The original experiment allowed only one model per path. Their results also indicated that the addition of P_g travel times did not significantly improve location accuracy.

This year, we have experimented with three additional methods of locating events with regional phases. The first, a modified HYLO method, incorporates an option for selecting crustal models at the source and receiver, and assumes a constantly dipping Moho between the two. Two other methods were tested, which require no previous knowledge of crustal structures, and which may incorporate phases other than P_n into the location process. The method of successive determinations involves alternately calculating a least squares fit to the travel times of the arrivals for a given event, and then relocating the event. Thus, this method determines an independent travel time table for each phase of each individual event. The method of simultaneous inversions does much the same, except that the new travel time relationships and locations are determined simultaneously, through matrix inversion, as opposed to alternately, as in successive determinations.

2. THE MODIFIED HYLO METHOD

2.1 Theory and Method of Investigation

The original HYLO method, of Herrin and Taggart (1962), replaced the travel time relationships for the phase P_n from the standard tables with travel times calculated by determining an average velocity for each travel path, using a P_n velocity which varies laterally as shown in Figure 1.

Our modified HYLO method allowed us to select a local or regional crustal model for the source and receiver crust from among those shown in Figures 2 and 3 and Table I. A constantly dipping Moho was assumed between source and receiver. Figure 1 was divided into a grid of one degree squares, defined by parallels of latitude and meridians of longitude. Each block of the grid has an associated P_n velocity. A computer program was developed to determine a theoretical travel time for a ray passing down the source model, across the grid of P_n velocities along the constantly dipping Moho, and up the receiver model. This theoretical time was subtracted from the expected travel time taken from the Herrin 68 table for the same distance, giving us a station correction factor to the Herrin table, which is valid for the given path and crustal models. Since we were using data from nuclear explosions, the true latitude and longitude were known to within one hundredth of a degree, and the true origin times were known to within one hundredth of a second. Therefore, the station correction factors were simply added to the observed P_n travel times, a standard location program was run on the corrected data, utilizing the Herrin 68 travel times, and absolute errors were obtained by comparing the computed locations with the true values. The results were compared to those obtained by running the same program on uncorrected data, as reported by Chang and Racine (1979).

2.2 Modified HYLO Method - Results and Discussion

Table II presents the results of our modified HYLO method. The average errors in location and origin time are slightly greater than those obtained by Chang and Racine (1979) for the same events, using uncorrected arrival times for P_n only and both P_n and P_g, and a Herrin 68 earth model.

The poor results of this experiment may be due to a number of reasons. The lateral variation in P_n velocity may be more complicated than is shown in Figure 1. Our assumption of a constantly dipping Moho may have been grossly

TABLE II

Comparison of Location Errors: Herrin 68 Versus Modified HYLO

	HERRIN P_n only		HERRIN (P_n + P_g)				HYLO			
	DEPTH REST		DEPTH REST		DEPTH FREE		DEPTH REST		DEPTH FREE	
	LOC E *	OT E #	LOC E	OT E	LOC E	OT E	LOC E	OT E	LOC E	OT E
FAULTLESS	18.3	1.5	15.04	1.3	15.04	1.4	12.32	0.2	12.32	-1.8
RULISON	7.3	0.5	1.58	0.3	1.58	-0.1	3.63	1.3	3.7]	1.0
PASSAIC	N/A	N/A	4.08	-0.4	4.08	-0.4	11.17	0.8	11.17	0.8
ROCKVILLE DAM	5.1	1.5	5.18	1.3	5.18	1.3	5.59	0.6	5.59	-0.4
DORMOUSE'	N/A	N/A	9.09	-0.2	9.09	0.2	10.47	-0.8	10.47	-1.4
KLICKITAT	7.0	0.4	6.53	0.0	6.53	0.0	9.56	-0.5	9.64	0.6
BANDICOOT	12.9	0.7	1.01	0.8	1.34	0.6	7.09	-0.6	7.09	-1.8
SHOAL	5.9	0	5.18	0.1	5.18	4.1*	11.26	-0.7	11.26	0
MERRIMAC	10.3	0.3	9.58	0.2	9.58	1.0	10.99	-0.2	10.89	4.7
GASBUGGY	5.2	0.6	11.43	0.4	11.43	0.4	5.60	1.1	5.81	0.4
PILEDRIVER	4.0	0.3	12.98	-0.4	12.98	1.2	24.54	-0.4	24.54	0.9
ROANOKE	8.3	0.4	8.15	0.4	8.24	1.5	2.68	-0.6	3.68	0.4
Average	8.4		7.49		7.52		9.68		9.68	

* LOC E: Error of location vector, in km
\# OT E: Error of origin time estimates $T_{est} - T_{true}$, in sec.

inaccurate, especially, for example, when a phase crosses two or more distinct geological provinces, as in a path from the Basin and Range to the Rocky Mountains. There is a possibility that our derived local models are not adequate. We find a great deal of variation among authors regarding local crustal models, and our limiting condition that the crust be two layers may have been an important factor. All the above are supported by Schilt et al. (1979) who in a review of the heterogeneity of the crust, with data from vibroseis surveys, carried out by the Consortium for Continental Reflection Profiling, conclude the following:

1. That the continental crust demonstrates heterogeneities on a scale of a few kilometers or less, as well as patterns on a continental scale.

2. That the Mohorovicic discontinuity has the characteristics of a complexly layered transition zone, as opposed to a continuous interface separating the crust and mantle.

Despite all those possible causes of error, we feel that our revised HYLO method is a better method than the original HYLO, which attempted to compensate only for the portion of the crust above sea level. We find that the HYLO method, as tested in the previous paper, and in this improved version, does not improve location accuracy if only a few stations are available for analysis; in Herrin's publications the number of stations was on the order of 100 and perhaps local fluctuations averaged out so that the removal of overall East-West bias resulted in a more accurate location.

3. METHOD OF SUCCESSIVE DETERMINATIONS

3.1 Review of the P_n and P_g Observations

Thus far, we have shown that the modified HYLO method was not effective in eliminating errors in location due to the earth's heterogeneity. We have discussed several possible explanations of why it did not work. We also discussed the fact that HYLO is difficult to use, especially for smaller regional events, because it utilizes only the phase P_n.

The reason P_g has not been used in the HYLO method is that it has been commonly understood that P_g is not a head wave and that P_g is not linear on the T-delta curve. Thus, it was not considered adequate for use in locating events. If this is so, it may also be possible that the earth is so heterogeneous that P_n travel times fluctuate widely from a linear relationship so that P_n may not be suitable for locating events. We have investigated this point.

Figure 4, a composite travel time curve for eight explosions at NTS, shows that the travel times for both P_n and P_g are linear. Thus, we conclude that both P_n and P_g may be useful for location purposes. Figure 4 also demonstrates that it is possible to get a reasonably good average velocity for phases P_n and P_g, thus explaining Chang and Racine's (1979) reasonably good results in locating the events with the Herrin 68 earth model. Close inspection of Figures 4a through 4n and Appendix I, however, shows that while the travel times for each individual event are linear, the slopes of the linear fits differ for sources distant from each other, and in no case are the velocities exactly equal to the Herrin 68 model. Thus we conclude that we may improve our location estimates, by evaluating P_n and P_g travel time relationships for each event and its unique station distribution. This is a paradox, of course; perhaps the P_n and P_g velocities are characteristic of the detailed source location and depth and not of the "broad-brush" path because a different set of rays (modes) escape the source for different near-source geologies.

This is the basis for our methods of successive determinations and simultaneous inversions. We are not trying to obtain or utilize crustal structures, which we have demonstrated may vary significantly across a small area. We are trying to determine the constant P_n and P_g velocities that best fit each particular event.

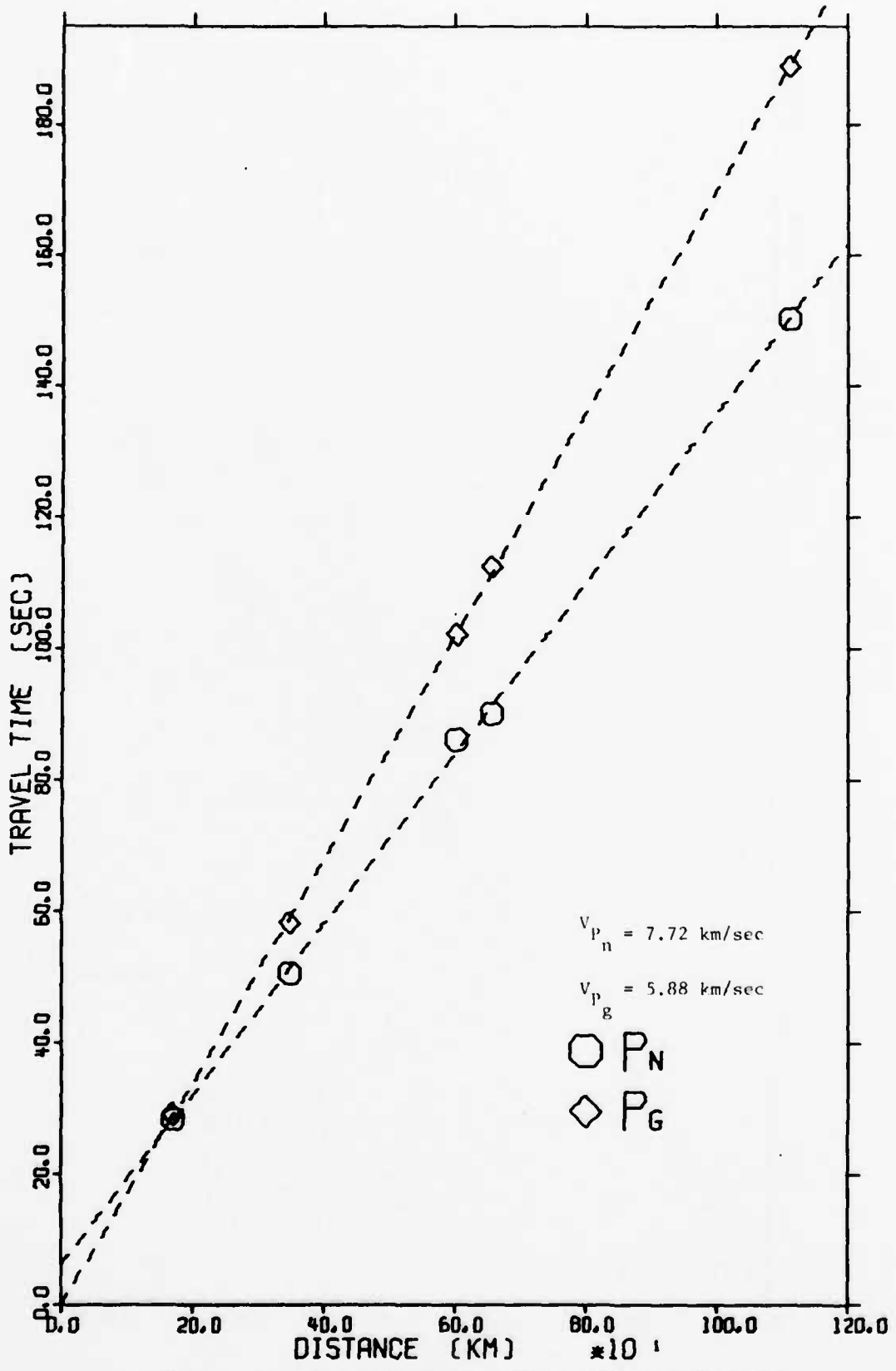

Figure 4a Observed P_n and P_g Travel Times for FAULTLESS

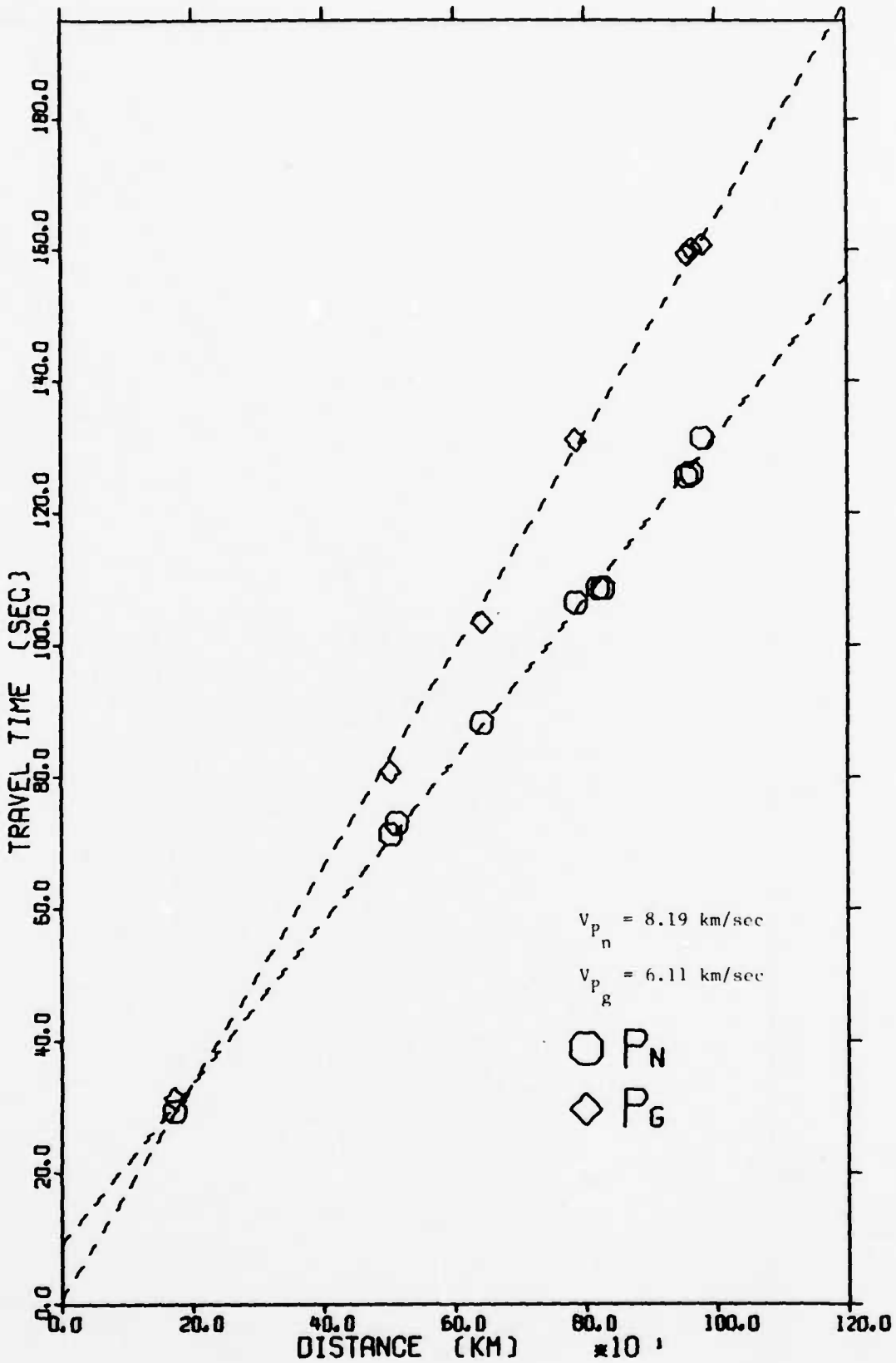

Figure 4b Observed P_n and P_g Travel Times for RULISON

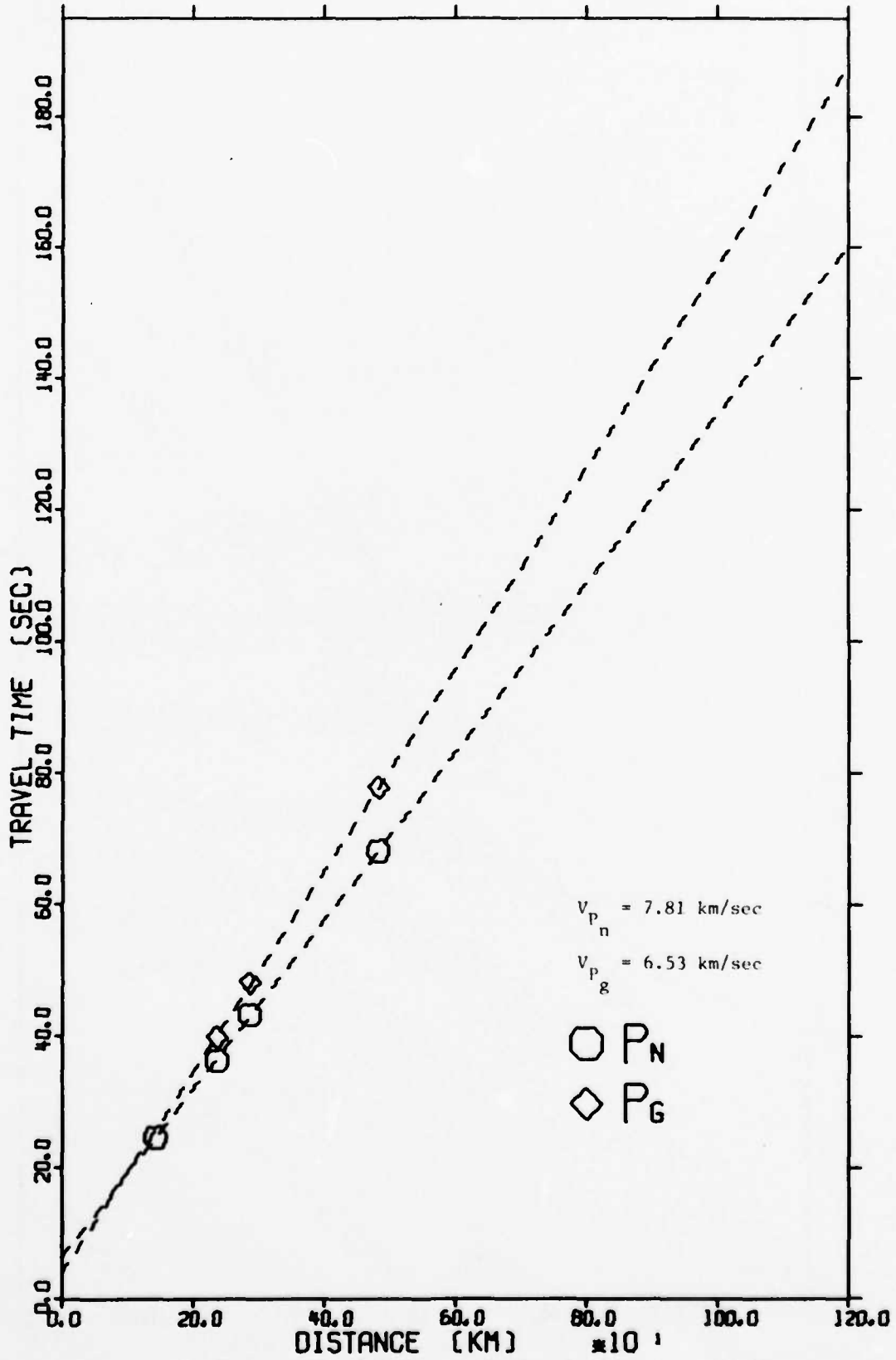

Figure 4c Observed P_n and P_g Travel Times for PASSAIC

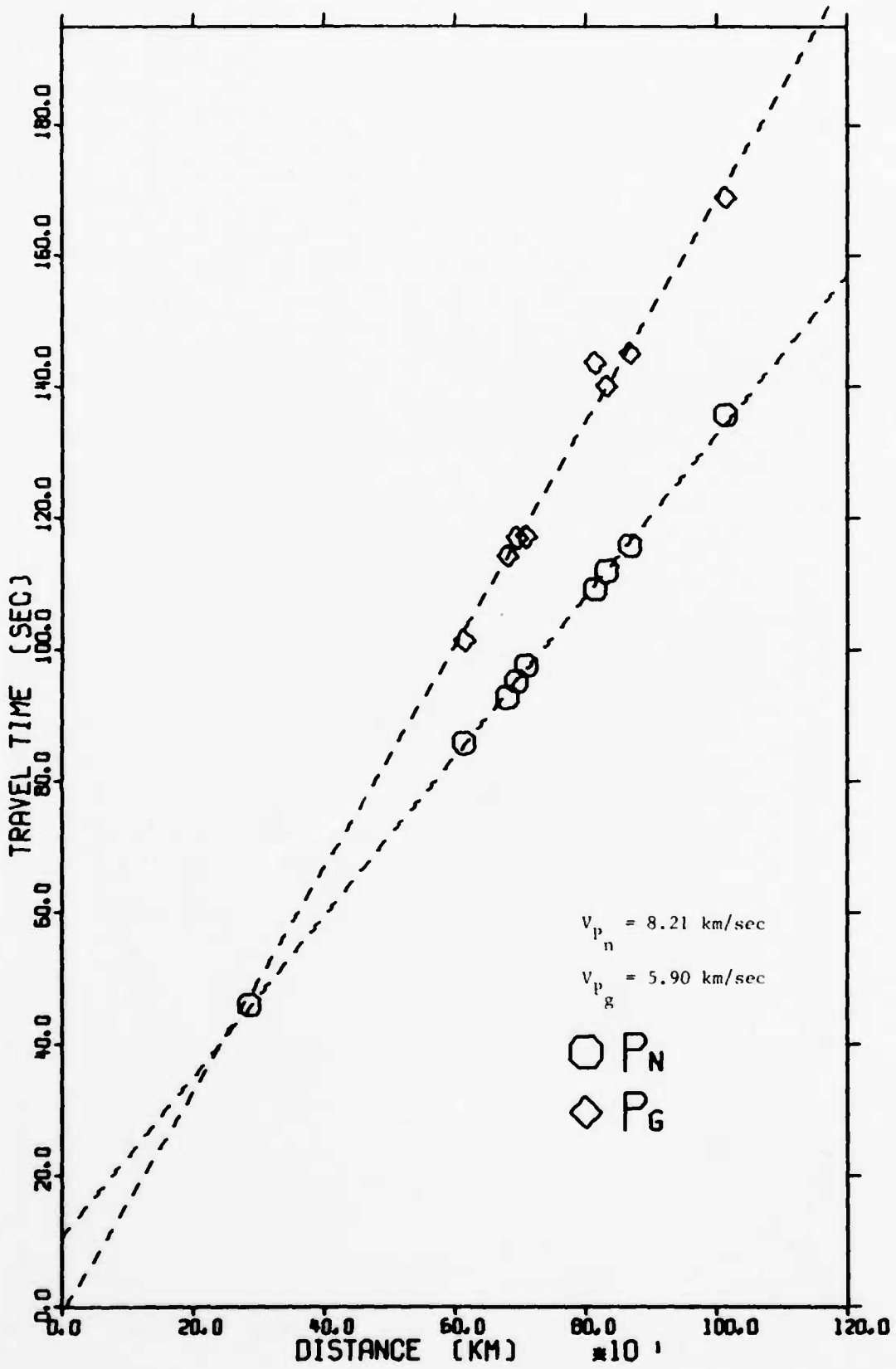

Figure 4d Observed P_n and P_g Travel Times for ROCKVILLE DAM

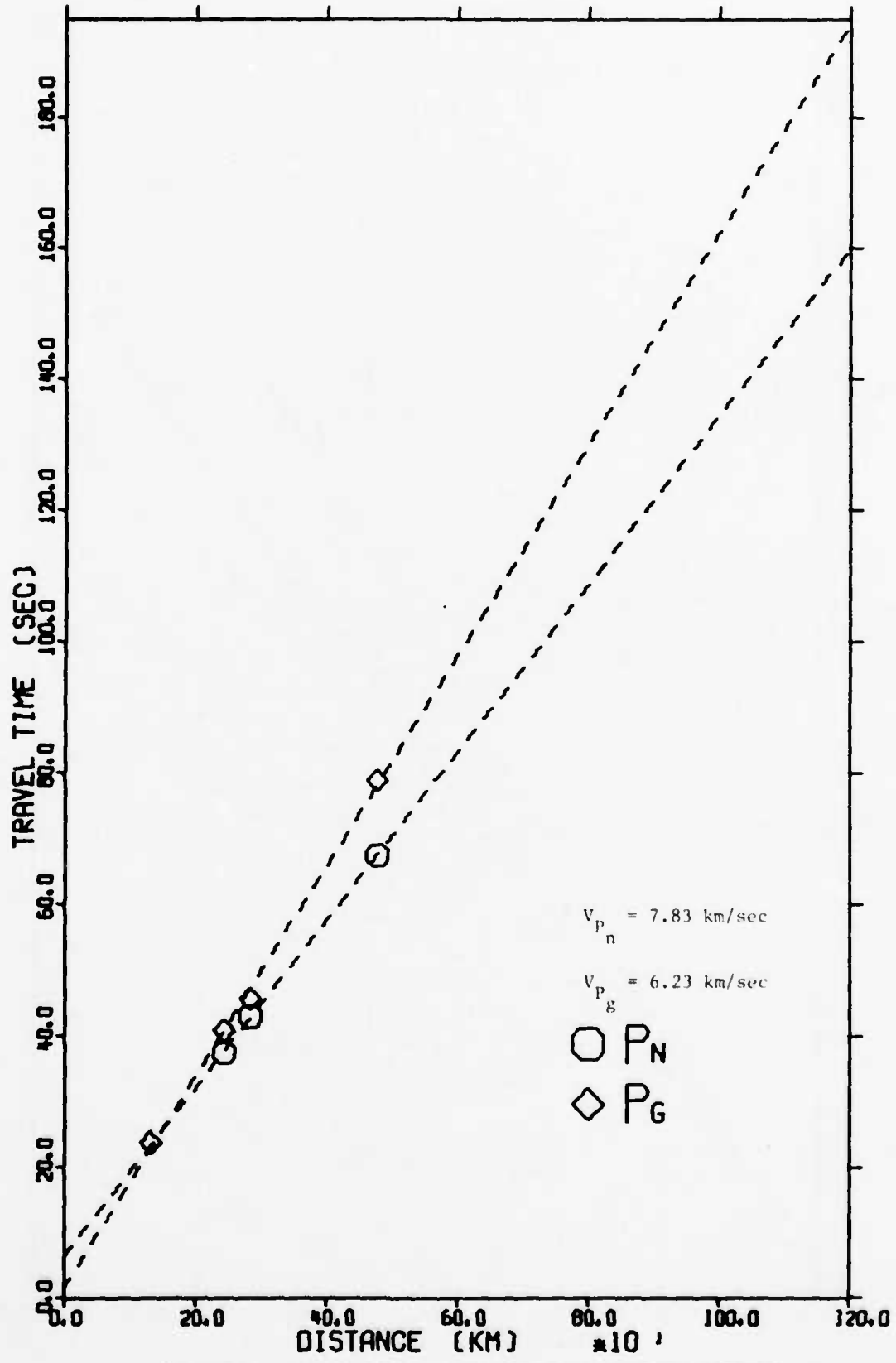

Figure 4e Observed P_n and P_g Travel Times for DORMOUSE'

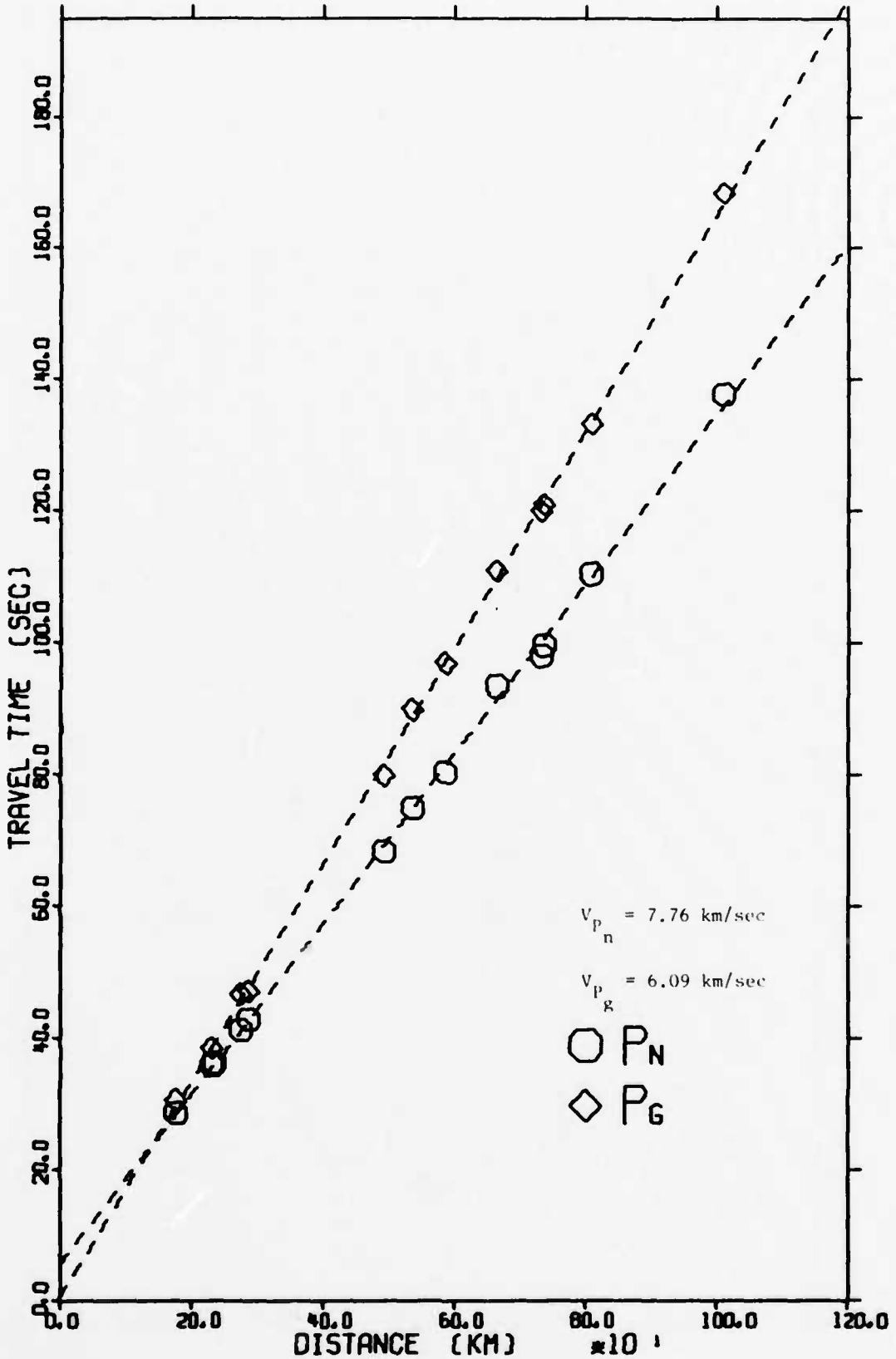

Figure 4f Observed P_n and P_g Travel Times for KLICKITAT

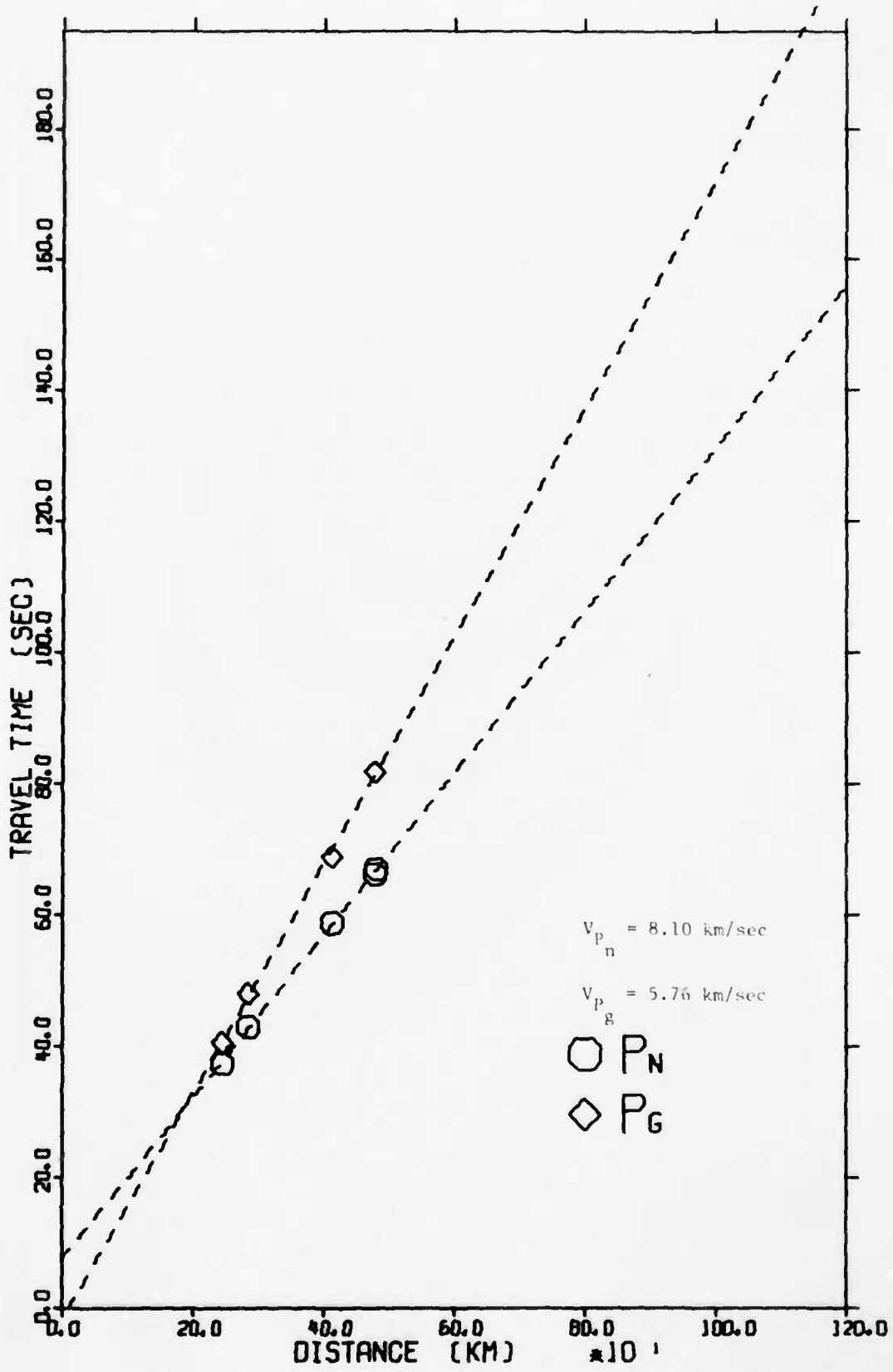

Figure 4g Observed P_n and P_g Travel Times for BANDICOOT

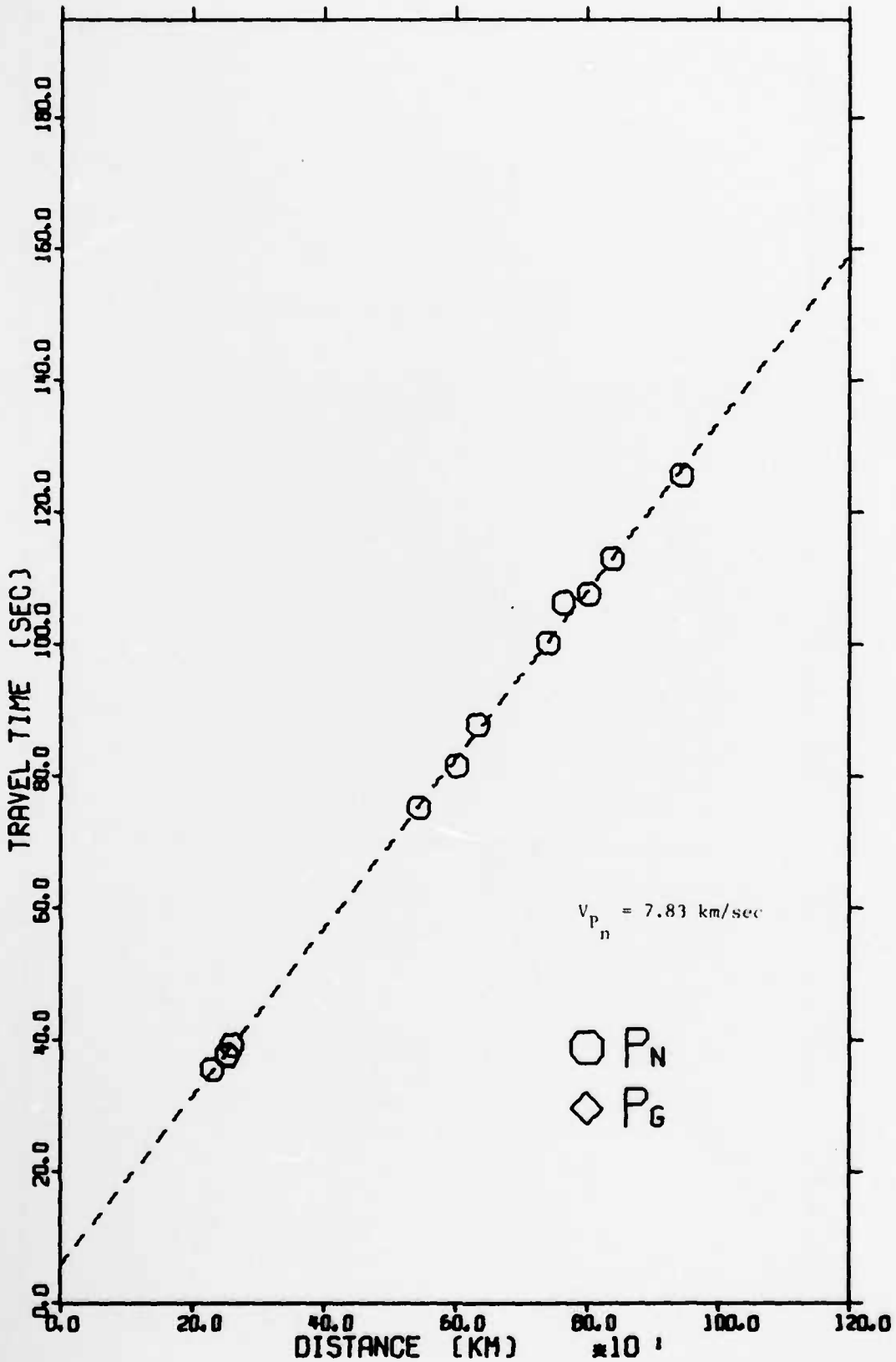

Figure 4h Observed P_n and P_g Travel Times for SHOAL

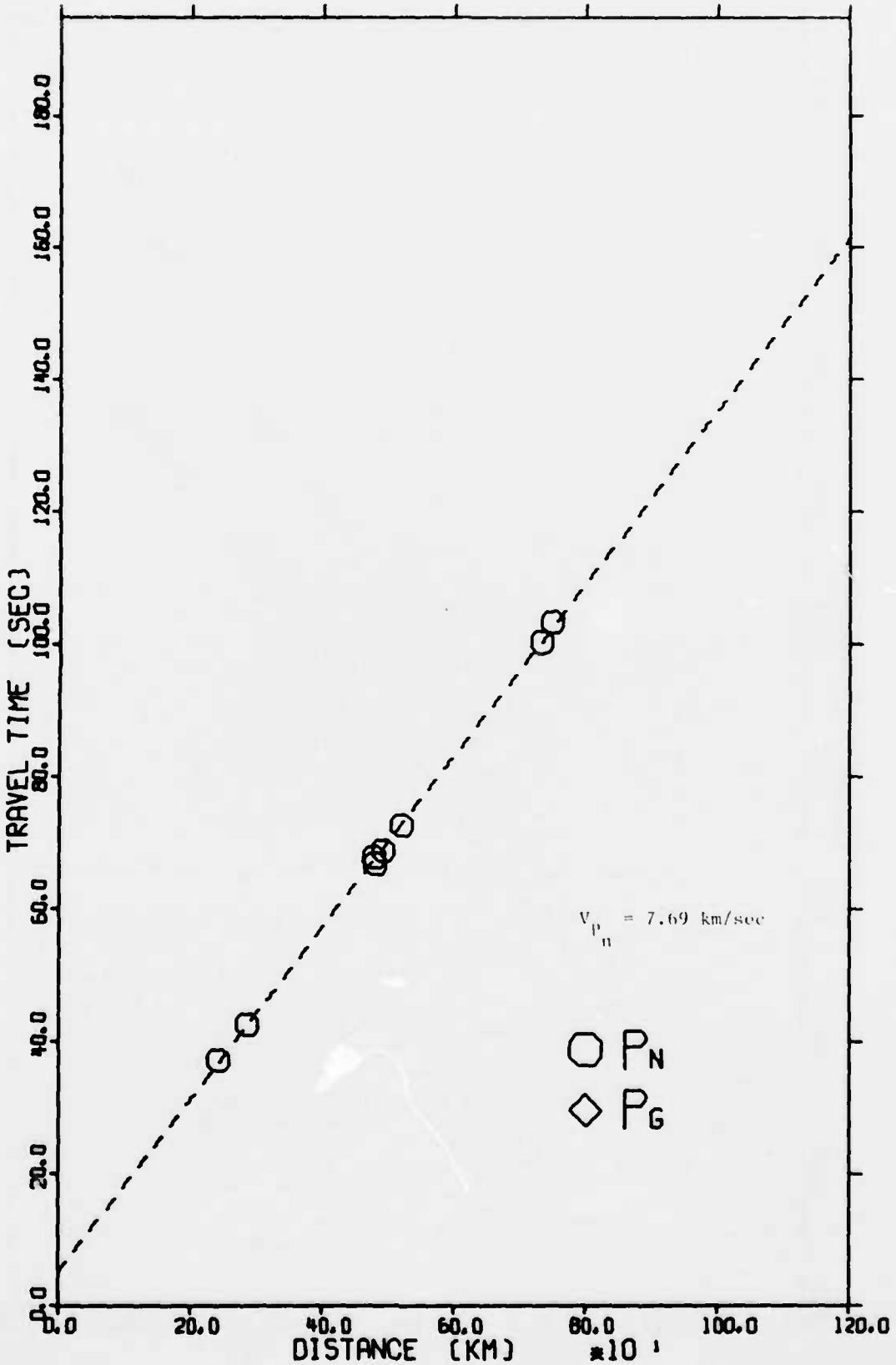

Figure 4i Observed P_n and P_g Travel Times for MERRIMAC

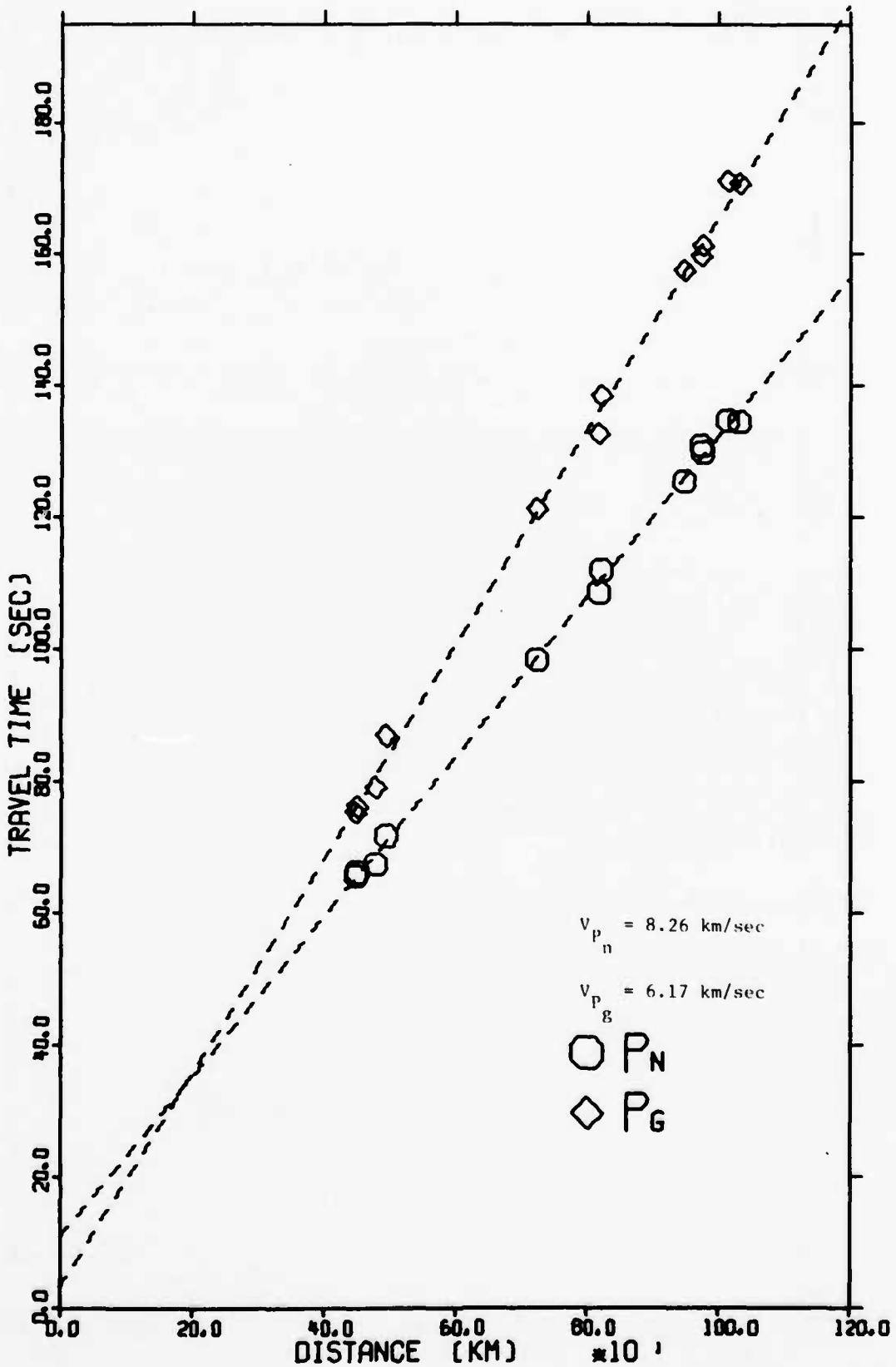

Figure 4j Observed P_n and P_g Travel Times for GASBUGGY

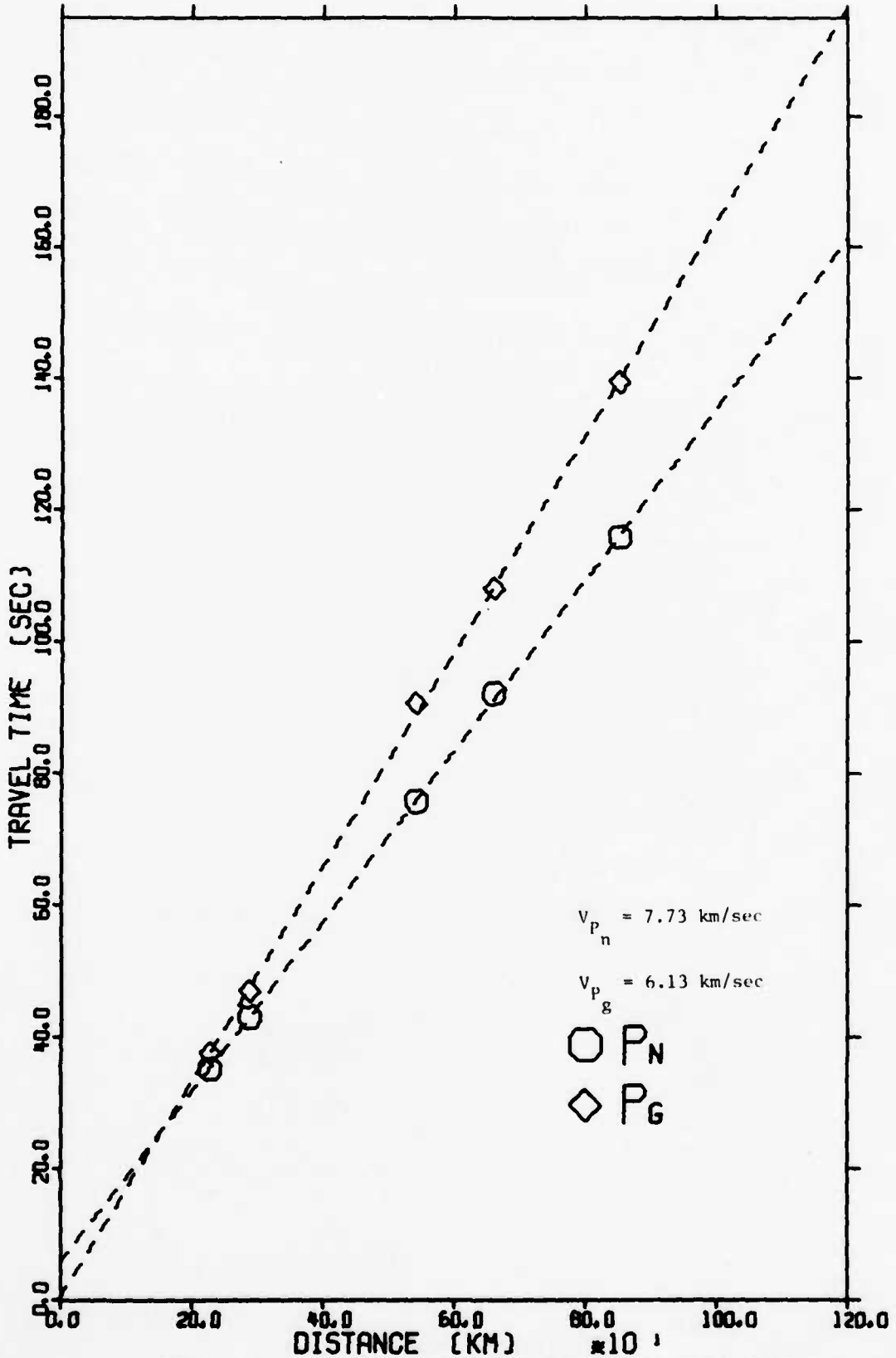

Figure 4k Observed P_n and P_g Travel Times for PILEDRIVER

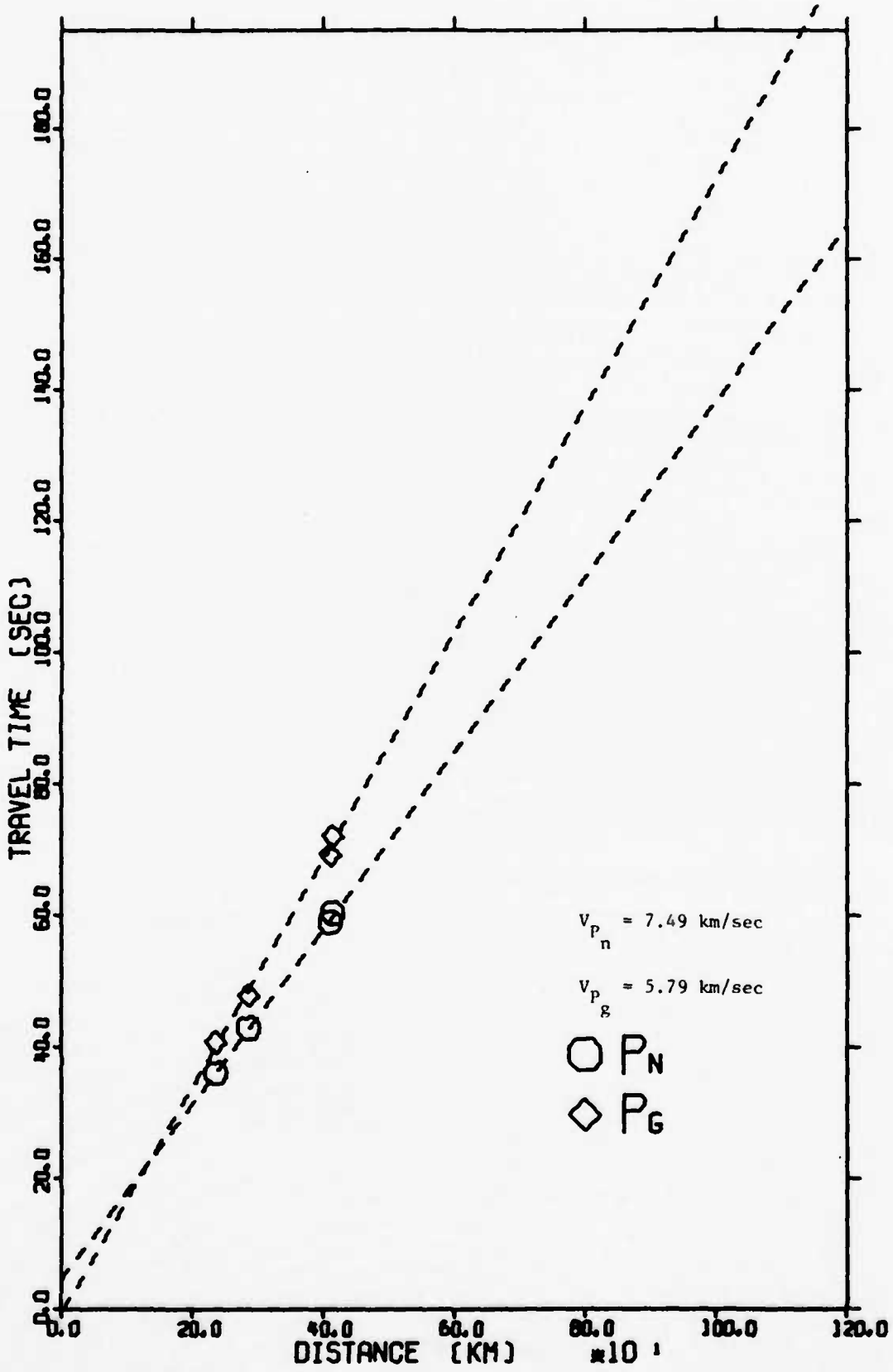

Figure 41 Observed P_n and P_g Travel Times for ROANOKE

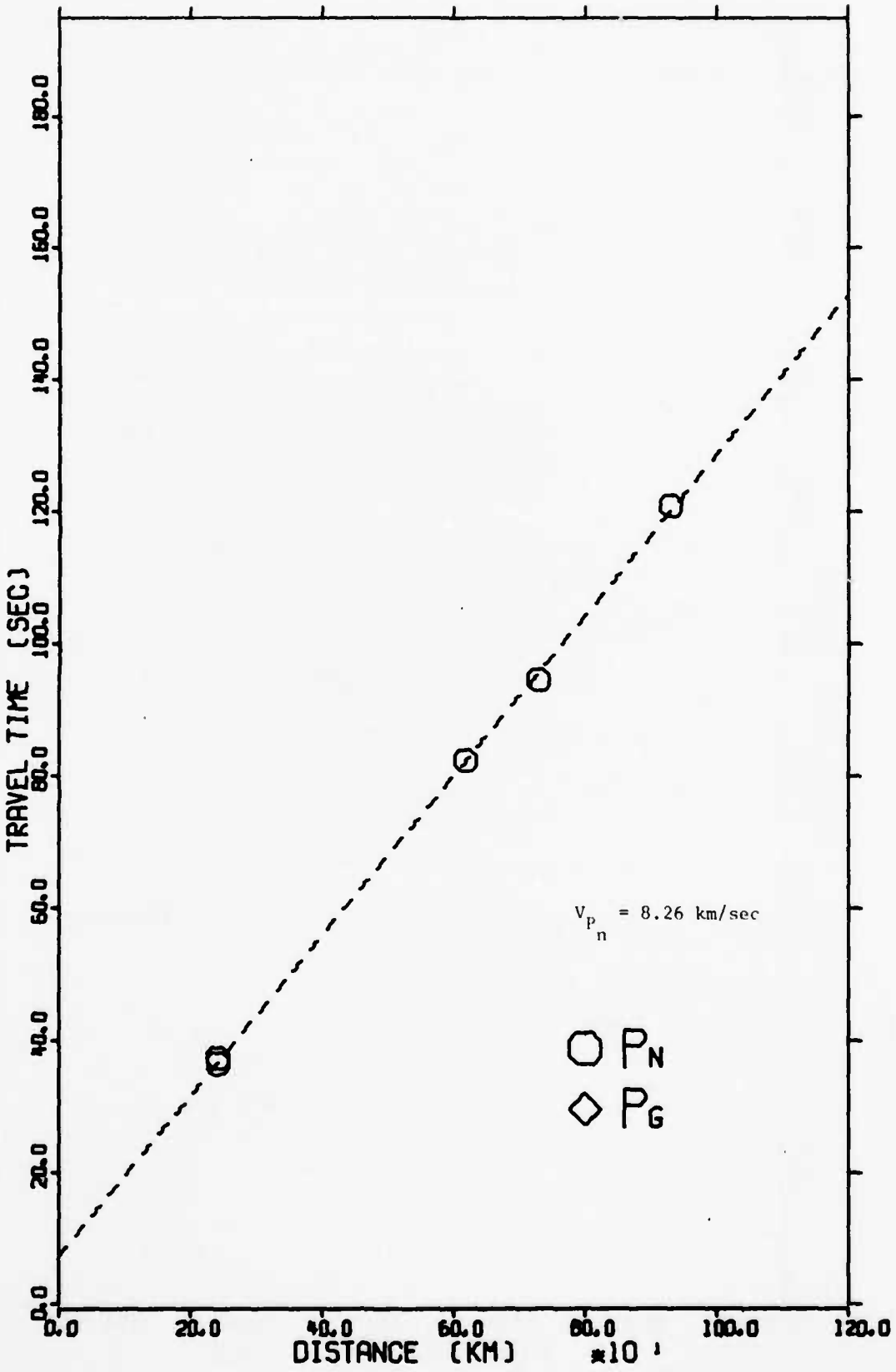

Figure 4m Observed P_n and P_g Travel Times for SALMON

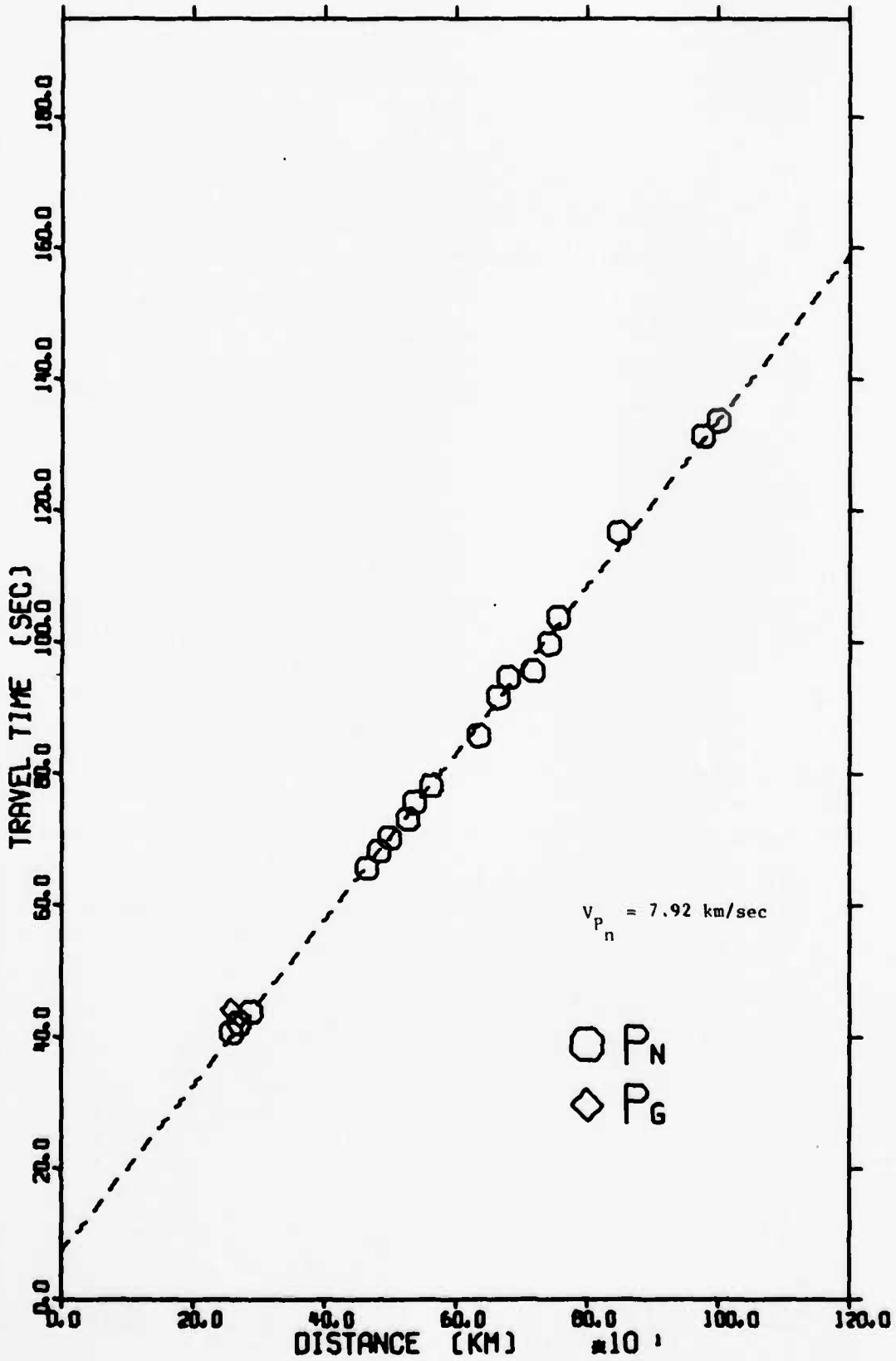

Figure 4n Observed P_n and P_g Travel Times for GNOME

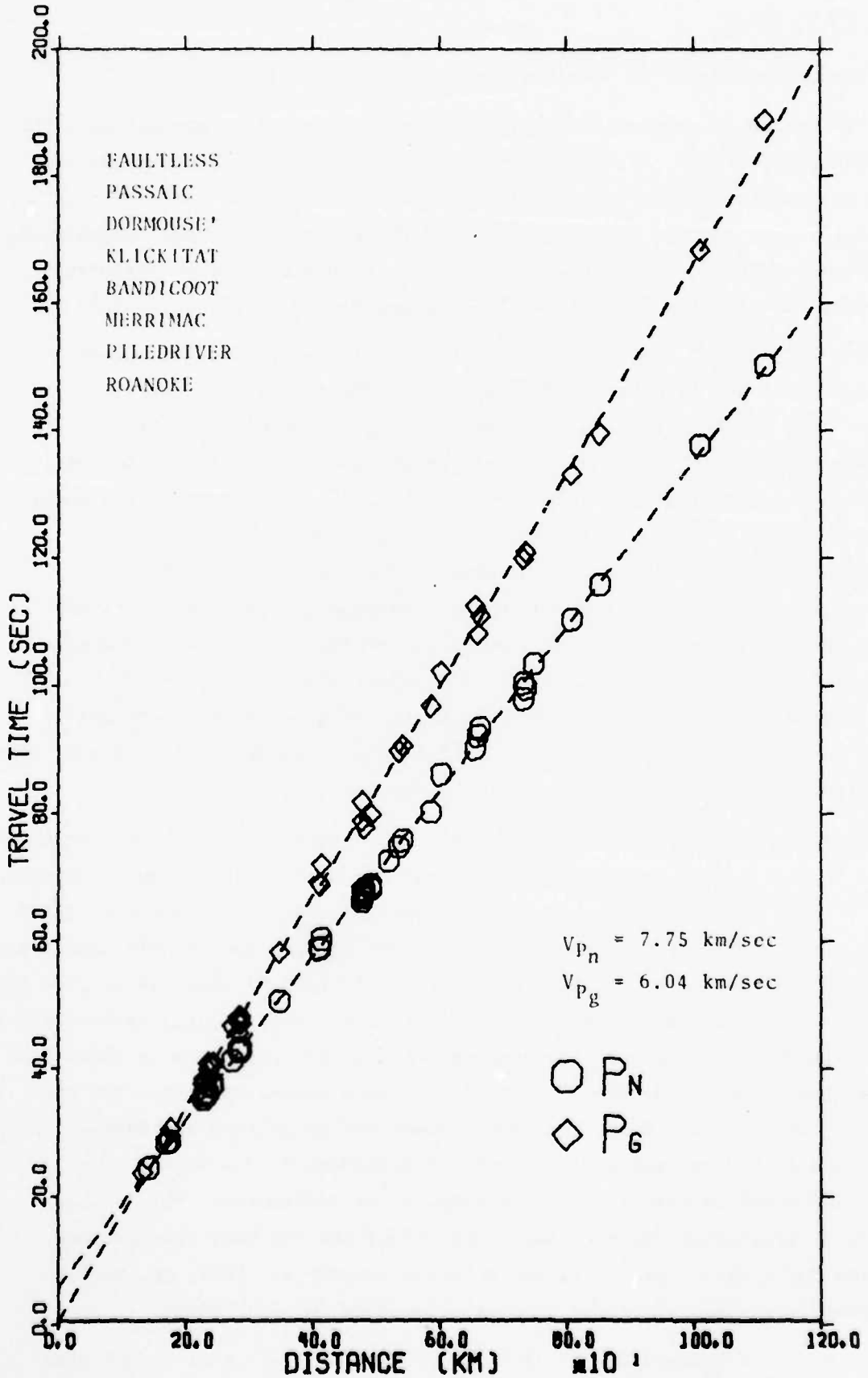

Figure 4o Observed P_n and P_g Travel Times for NTS COMPOSITE

3.2 Theory and Method of Investigation

The method of successive determinations has several advantages over the modified HYLO method. No previous knowledge of the crust is necessary, and it is then applicable anywhere in the world. The method is applicable to any regional phase, whereas HYLO utilizes only the phase P_n. In this experiment, we limited ourselves to the phases P_n and P_g, in order to allow ourselves to compare the results directly with Chang and Racine's (1979) results.

The method of successive determinations utilizes an initial epicenter location which may be determined using any of the standard travel time tables. The location used in this manner will, of course, be only approximately correct, and the size of the absolute error of location will depend on the difference between the P_n and P_g velocities used in the model selected and the true velocities for these phases measured along the particular source to receiver paths used in the location. In this particular study, our original epicenter determination was made using the Herrin 68 travel time tables and a Herrin 68 crustal model. We now make the critical assumption that for each individual event the P_n and P_g velocities have constant values for all paths and hence that the P_n and P_g travel time "curves" are in fact straight lines. Evidence substantiating this assumption has been presented in the previous section.

We shall therefore attempt to correct the approximate locations for the errors in the assumed travel-time relations, but in practice we must, of course, do so without any reference to the true locations, which were known *a priori* in the construction of Figures 4a-4o. In order to make such a correction, we construct travel-time curves similar to those in Figure 4, but now we plot the observed arrival times versus the distance from the approximate, rather than the true, epicenters. A linear least-squares fit is then performed on these observations, and the slopes of these lines yield corrected values for the P_n and P_g velocities. Next, the newly determined velocities are used as layer velocities in a crust which is otherwise appropriate to the Herrin travel times, and complete travel times are computed by raytracing. This process continues, alternately determining phase velocities and then travel-times, location and origin time, until the solution converges. Thus, the method determines a new set of travel time relationships for each event.

An option was installed to allow for two separate sets of travel time relationships for each event. This option may be useful, for example, in

allowing the use of separate travel time relationships for paths crossing very dissimilar geological provinces, or for differentiating between stations on opposite sides of a dipping slab.

3.3 Results and Discussion

Table III presents the results of the method of successive determinations. Unlike Chang and Racine's (1979) earlier findings using a standard location program and local or regional crustal models, the addition of P_g arrival times to the data base of the method of successive determinations significantly improves the location accuracy. Thus, it may be that the tabulated travel times for the phase P_g are not applicable to wide areas, and better location accuracy is obtained by determining the travel time relationships for P_g for each individual event. This may be due to the fact that P_g propagates through the upper layer of the crust, which is more laterally heterogeneous in its physical properties than the crust-mantle interface along which the P_n ray propagates. Or it may be possible that a wider variety of P_g rays are emitted as a function of source depth and geology.

Table IV compares the results of successive determinations versus the location and origin time determined using a standard location algorithm and Herrin 68 earth model. Substantial improvement in location is seen using the method of successive determinations.

Table V compares the results of successive determinations versus the modified HYLO method. Successive determination yields a more accurate location, requires no previous knowledge of the velocity structure of the earth's crust, and allows the use of phases other than P_n.

Table VI shows the results of the double successive determination experiment. This experiment invoked the option of separating the detecting stations into two azimuthal sectors and then fitting the travel times for each sector separately. As is shown in the table, dividing the arrival times for GNOME into eastward-going and westward-going paths does reduce the location error somewhat. However, this technique fails in the case of SHOAL, as might be expected since all directions out of SHOAL lie within the Western United States. Note that the P_n velocity for the second group of stations observing SHOAL defaulted to the Herrin 68 values, when the least-squares fit to the arrival data showed too much variance. Further, for SHOAL the first seven iterations appeared to diverge.

Figures 5a-n show the actual location of each event studied, the initial epicenter determination and the successive locations determined by our program as it converges on a solution. The open circles for SHOAL and GNOME illustrate the successive locations determined by the program allowing two separate travel time relationships. It may be seen that most solutions converged after about seven successive approximations. However, the event ROCKVILLE DAM, which gave a good solution after seven successive approximations, did not converge to a final solution.

TABLE III

Method of Successive Determinations - Absolute Errors

	# P_n's	# P_g's	Error (km) P_n only Depth Free	Error (km) P_n & P_g Depth Free	Error (km) P_n only Depth Rest.	Error (km) P_n & P_g Depth Rest.
FAULTLESS	5	5	18.64	(3.95)	18.64	4.05
RULISON	10	7	restr.	restr.	2.65	3.38
PASSAIC	4	3	(2.66)	restr.	2.66	2.14
ROCKVILLE DAM	9	8	restr.	restr.	2.04	a 3.75 b 5.00*
DORMOUSE'	3	4	diverges	(9.39)	diverges	10.70
KLICKITAT	13	12	diverges	(3.11)	4.34	4.11
BANDICOOT	5	4	N/A	restr.	N/A	9.50
SHOAL	12	0	diverges	no P_g	2.34	no P_g
MERRIMAC	8	0	restr.	no P_g	5.17	no P_g
GASBUGGY	12	12	10.51	restr.	10.51	10.02
PILEDRIVER	5	5	diverges	(1.83)	10.41	2.56
ROANOKE	4	4	(4.41)	ignores P_g**	4.38	4.24
GNOME	18	1	restr.	restr.	7.10	7.06
Mean Error (km):			8.08	4.57	6.39	a 5.59 b 5.71

DIVERGES = Does not converge to solution
RESTR = Restricted to 0 depth

Unlike HYLO - can use P_g (bigger than P_n, especially in WUS)

Unlike Chang & Racine - P_g improves location.

* Solution alternates between two epicenters

** Residuals too large - data rejected

TABLE IV

Accuracy of Location
Successive Determination Versus Herrin 68
Depth Free

	HERRIN 68			SUCCESSIVE DETERMINATIONS		
	LOC E[1]	OT E[2]	DEPTH[3]	LOC E	OT E	DEPTH
FAULTLESS	15.04	1.4	0.0	3.96	1.0	3.6
RULISON	1.58	0.0	0.0	3.39	2.6	0.0
PASSAIC	4.08	-0.2	0.0	2.14	-0.6	0.0
ROCKVILLE DAM	5.18	1.5	0.0	a 3.75 b 5.00	1.9 1.9	0.0 0.0
DORMOUSE'	9.09	0.2	0.0	9.87	0.7	4.3
KLICKITAT	6.53	0.1	0.0	2.78	0.7	8.1
BANDICOOT	1.24	0.6	7.8	4.58	0.0	0.0
SHOAL*	5.18	0.0	0.0	2.34	-0.9	0.0
MERRIMAC	9.58	0.3	0.0	5.16	0.2	15.9
GASBUGGY	11.43	0.6	0.0	10.04	2.0	0.0
PILEDRIVER	12.98	0.0	0.0	1.66	-0.1	8.9
ROANOKE	8.24	1.3	7.9	4.20	1.1	28.1
Average	7.52			a 4.49 b 4.59		

* Depth restricted

1. LOC E: Error of location vectors in km
2. OT E: Error of origin time estimates, $T_{est} - T_{true}$, in sec
3. when depth is zero, the depth is restricted to 0 km
4. Solution alternates between two epicenters.

TABLE V

Successive Determination Versus HYLO

	HYLO		SUCCESSIVE DETERMINATION		
	LOC E	OT E	LOC E	OT E	
FAULTLESS	12.32	-1.8	3.96	1.0	
RULISON	3.72	1.0	3.39	2.6	
PASSAIC	11.17	0.8	2.14	-0.6	
ROCKVILLE DAM	5.59	-0.4	a 3.75 b 5.00	1.9 1.9	*
DORMOUSE'	10.47	-1.4	9.87	0.7	
KLICKITAT	9.64	0.6	2.78	0.7	
BANDICOOT	7.09	-1.8	4.58	0.0	
SHOAL	11.26	0	2.34	-0.9	
MERRIMAC	10.89	4.7	5.16	0.2	
GASBUGGY	5.81	0.4	10.04	2.0	
PILEDRIVER	24.54	0.9	1.66	-0.1	
ROANOKE	3.68	0.4	4.20	1.1	
Average	9.68		a 4.49 b 4.59		

* Solution alternates between two epicenters.

TABLE VI

Double Successive Determinations

GNOME		SHOAL	
Group #1	Group #2	Group #1	Group #2
LC-NM	PO-TX	EK-NV	BMO
ML-NM	SS-TX	WI-NV	
RT-NM	SM-TX	MV-CL	CP-CL
SV-AZ	LP-TX	CU-NV	UBO
SF-AZ	HB-OK	KN-UT	BX-UT
DR-CO	AM-OK	HL-ID	TFO
FS-AZ	TO-OK		DR-CO
WM-AZ	SJ-TX		
KN-UT			
PM-WY			
Vel P_n 7.887	8.244	8.108	***

	SUCCESS			DOUBLE SUCCESS		
	LOC Error (km)	OT Error (sec)	H (km)	LOC Error (km)	OT Error (sec)	H (km)
GNOME	7.07	+0.3	0.0*	5.73	+1.5	4.965
SHOAL	2.34	-0.9	0.0*	11.04 (diverges)	+0.9	0.0*

* RESTRICTED

*** DEFAULTED to Herrin 68 Model

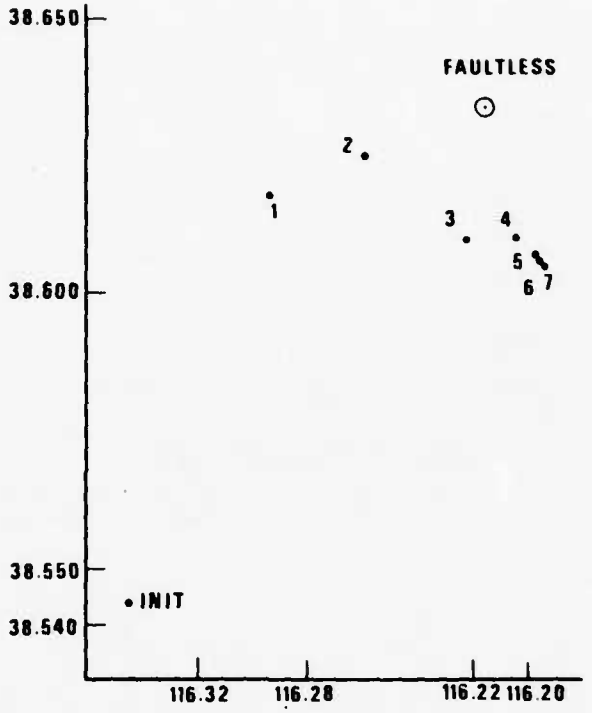

Figure 5a Convergence of calculated epicenters toward true epicenters - Method of successive determinations.

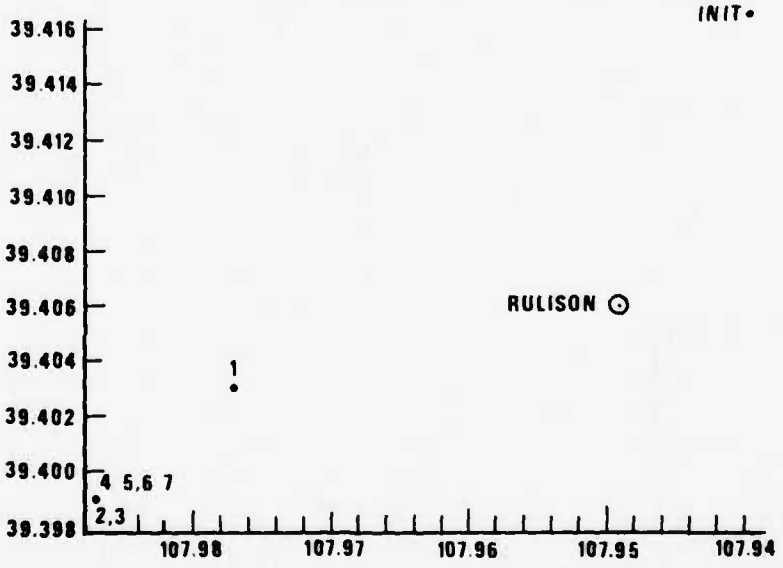

Figure 5b Convergence of calculated epicenters toward true epicenters - Method of successive determinations.

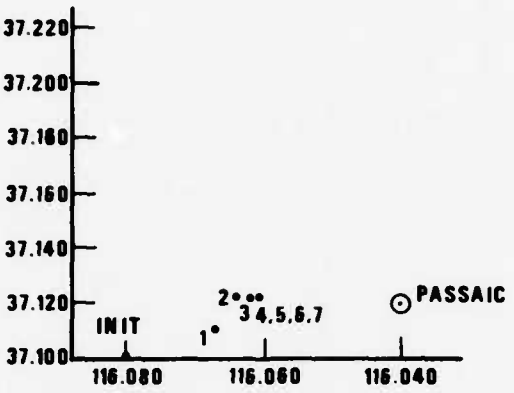

Figure 5c Convergence of calculated epicenters toward true epicenters - Method of successive determinations.

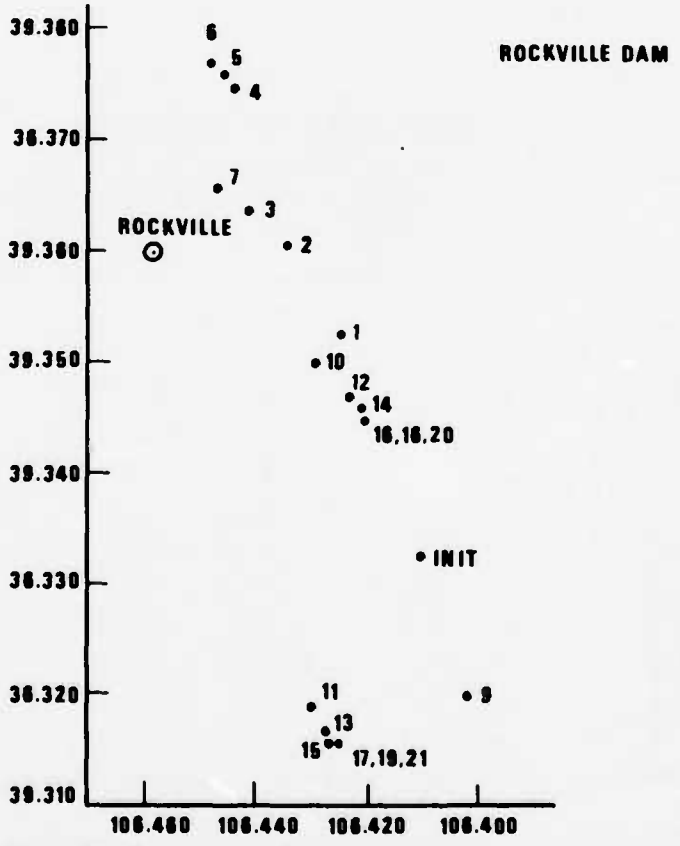

Figure 5d Convergence of calculated epicenters toward true epicenters - Method of successive determinations.

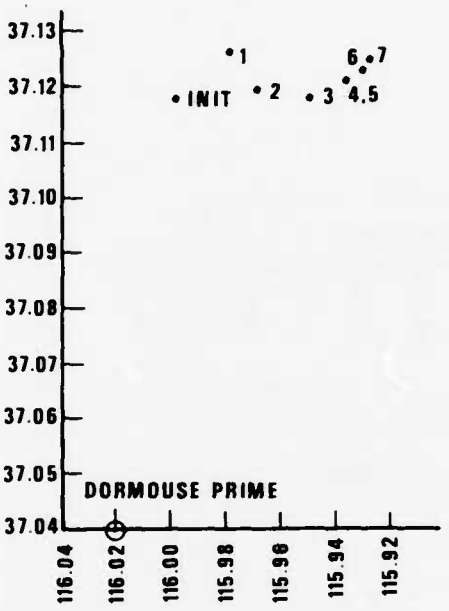

Figure 5e Convergence of calculated epicenters toward true epicenters - Method of successive determinations.

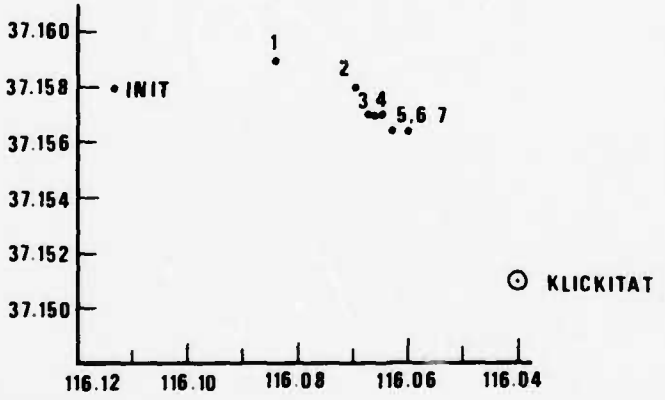

Figure 5f Convergence of calculated epicenters toward true epicenters - Method of successive determinations.

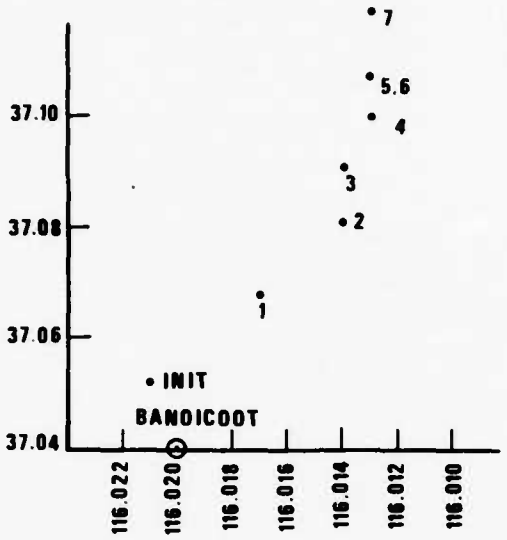

Figure 5g Convergence of calculated epicenters toward true epicenters - Method of successive determinations.

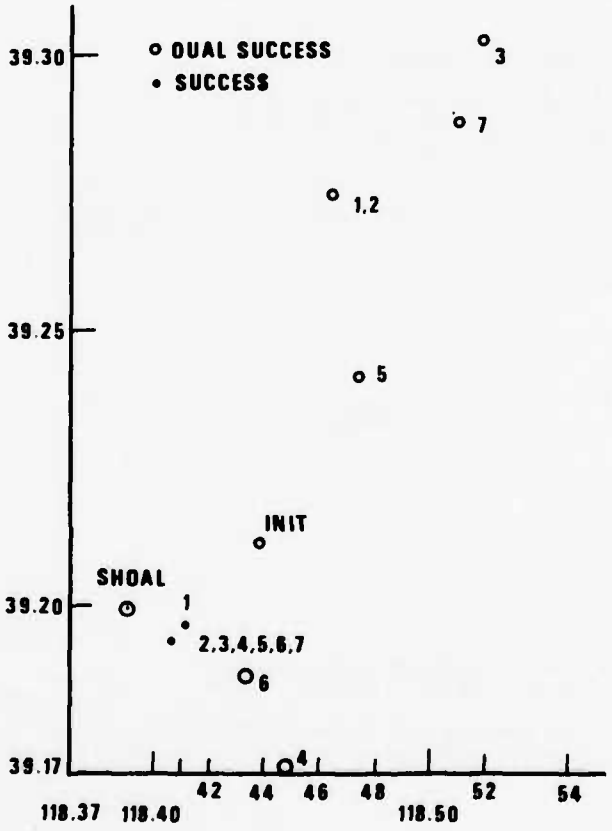

Figure 5h Convergence of calculated epicenters toward true epicenters - Method of successive determinations.

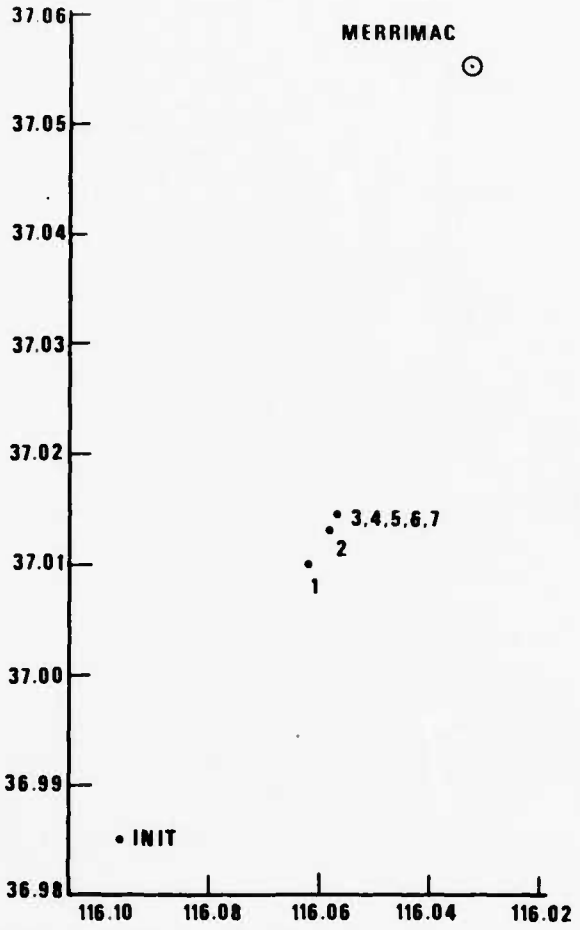

Figure 5i Convergence of calculated epicenters toward true epicenters - Method of successive determinations.

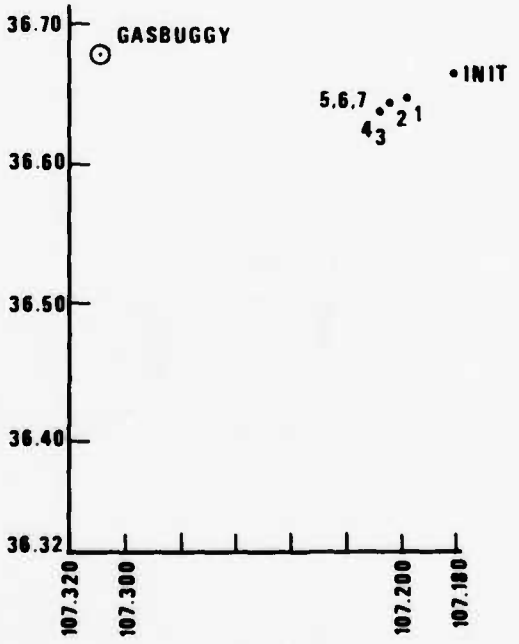

Figure 5j Convergence of calculated epicenters toward true epicenters - Method of successive determinations.

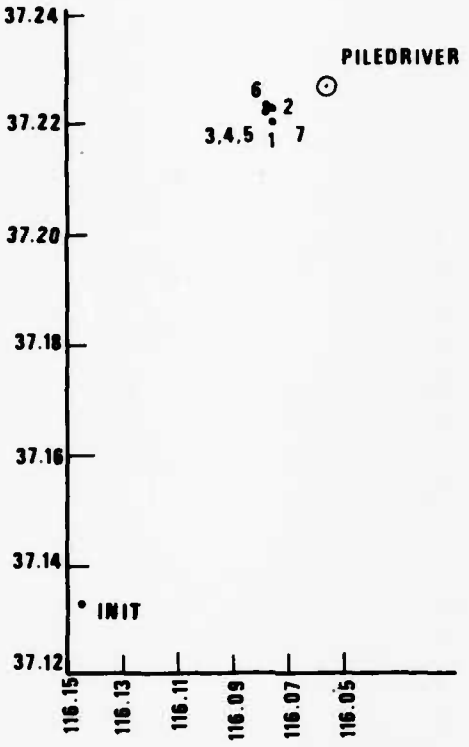

Figure 5k Convergence of calculated epicenters toward true epicenters - Method of successive determinations.

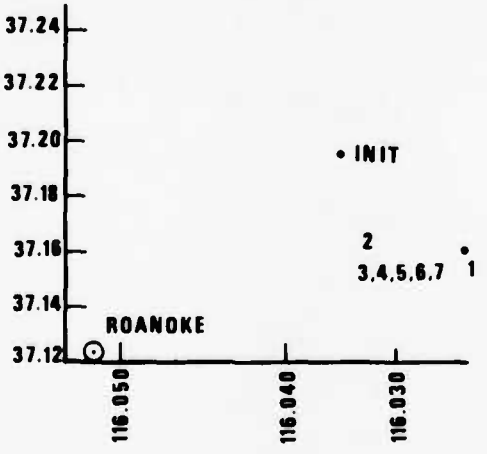

Figure 51 Convergence of calculated epicenters toward true epicenters - Method of successive determinations.

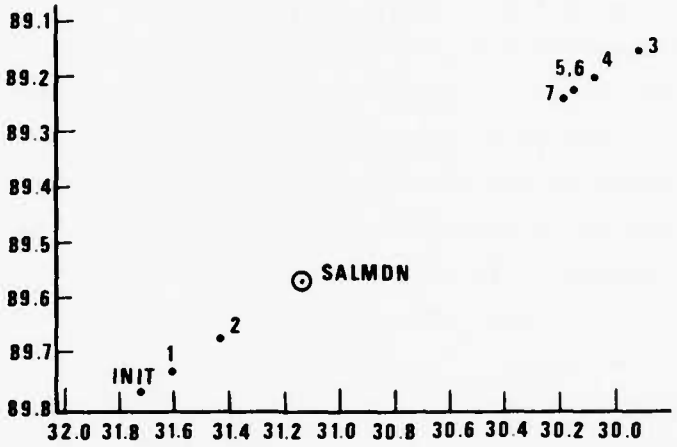

Figure 5m Convergence of calculated epicenters toward true epicenters - Method of successive determinations.

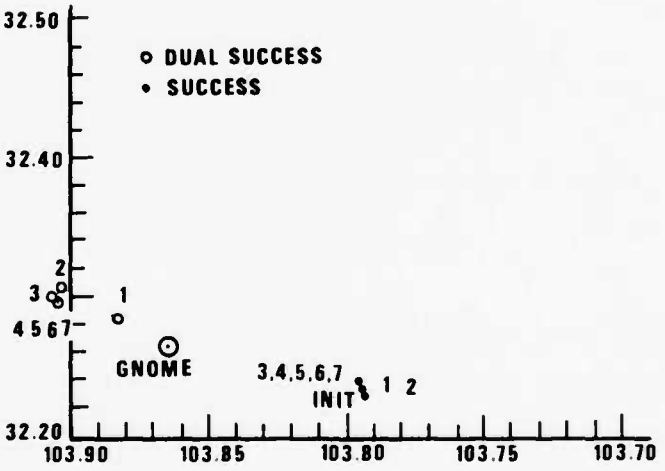

Figure 5n Convergence of calculated epicenters toward true epicenters - Method of successive determinations.

4. METHOD OF SIMULTANEOUS INVERSIONS

4.1 Theory

Thus far in this report two approaches have been taken to the problem of overcoming inaccuracies introduced into the location of regional events by an inadequate knowledge of the P_n and P_g travel-time relations. The first approach, HYLO, involved the construction of improved travel-time curves using velocities measured by crustal refraction methods. The second approach, the method of successive determinations, assumes no such *a priori* information (except as an initial guess), but instead determines corrections to the assumed travel-time curves alternately with corrections to the assumed event locations in a successive approximations scheme. We shall now describe a third approach, the method of simultaneous inversions, whereby the corrections to the travel-time curves and to the event locations are computed at the same time rather than alternately. We shall present a detailed comparison of these latter two methods in order to determine which approach ought to be taken in order to improve the location of events at regional distances in the absence of *a priori* knowledge of the true travel-time relations.

The standard technique for locating seismic events, at both regional and teleseismic distances, involves assuming a trial value of the hypocenter and origin time, calculating predicted arrival times at a set of stations for signals originating at the trial hypocenter, expanding the travel time residual at the i^{th} station, $\delta t_i = t_{i,\text{observed}} - t_{i,\text{calculated}}$, in the first-order Taylor series

$$\delta t_i = \left(\frac{\partial t}{\partial T}\right)_i dT + \left(\frac{\partial t}{\partial x}\right)_i dx + \left(\frac{\partial t}{\partial y}\right)_i dy + \left(\frac{\partial t}{\partial h}\right)_i dh, \tag{1}$$

forming a system of such equations for all residuals δt_i, solving for the location corrections dT, dx, dy, and dh by means of matrix inversion and then adding these corrections to the assumed values of the event's origin time, east, north, and depth coordinates. In order to evaluate the derivatives in this equation, one may set

$$\frac{\partial t}{\partial T} = 1 \tag{2}$$

$$\frac{\partial t}{\partial x} = \frac{\partial t}{\partial \Delta} \cdot \frac{\partial \Delta}{\partial x} = - \sin \zeta_0 \cdot \frac{\partial t}{\partial \Delta} \tag{3}$$

$$\frac{\partial t}{\partial y} = \frac{\partial t}{\partial \Delta} \cdot \frac{\partial \Delta}{\partial y} = - \cos \zeta_0 \cdot \frac{\partial t}{\partial \Delta} \tag{4}$$

where ζ_0 is the azimuth from the epicenter to the station. If the travel-time relations are accurately known, then the derivatives $\frac{\partial t}{\partial \Delta}$ and $\frac{\partial t}{\partial h}$ may be calcuated at the distance Δ_i and the matrix inversion thereby made tractable. Evidence has been presented in Figure 4 and Table III that the travel-time curves for P_n and P_g are linear, and we shall therefore assume that the travel times may be defined analytically as

$$t_{P_n} = T + a_{P_n}(h) + b_{P_n} \cdot \Delta \tag{5}$$

$$t_{P_g} = T + a_{P_g}(h) + b_{P_g} \cdot \Delta. \tag{6}$$

In these expressions we have made it explicit that the coefficients a_{P_n} and a_{P_g} depend on the depth of the event, since they represent the delay between the event origin time and the first motion at the surface. The travel-time residuals at regional distances may thus be expanded as

$$(\delta t_{P_n})_i = (\partial t_{P_n}/\partial T)_i \, dT + (\partial t_{P_n}/\partial x)_i \, dx + (\partial t_{P_n}/\partial y)_i \, dy + (\partial t_{P_n}/\partial a_{P_n})_i \, da_{P_n} + (\partial t_{P_n}/\partial b_{P_n})_i \, db_{P_n} \tag{7}$$

$$(\delta t_{P_g})_i = (\partial t_{P_g}/\partial T)_i \, dT + (\partial t_{P_g}/\partial x)_i \, dx + (\partial t_{P_g}/\partial y)_i \, dy + (\partial t_{P_g}/\partial a_{P_g})_i \, da_{P_g} + (\partial t_{P_g}/\partial b_{P_g})_i \, db_{P_g}. \tag{8}$$

These expressions are not explicitly a function of depth, since the depth dependence is contained within the coefficients a_{P_n} and a_{P_g}. Evaluation of the derivatives in these expressions is straightforward:

$$\partial t_{P_n}/\partial T = \partial t_{P_g}/\partial T = \partial t_{P_n}/\partial a_{P_n} = \partial t_{P_g}/\partial a_{P_g} = 1 \tag{9}$$

$$\partial t_{P_n}/\partial x = -\sin \zeta_0 \cdot (\partial t_{P_n}/\partial \Delta) = -\sin \zeta_0 \cdot b_{P_n} \tag{10}$$

$$\partial t_{P_g}/\partial x = -\sin \zeta_0 \cdot b_{P_g} \tag{11}$$

$$\partial t_{P_n}/\partial y = -\cos \zeta_0 \cdot (\partial t_{P_n}/\partial \Delta) = -\cos \zeta_0 \cdot b_{P_n} \tag{12}$$

$$\partial t_{P_g} / \partial y = - \cos \zeta_0 \cdot b_{P_g} \tag{13}$$

$$(\partial t_{P_n} / \partial b_{P_n})_i = \Delta_i \tag{14}$$

$$(\partial t_{P_g} / \partial b_{P_g})_i = \Delta_i . \tag{15}$$

The addition of the travel-time residuals δt_{P_n} and δt_{P_g} to the conventionally calculated residuals $\delta t_{P\ \text{teleseismic}}$ enables the event location to be expressed in terms of an expanded set of coordinates $(x,y,h,T,a_{P_n},b_{P_n},a_{P_g},b_{Pg})$. For an over-determined system of more than eight observations, the matrix inversion may be carried out as before and a solution, in the least-squares sense, may be found for the newly defined eight-dimensional hypocenter. The first four coordinates give the event location, and the last four determine the slopes and intercepts of the P_n and P_g travel-time curves. If there are no observations of teleseismic P, then the system of equations does not involve h explicitly and so the depth cannot be determined, but the other seven hypocentral coordinates still can be. Similarly the absence of P_n or P_g arrival time data presents no difficulties in the computation since the matrix manipulation is simply carried out in a six-dimensional subspace by restraining the unmeasured coefficients a_{P_n} and b_{P_n} or a_{P_g} and b_{P_g} to have some arbitrary fixed value.

In the event that no teleseismic P arrival times are available and that all of the regional data consist of measurements made upon a single phase only (i.e., all P_n or all P_g), then the origin time as well as the depth of the event becomes indeterminate. That this is so can be seen by examining equations (5) and (6), wherein it is shown that in the absence of P_g measurements one may calculate only the sum of T and a_{P_n} rather than the two individual coefficients, with a similar indeterminacy occurring in the case of no P_n data.

A consideration of the physical meaning of the coefficients a_{P_n}, b_{P_n}, a_{P_g}, and b_{P_g} permits the depth to be estimated when it cannot be directly calculated on account of the absence of teleseismic data. Consider a simple earth model consisting of an upper crustal layer of thickness h_1 and P-wave velocity, V_1, a lower crustal layer of thickness h_2 and velocity V_2, and a mantle with velocity V_3. The ray diagram in Figure 6 shows that

$$t_{P_g} = h/2V_1 + \Delta/V_1, \tag{16}$$

so we may set

Theoretical Travel Time for P_g in a Simple Earth Model

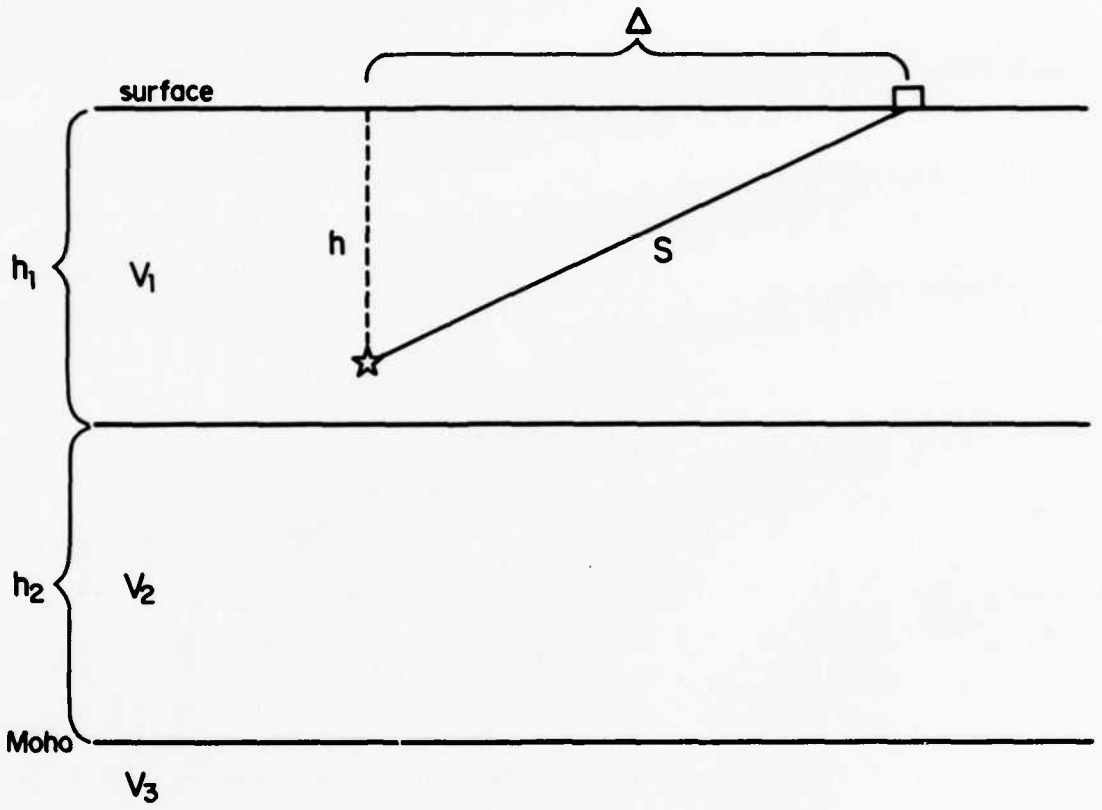

$$t_{Pg} = S/V$$
$$= (h^2+\Delta^2)^{1/2}/V_1$$
$$\approx \Delta/V_1 + h/2V_1$$

Figure 6 Raypath for P_g.

$$a_{P_g} = h/2V_1 \tag{17}$$

$$b_{P_g} = 1/V_1. \tag{18}$$

In a like manner we find that for an event occurring in the upper crustal layer (cf. Figure 7a)

$$a_{P_n} = 2h_1/V_1 \cos\theta_1 + 2h_2/V_2 \cos\theta_2 - (2h_1 \tan\theta_1 + 2h_2 \tan\theta_2)/V_3 + (\tan\theta_1/V_3 - 1/V_1 \cos\theta_1) \cdot h \tag{19}$$

and for an event occurring in the lower layer (cf. Figure 7b)

$$a_{P_n} = (h_1 + 2h_2)/V_2 \cos\theta_2 + h_1/V_1 \cos\theta_1 - [(h_1 + 2h_2) \tan\theta_2 + h_1 \tan\theta_1]/V_3 + (\tan\theta_2/V_3 - 1/V_2 \cos\theta_2) \cdot h \tag{20}$$

and in both cases

$$b_{P_n} = 1/V_3 \tag{21}$$

where the angles in these expressions are given by Snell's law as

$$\sin\theta_1 = V_1/V_3 \tag{22}$$

$$\sin\theta_2 = V_2/V_3. \tag{23}$$

We shall abbreviate the preceding expressions for a_{P_g} and a_{P_n} (for both the upper and lower crustal layers) as

$$a_{P_g} = k_1 \cdot h \tag{24}$$

$$a_{P_n} = k_2 \cdot h + k_3 \tag{25}$$

and form the difference

$$a_{P_g} - a_{P_g} = (k_1 - k_2) \cdot h - k_3. \tag{26}$$

Substituting into the above formula the values which are found for a_{P_g} and a_{P_n} by the method of simultaneous inversions, we may now calculate the depth in terms of the model parameters k_1, k_2, and k_3. We emphasize that such a calculation is only approximate, since the impetus for using the simultaneous inversion approach is the assumption that the *a priori* earth model is inaccurate. Equations (24) and (25) cannot be used to determine the depth if only P_n or P_g data are used, since in these cases only $T + a_{P_n}$ or $T + a_{P_g}$ can be determined. If, however, the location is constrained to the surface, then these expressions show that the origin time may be approximated by means of relations

$$a_{P_g}(\text{measured}) = k_1 \cdot h + T = T \tag{27}$$

$$a_{P_n}(\text{measured}) = (k_1 - k_2) \cdot h - k_3 + T = -k_3 + T. \tag{28}$$

Table VII presents a summary of which variables can be determined when different types of data are used. The indeterminate variables represent a difference between the method of simultaneous inversions and the method of successive determinations. Even though both methods are based upon the determination of the slopes and intercepts of the P_n and P_g travel-time curves and hence they both should be indeterminate under the same circumstances, differences in the operational approaches which were taken to the implementation of the two techniques create discrepancies in their applicability. The simultaneous inversions technique is based directly on equations (5) and (6), which cause the indeterminations shown in Table VII; the implementation of the successive determinations method, however, uses a hybrid approach which calculates the slopes and intercepts in equation (5) and (6) but then ignores the intercepts and substitutes the resulting velocities in a Herrin structure which may be used to calculate $dT/d\Delta$ and dT/dh for regional phases, equations (17) - (23). During each iterative calculation of the hypocenter, the travel-time curves are thus taken to be pre-determined, so the indeterminations shown in Table VII do not occur. In the comparison of results of the two methods which will be presented in the next section, there are therefore several instances of the calculation of some variable by the successive determinations method even though no corresponding value can be calculated by the simultaneous inversions method.

TABLE VII

Variables Which May Be Determined Using the Method of Simultaneous Inversions

Data	Determinate Variables
P_n, P_g, $P_{teleseismic}$	x,y,h,T,a_{P_n}, b_{P_n}, a_{P_g}, b_{P_g}
P_n, $P_{teleseismic}$	x,y,h,T,a_{P_n}, b_{P_n}
P_g, $P_{teleseismic}$	x,y,h,T,a_{P_g}, b_{P_g}
$P_{teleseismic}$	inapplicable
P_n, P_g	x,y,T,a_{P_n}, b_{P_n}, a_{P_g}, b_{P_g} h (by approximation)
P_n	x,y,b_{P_n}, $(T + a_{P_n})$ T (by approximation if depth is restrained)
P_g	x,y,b_{P_g}, $(T + a_{P_g})$ T (by approximation if depth is restrained)

For events with epicenters close to each other and at the same depth, the coefficients a_{P_g} , b_{P_g} , a_{P_n} , b_{P_n} should be nearly constant from event to event. The accuracy of the determination of these coefficients, and hence of the event location, may therefore be improved by inverting the arrival-time measurements from several nearby events simultaneously, a process known as joint epicenter determination (JED). Applying JED to data from N events has the effect of transforming N systems of equations in 8N unknowns to a single system (with the same total number of equations) in 4N + 4 unknowns. Extension of conventional location to encompass JED is a straightforward technique described by Douglas (1967) and by Ahner, Blandford and Shumway (1971). We shall examine whether this same extension can be performed for the method of simultaneous inversions.

4.2 Results

In order to implement the method, the standard location program LOCATION was rewritten to solve for eight, rather than four, unknowns. The revised program was tested using the same data set as was used for testing the method of successive determinations. (There were a few small changes from the data used in the previous section of this report.) Table VIII presents the results of eight trials which should be examined in comparing the two methods. The first trial represents the "correct" results, namely the travel-time curves which are constructed as least-squares fits using the known hypocenter and origin time, as shown in Figure 4. Next are presented the results of applying the method of successive determinations for P_n data only and for combined P_n and P_g data. These two trials are then repeated with the depth restrained to the surface. The simultaneous inversions results, which follow, ought to be compared with those obtained by the successive determinations techniques run in both the depth-free and depth-restrained modes. The reason for this ambiguity is that even though the method of simultaneous inversions was run in the depth-restrained mode (since no teleseismic data were used), the depth does nevertheless vary indirectly through the coefficients a_{P_n} and a_{P_g}, hence the results are perhaps more nearly analogous with those obtained for the depth-free mode of the other technique.

It was not possible in every case to run the successive determinations program successfully in the depth-free mode. The depth would frequently turn out to be negative, in which case it would be restrained to the surface; no results are given for these cases, since they are identical to those which are produced by the running of the program in the depth-restrained mode directly. Some other cases resulted in negative depths which were restrained to the surface at the end of the first iteration, but they yielded positive depths when the improved travel-time curves were applied to them in the second iteration. These once-restrained cases are denoted by parentheses placed around the value of the absolute error.

There are many gaps in the values given in Table VIII for the method of simultaneous inversions which reflect the indeterminations listed in Table VII. As has been discussed previously, the indetermination of the depth can be removed by approximation if one assumes an earth model such as is shown in Figures 6 and 7. We have assumed the following parameters for such a model:

Theoretical Travel Time for P_n in a Simple Earth Model

(1) Hypocenter in Upper Crustal Layer

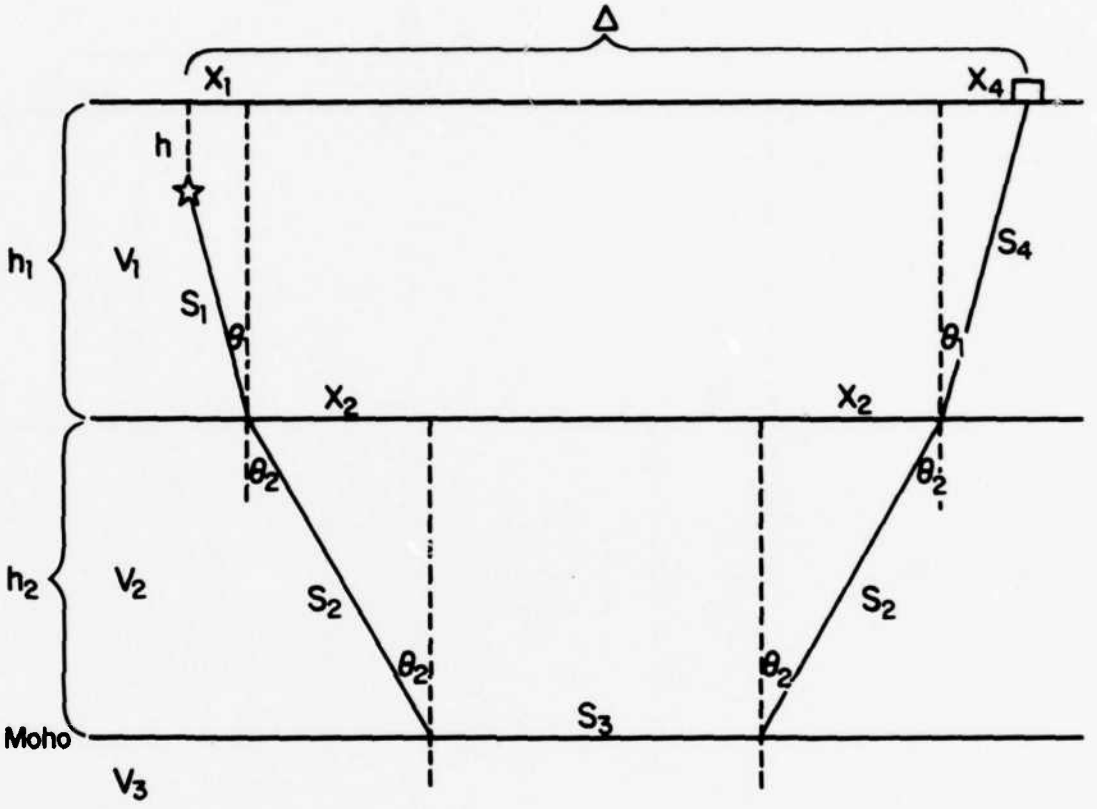

$X_1 = (h_1 - h)\tan\theta_1$ $\qquad$ $S_1 = X_1/\sin\theta_1$

$X_2 = h_2 \tan\theta_2$ $\qquad$ $S_2 = X_2/\sin\theta_2$

$X_4 = h_1 \tan\theta_1$ $\qquad$ $S_4 = X_4/\sin\theta_1$

$S_3 = \Delta - X_1 - 2X_2 - X_4$

$$t_{Pn} = S_1/V_1 + 2S_2/V_2 + S_3/V_3 + S_4/V_1$$
$$= (2h_1 - h)/V_1\cos\theta_1 + 2h_2/V_2\cos\theta_2 + \left[\Delta - (2h_1 - h)\tan\theta_1 - 2h_2\tan\theta_2\right]/V_3$$

Figure 7a Raypath for P_n.

Theoretical Travel Time for P_n in a Simple Earth Model
(2) Hypocenter in Lower Crustal Layer

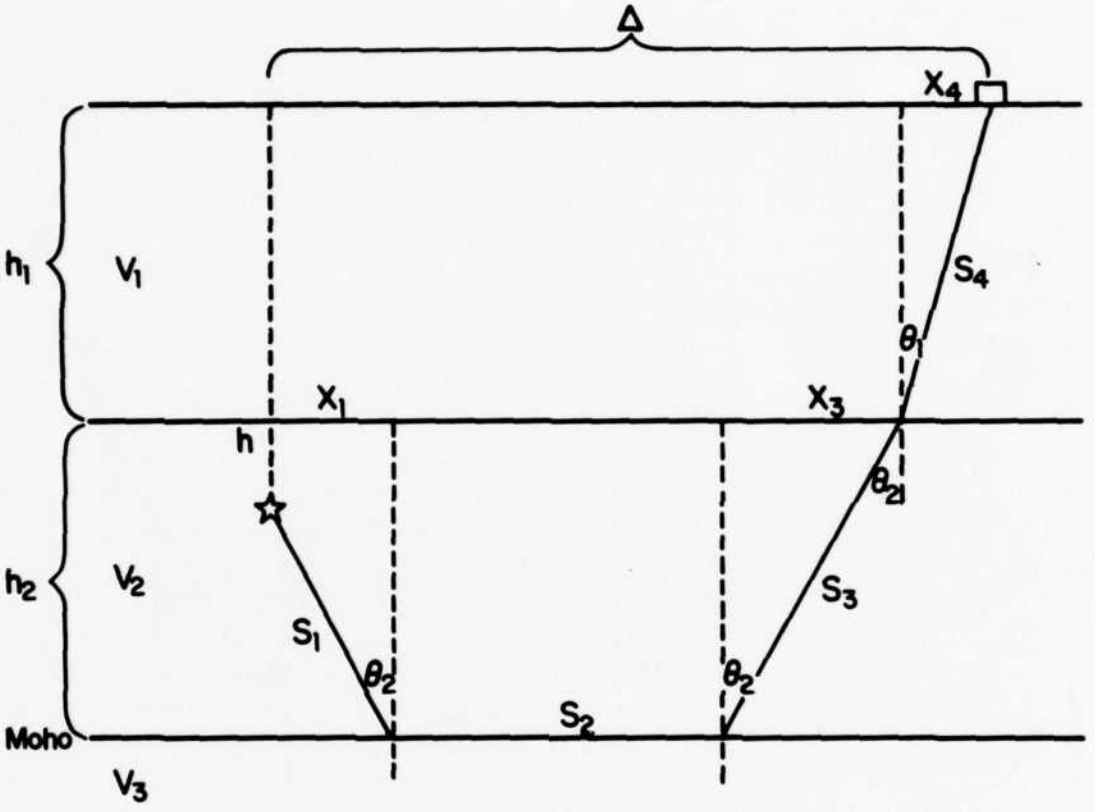

$$X_1 = (h_1+h_2-h)\tan\theta_2 \qquad S_1 = X_1/\sin\theta_2$$
$$X_3 = h_2\tan\theta_2 \qquad S_3 = X_3/\sin\theta_2$$
$$X_4 = h_1\tan\theta_1 \qquad S_4 = X_4/\sin\theta_1$$
$$S_2 = \Delta - X_1 - X_3 - X_4$$

$$t_{Pn} = S_1/V_2 + S_2/V_3 + S_3/V_2 + S_4/V_1$$
$$= (h_1+2h_2-h)/V_2\cos\theta_2 + \left[\Delta-(h_1+2h_2-h)\tan\theta_2 - h_1\tan\theta_1\right]/V_3 + h_1/V_1\cos\theta_1$$

Figure 7b Raypath for P_n.

TABLE VIII

Comparison of Method of Simultaneous Inversions
with Method of Successive Determinations

Trial 1: least-squares fit of travel times from the known epicenter
Trial 2: successive determinations, P_n data only; depth free
Trial 3: successive determinations; P_n and P_g data; depth free
Trial 4: successive determinations; P_n data only; depth restrained
Trial 5: successive determinations; P_n and P_g data; depth restrained
Trial 6: simultaneous inversions; P_n data only
Trial 7: simultaneous inversion; P_n and P_g data
Trial 8: simultaneous inversion; P_n and P_g data; joint epicenter determination

Event	Trial #	Lat(N)	Long(W)	Depth (km)	Absolute O. T. Error	(km)	V_{P_g} (km/sec)	V_{P_n} (km/sec)	χ^2	Degrees of Freedom
FAULTLESS	1	38.634	11.216		18:15:00.1		5.882	7.719	0.64, 1.61	3,3
	2	.524	.378	7.8	:02.0	18.64		8.089	1.72	1
	3	.625	.260	3,6	:01.1	(3.95)	5.967	7.922	1.26	6
	4	.524	.378		:01.7	18.64		8.088	1.72	2
	5	.628	.262		:00.9	4.05	5.967	7.922	1.30	7
	6	.433	.217			22.35		7.640	1.26	4
	7	.468	.212	-4.2	:59.8	18.46	5.834	7.648	1.26	4
	8	.471	.247		:01.6	18.31				
RULISON	1	39.406	107.949		21:00:00.1		6.111	8.192	2.67, 14.06	5,8
	2	[depth restrained]								
	3	[depth restrained]								
	4	.421	.937		:01.2	2.65		8.161	1.91	7
	5	.398	.987		:02.7	3.38	6.169	8.292	8.62	14
	6	.420	.939			1.78		8.177	13.63	6
	7	.412	.915	-7.8	:00.3	0.69	6.111	8.184	16.44	11
	8	[too far]								
PASSAIC	1	37.120	116.040		18:00:00.2		6.536	7.812	0.04, 0.16	1,2
	2	.120	.070	0.9	:59.7	(2.66)		7.910	0.00	0
	3	[depth restrained]								
	4	.120	.070		:59.6	2.66		7.909	0.00	1
	5	.122	.064		:59.6	2.14	restr.	7.881	1.04	4
	6	.120	.070			2.66		7.907	0.00	0
	7	.120	.071	17.6	:06.0	2.75	6.630	7.909	0.00	1
	8	.133	.039		:00.7	1.45				
ROCKVILLE DAM	1	39.360	106.460		16:21:33.6		5.900	8.213	6.27, 6.80	6,7
	2	[depth restrained]								
	3	.361	.436	12.9	:37.5	(2.07)	6.129	8.139	16.15	13
	4	[depth restrained]								
	5a	.345	.421		:35.5	1.90	5.813	8.127	19.25	14
	5b	.316	.426		:35.5	1.90	5.884	8.136	7.99	14
	6	.372	.440			2.59		7.800	2.81	5
	7	.336	.419	-31.9	:27.9	4.42	5.808	8.102	8.86	11
	8	[too far]								

TABLE VIII (con't)

Event	Trial #	Lat(N)	Long(W)	Depth (km)	Absolute O. T.	Error (km)	V_{P_g} (km/sec)	V_{P_n} (km/sec)	χ^2	Degrees of Freedom
DORMOUSE'	1	37.040	116.020		18:00:00.1		6.234	7.829	0.39, 0.04	2,1
	2	[fails to converge]								
	3	.116	.974	4.3	:00.8	(9.39)	6.134	7.969	0.18	3
	4	[fails to converge]								
	5	.126	.966		:00.5	10.70	6.119	7.985	0.19	4
	6	[insufficient data]								
	7	.111	.993	-6.7	:00.4	8.25	6.159	7.995	0.24	1
	8	.077	.994		:00.8	4.72				
KLICKITAT	1	37.151	116.040		15:30:00.1		6.091	7.762	1.26, 14.88	10,11
	2	[fails to converge]								
	3	.158	.074	8.1	:00.8	(3.11)	6.108	7.935	6.22	21
	4	.152	.089		:59.6	4.34		7.916	3.31	10
	5	.158	.089		:00.2	4.41	6.112	7.891	8.01	22
	6	.146	.031			0.97		7.900	15.24	9
	7	.148	.034	2.5	:00.9	0.63	6.088	7.759	16.55	19
	8	.149	.027		:00.2	1.18				
BANDICOOT	1	37.040	116.020		18:00:00.0		5.763	8.101	0.17, 0.38	2,3
	2	.077	.012	0.0	:00.3	4.18		8.205	0.25	1
	3	[depth restrained]								
	4	.077	.012		:00.3	4.18		8.205	0.25	2
	5	.079	.014		:00.5	4.37	6.115	8.217	2.40	6
	6	.140	.013			11.14		7.900	0.03	1
	7	.118	.021	-18.9	:58.9	8.67	5.983	8.453	0.32	3
	8	.995	.012		:00.1	5.05				
SHOAL	1	39.200	118.380		17:00:00.1		no data	7.831	12.02	10
	2	[fails to converge]								
	3	[no P_g data]								
	4	.194	.406		:59.2	2.34		7.893	2.92	3
	5	[no P_g data]								
	6	.187	.394			1.88		7.835	12.02	8
	7	[no P_g data]								
	8	[too far]								
MERRIMAC	1	37.055	116.033		16:00:00.1		no data	7.689	2.62	6
	2	[depth restrained]								
	3	[no P_g data]								
	4	.013	.058		:58.6	5.17		7.731	1.10	5
	5	[no P_g data]								
	6	.013	.058			5.17		7.731	1.44	5
	7	[no P_g data]								
	8	.012	.059		:58.3	5.31				
GASBUGGY	1	36.678	107.308		19:30:00.1		6.166	8.260	4.90, 13.88	10,10
	2	.635	.203	-0.1	:02.3	10.51		8.203	2.71	8
	3	[depth restrained]								
	4	.635	.203		:02.3	10.51		8.203	2.71	9
	5	.644	.204		:02.0	10.02	5.940	8.198	17.73	21
	6	.634	.203			10.56		8.208	2.07	8
	7	.633	.210	-5.5	:01.9	10.07	6.142	8.214	5.78	18
	8	[too far]								

TABLE VIII (con't)

Event	Trial #	Lat(N)	Long(W)	Depth (km)	O. T.	Absolute Error (km)	V_{P_g} (km/sec)	V_{P_n} (km/sec)	χ^2	Degrees of Freedom
PILEDRIVER	1	37.227	116.056		15:30:00.1		6.128	7.729	0.29, 1.11	3,3
	2	[fails to converge]								
	3	.223	.076	8.9	:00.1	(1.83)	6.095	7.740	0.67	6
	4	.153	.128		:59.0	10.41		7.823	0.22	2
	5	.217	.082		:59.3	2.56	6.095	7.740	1.02	7
	6	.165	.118			8.81		7.789	0.46	1
	7	.190	.100	0.9	:00.6	5.67	6.158	7.764	1.01	4
	8	.179	.090		:00.3	6.13				
ROANOKE	1	37.123	116.051		15:00:00.2		5.788	7.494	0.44, 0.29	2,2
	2	.160	.033	2.5	:59.2	(4.41)		7.576	0.02	0
	3	[drops P_g on account of depth]								
	4	.160	.034		:58.9	4.38		7.576	0.02	0
	5	.156	.027		:59.0	4.24	5.893	7.557	3.48	5
	6	.156	.033			4.00		7.539	0.00	0
	7	.153	.024	0.9	:59.9	4.11	5.814	7.529	0.18	2
	8	.186	.020		:01.0	7.52				
SALMON	1	31.142	89.570		16:00:00.0		no data	8.263	1.61	3
	2	[fails to converge]								
	3	[no P_g data]								
	4	.426	.671		:01.1	33.00		8.138	0.31	2
	5	[no P_g data]								
	6	30.211	.246			107.75		8.290	0.18	1
	7	[no P_g data]								
	8	[too far]								
GNOME	1	32.263	103.865		19:00:00.0		1 data pt	7.920	20.80	16
	2	[depth restrained]								
	3	[depth restrained]								
	4	.239	.795		:00.3	7.10		7.983	5.81	15
	5	.238	.796		:00.3	7.06	restr.	7.988	5.90	16
	6	.238	.795			7.15		7.993	9.02	14
	7	.238	.795	-0.4	:00.5	7.15	6.095	7.993	9.02	13
	8	[too far]								

h_1 = 20.0 km
h_2 = 10.0 km
V_1 = 6.20 km/sec
V_2 = 7.00 km/sec
V_3 = 7.90 km/sec.

Some idea of the validity of this model and hence, of the depth approximation, may be gained by comparing V_1 with the value listed for the velocity of P_g, $V_{P_g} = 1/b_{P_g}$, and by comparing V_3 with $V_{P_n} = 1/b_{P_n}$.

The absolute errors shown in Table VIII are summarized in Table IX. It is apparent that the addition to the data base of P_g arrival times frequently improves the location relative to that which would be determined using P_n data alone, and it seldom worsens it. This improvement holds for both the method of successive determinations and the method of simultaneous inversions, and it represents an important departure from the results obtained by conventional location techniques (Herrin and Taggart, 1962; McCowan and Needham, 1978; Chang and Racine, 1979). A comparison of the results obtained by the method of successive determinations and by the method of simultaneous inversions shows that even though one or the other of the two methods yields a better location for particular events, on the whole the results are about the same. A notable exception is SALMON, for which the method of successive approximations yielded a poor result and the method of simultaneous inversions failed. This failure is due to the fact that the least-squares solution had only one degree of freedom (cf. Table VIII). The fact that there are discrepancies between the two methods suggests that in practice perhaps both techniques should be used in the location of unknown events; subjective judgment would then be necessary to select one of the two resulting epicenters as "the" location.

Tables VIII and IX also show the results of applying JED to those eight NTS events for which the composite travel-time curves are shown in Figure 4o. As one might expect for a technique such as this which effectively performs an average over events, in some cases the location was improved but in other cases it was worsened. The net effect seems to be small. No depths are approximated for the trial using JED since this technique assumes the a_{P_n} and a_{P_g} are the same for all events and hence that each event is at the same depth. The slopes of the calculated travel-time curves imply that V_{P_g} = 6.021 km/sec and V_{P_n} = 7.736 km/sec, values which are to be compared with those given by the least-squares fit (Appendix I) of V_{P_g} = 6.036 km/sec and V_{P_n} = 7.745 km/sec.

TABLE IX

Absolute errors (km) resulting from the application of two location techniques to a common data set.

Successive Determinations

Event	# P_n	# P_g	P_n only Depth Free	P_n and P_g Depth Free	P_n only Depth Restrained	P_n and P_g Depth Restrained
FAULTLESS	5	5	18.64	(3.95)	18.64	4.05
RULISON	10	7	restr.	restr.	2.65	3.38
PASSAIC	4	3	(2.66)	restr.	2.66	2.14
ROCKVILLE DAM	9	8	restr.	restr.	2.04	a 3.75 b 5.00 *
DORMOUSE'	3	4	diverges	(9.39)	diverges	10.70
KLICKITAT	13	12	diverges	(3.11)	4.34	4.11
BANDICOOT	5	4	4.18	restr.	4.18	4.37
SHOAL	12	0	diverges	no P_g	2.34	no P_g
MERRIMAC	8	0	restr.	no P_g	5.17	no P_g
GASBUGGY	12	12	10.51	restr.	10.51	10.02
PILEDRIVER	5	5	diverges	(1.83)	10.41	2.56
ROANOKE	4	4	(4.41)	ignores P_g	4.38	4.24
SALMON	5	0	diverges	no P_g	33.00	no P_g
GNOME	18	1	restr.	restr.	7.10	7.06

Simultaneous Inversion

Event	P_n only	P_n and P_g	J.E.D.
FAULTLESS	22.35	18.46	18.31
RULISON	1.78	0.69	
PASSAIC	2.66	2.75	1.45
ROCKVILLE DAM	2.59	4.42	
DORMOUSE'	insuf. P_n	8.25	4.72
KLICKITAT	0.97	0.63	1.18
BANDICOOT	11.14	8.67	5.05
SHOAL	1.88	no P_g	
MERRIMAC	5.17	no P_g	5.31
GASBUGGY	10.56	10.07	
PILEDRIVER	8.81	5.67	6.13
ROANOKE	4.00	4.11	7.52
SALMON	107.75	no P_g	
GNOME	7.15	7.15	

* Solution alternates between two epicenters.

In all versions of the program LOCATION, arrival time residuals for each seismic phase are weighted by the reciprocals of the standard deviations which are anticipated for residuals of that phase. We have heretofore applied weights of $W_{P_n} = 1/\sigma_{P_n} = 1.0$ and $W_{P_g} = 1/3.0$. Table X presents the results of changing these weighting factors in the method of simultaneous inversions. In accordance with the observed scatter of data points about the least-squares lines in Figure 4o, we have tried alternate values of $W_{P_n} = 1/\sigma_{P_n} = 1/0.84$ and $W_{P_g} = 1/1.58$. It is not the values of these weights but rather their ratio which affects the location, so we anticipate that the locations which will be subject to the most change by these new weighting factors will be those which utilize the most values of P_g relative to the number of P_n values. Table X shows that only in the case of PILEDRIVER does the change in weights significantly improve the location, and in the case of ROCKVILLE DAM, which was not one of the eight NTS events used to determine the new standard deviations, the new location is significantly worse. The value of JED appears to be enhanced if the new weighting scheme is applied; this improvement is illusory, however, since in fact the locations failed to converge in this case. The values which are shown for the absolute errors are thus unstable, and hence they are sensitive to the locations chosen as a first approximation.

TABLE X

Absolute errors (km) resulting from assigning more weight to P_n data in the method of simultaneous inversions

Event	No. P_n	No. P_g	$\sigma_{P_n} = 1.0$ $\sigma_{P_g} = 3.0$ P_n and P_g	$\sigma_{P_n} = 0.84$ $\sigma_{P_g} = 1.58$ P_n and P_g	$\sigma_{P_n} = 1.0$ $\sigma_{P_g} = 3.0$ J.E.D.	$\sigma_{P_n} = 0.84$ $\sigma_{P_g} = 1.58$ J.E.D.[2]
FAULTLESS	5	5	18.46	21.05[1]	18.31	13.35
RULISON	10	7	0.69	0.83		
PASSAIC	4	3	2.75	2.84	1.45	2.61
ROCKVILLE DAM	9	8	4.42	8.63		
DORMOUSE'	3	4	8.25	9.21	4.72	7.41
KLICKITAT	13	12	0.63	0.32	1.18	1.00
BANDICOOT	5	4	8.67	6.05	5.05	4.25
MERRIMAC	8	0			5.31	3.78
GASBUGGY	12	12	10.07	9.66		
PILEDRIVER	5	5	5.67	2.48	6.13	1.03
ROANOKE	4	4	4.11	4.30	7.52	5.94
GNOME	18	1	7.15	7.15		

[1] 2 P_g data points deleted

[2] failed to converge; values represent the minimum found for χ^2

4.3 Error Ellipses

Thus far we have discussed only the absolute error resulting from applying the method of simultaneous inversions to fourteen events whose hypocenters and origin times were known *a priori*. We now address the question which would be encountered in the location of unknown events, namely the *a posteriori* estimation of the location error using only the observed data. In the case of conventional location determination used fixed travel-time relations, the procedure for this error estimation is well known (Flinn, 1965). Abbreviating the system of equations upon which the location algorithm is based as

$$\vec{\delta}_t = \underset{\sim}{B}\,(\vec{x} - \vec{x}_0), \tag{29}$$

where $\vec{\delta}_t$ is the vector of arrival time residuals, $\vec{x}$ is the unknown location, and $\vec{x}_0$ is the trial location, the standard error of the i^{th} component of $\vec{x}$ is given by

$$S_i = [(\underset{\sim}{B}^T\,\underset{\sim}{B})^{-1}]^{1/2}_{ii} \tag{30}$$

and the "error ellipsoid" surrounding the computed hypocenter $\hat{\vec{x}}$ is given by

$$(\vec{x} - \hat{\vec{x}})^T\,\underset{\sim}{E}^{-1}(\vec{x} - \hat{\vec{x}}) \leq N\,\hat{\sigma}_0^2\,F_{N,N-4:0.05} \tag{31}$$

where N is the number of dimensions of $\vec{x}$, where $\underset{\sim}{E}$ is an NxN submatrix of $(\underset{\sim}{B}^T\,\underset{\sim}{B})^{-1}$, and where $\hat{\sigma}_0^2$ is the weighted variance of the final residuals. We see that the method of simultaneous inversions presents no new difficulties for the error estimation, since it can operate in eight dimensions as well as in four. In Table XI we present the standard errors corresponding to the absolute location errors already presented. On account of the previously discussed indetermination of the origin time, δa_{P_g} is understood to mean the standard error of $(T + a_{P_g})$, and similarly for δa_{P_n}. The standard errors in the slopes of the travel-time curves b_{P_g} and b_{P_n} have been used to compute the errors in their reciprocals, the velocities V_{P_g} and V_{P_n}. By setting the number of dimensions N equal to 2, we may calculate the error ellipses surrounding the computed epicenters; Figures 8a-n show these ellipses along with the actual epicenters.

For those events for which the degrees of freedom (= number of arrival times - number of parameters solved for by inversion) are small, the error ellipses are unrealistically large. This situation can be alleviated by using χ^2, rather than F, statistics in the computation (Evernden, 1969).

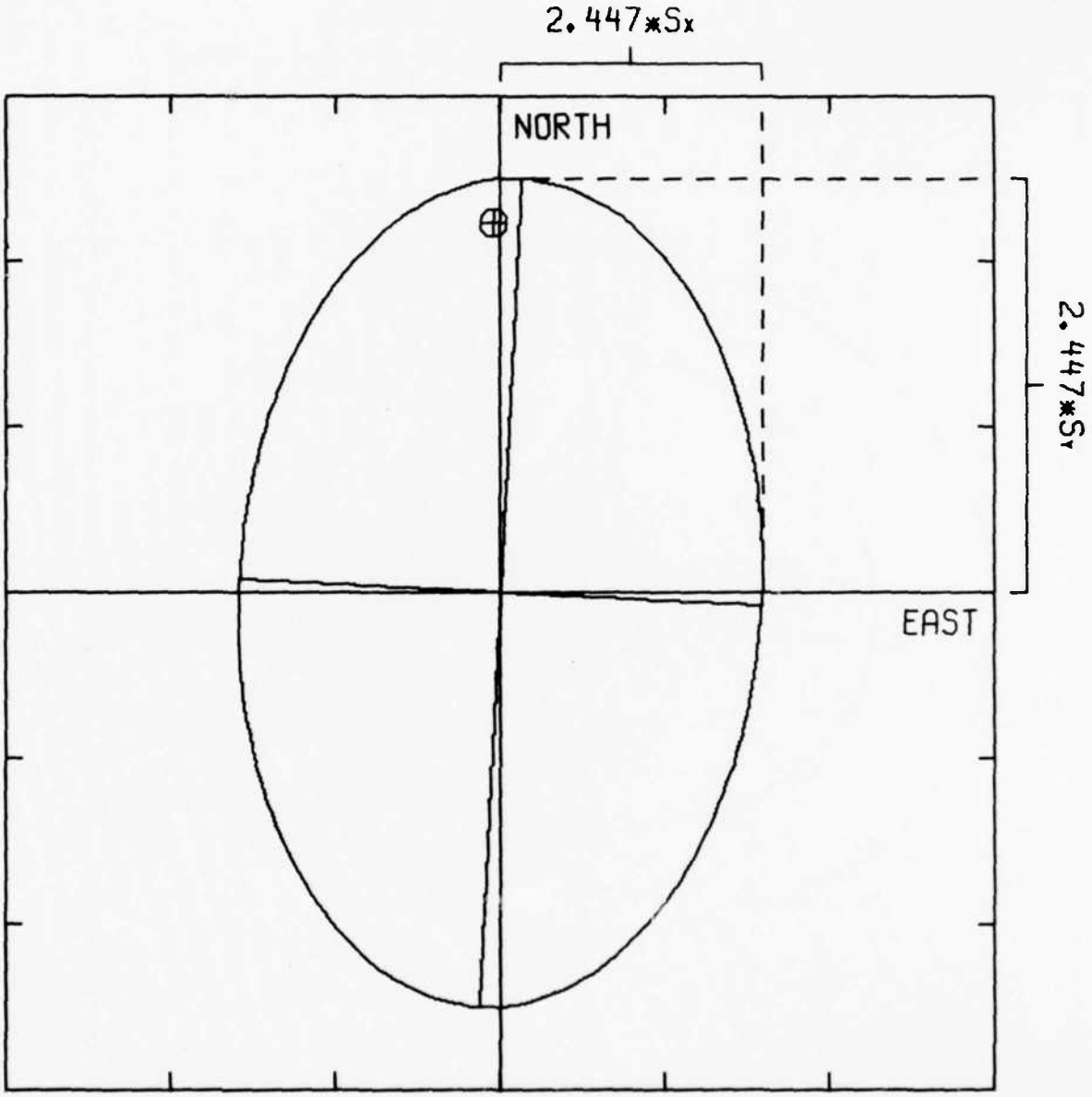

Sx : STANDARD ERROR (EAST)
Sy : STANDARD ERROR (NORTH)

⊕ TRUE EPICENTER
8.254 KM

ELLIPSE IS FOR CHI-SQUARED STATISTIC

Figure 8a - Error Elipses for FAULTLESS

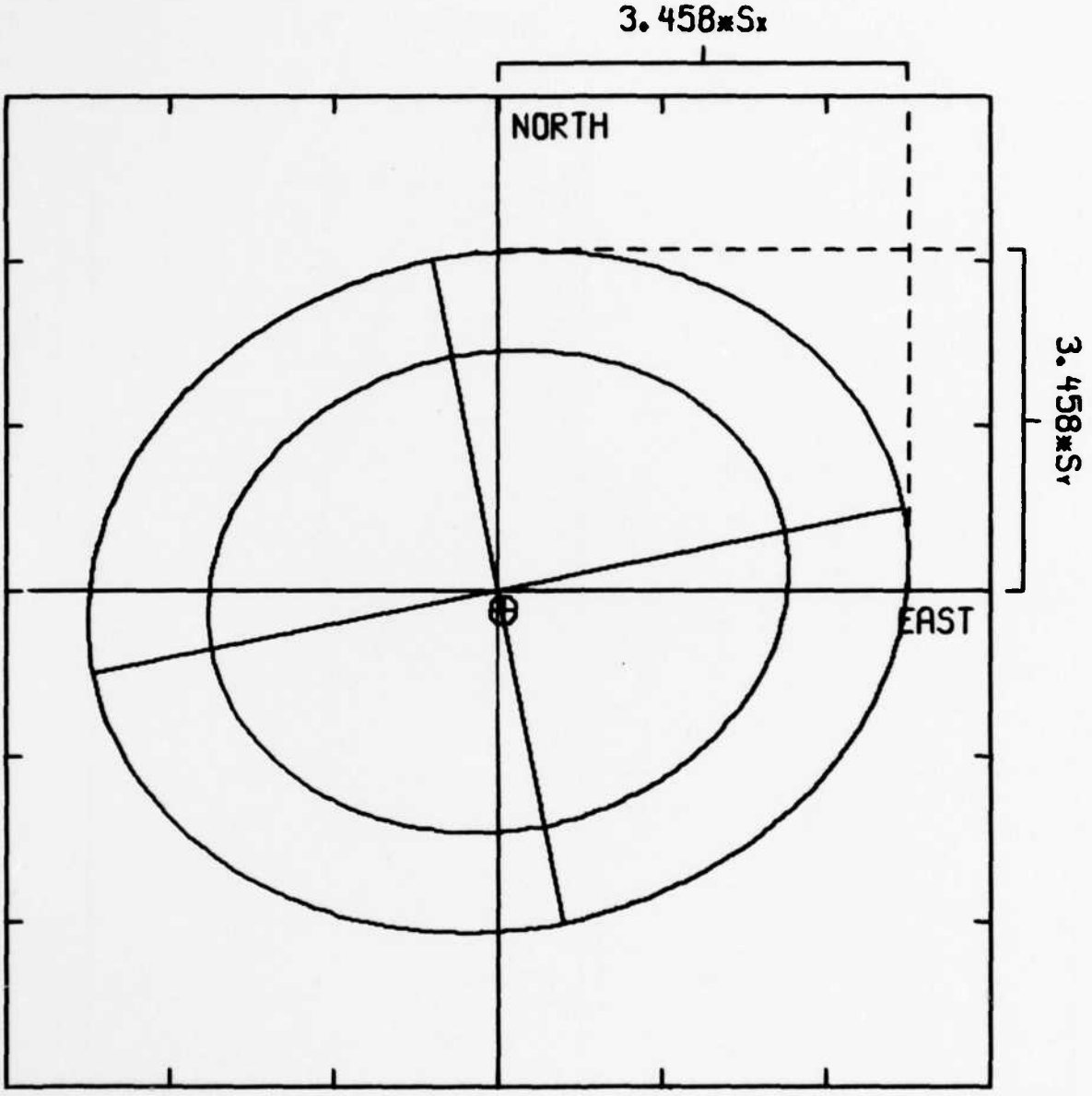

Sx : STANDARD ERROR (EAST)
Sy : STANDARD ERROR (NORTH)

⊕ TRUE EPICENTER
5.729 KM

OUTER ELLIPSE : F-STATISTIC
INNER ELLIPSE : CHI-SQUARED STATISTIC

Figure 8b - Error Ellipses for RULISON

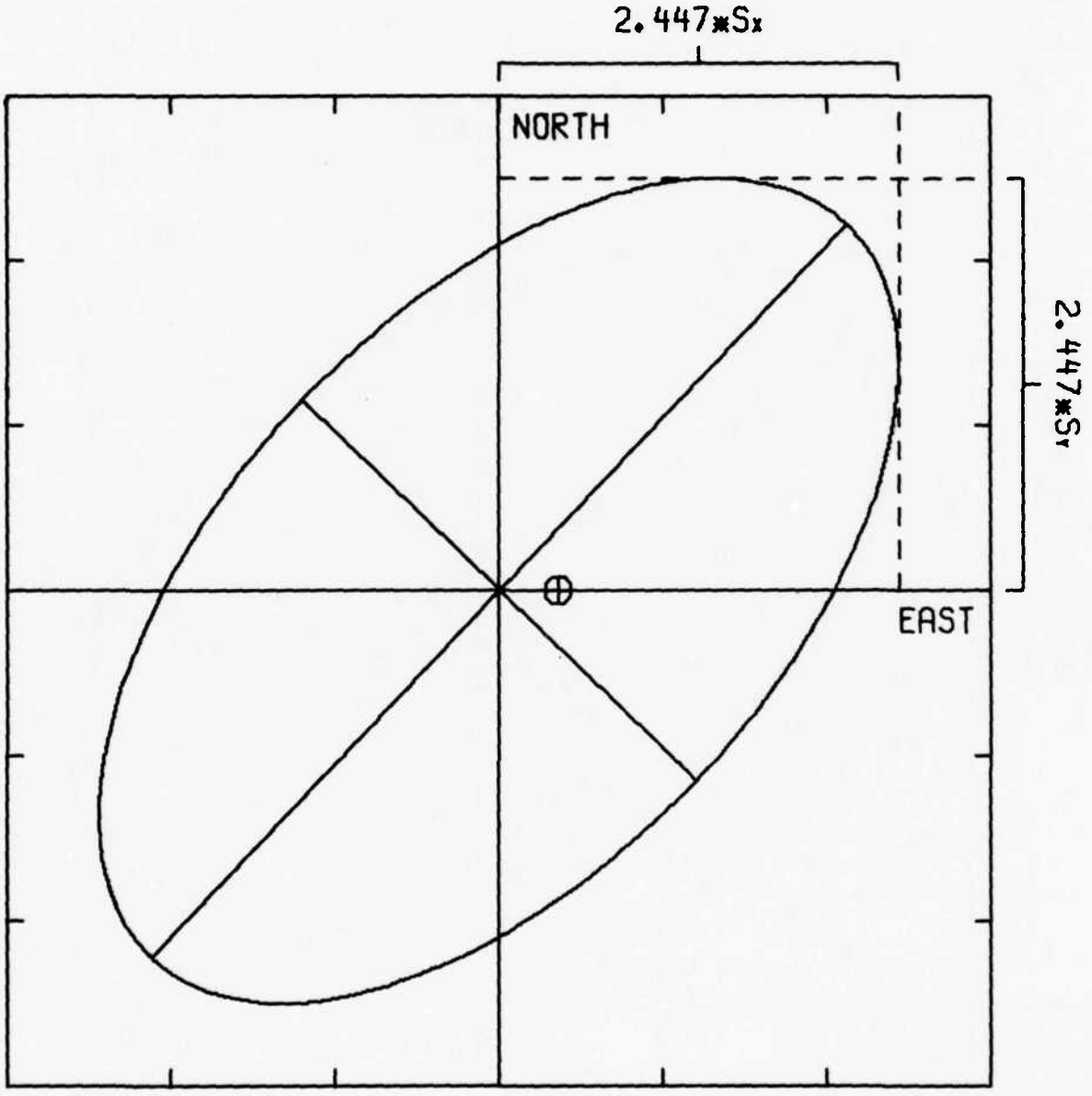

Sx : STANDARD ERROR (EAST)
Sy : STANDARD ERROR (NORTH)

⊕ TRUE EPICENTER
7.713 KM

ELLIPSE IS FOR CHI-SQUARED STATISTIC

Figure 8c - Error Ellipses for PASSAIC

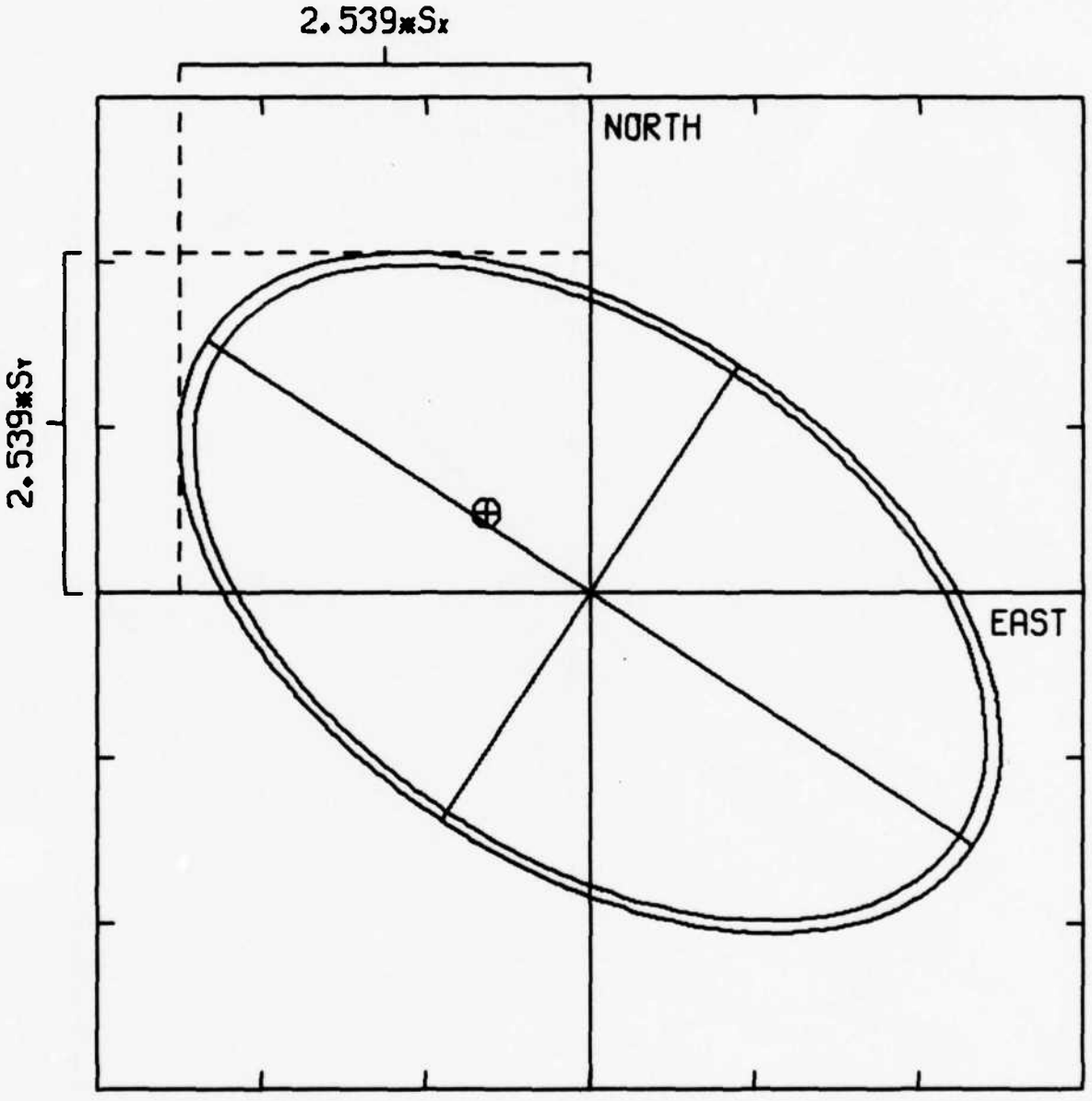

Sx : STANDARD ERROR (EAST)
Sy : STANDARD ERROR (NORTH)

⊕ TRUE EPICENTER
5.603 KM

OUTER ELLIPSE : F-STATISTIC
INNER ELLIPSE : CHI-SQUARED STATISTIC

Figure 8d - Error Ellipses for ROCKVILLE DAM

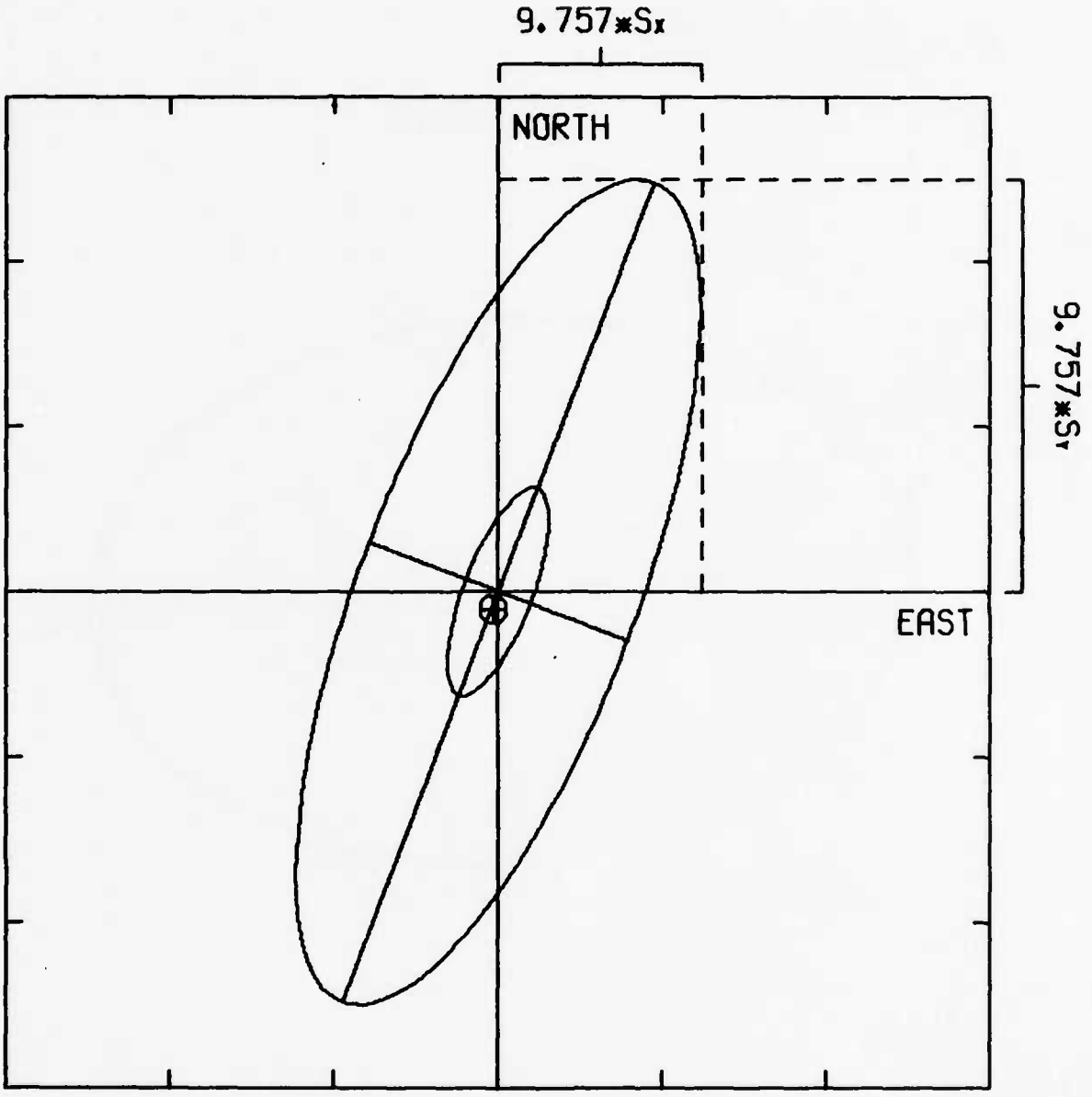

Sx : STANDARD ERROR (EAST)
Sy : STANDARD ERROR (NORTH)

⊕ TRUE EPICENTER
⊢——⊣ 69.665 KM

OUTER ELLIPSE : F-STATISTIC
INNER ELLIPSE : CHI-SQUARED STATISTIC

Figure 8e - Error Ellipses for DORMOUSE'

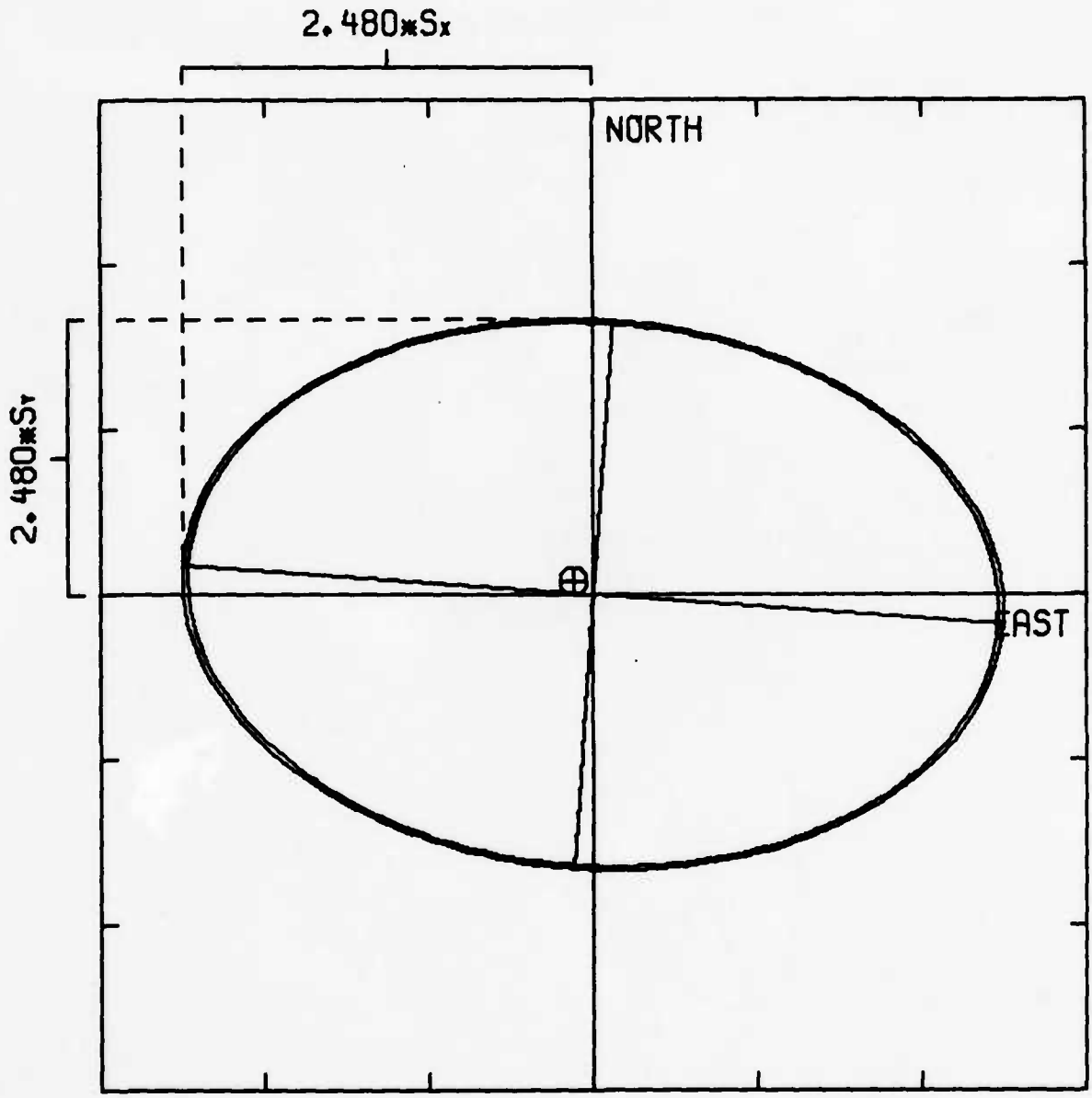

Sx : STANDARD ERROR (EAST)
Sy : STANDARD ERROR (NORTH)

⊕ TRUE EPICENTER
4.299 KM

OUTER ELLIPSE : F-STATISTIC
INNER ELLIPSE : CHI-SQUARED STATISTIC

Figure 8f - Error Ellipses for KLICKITAT

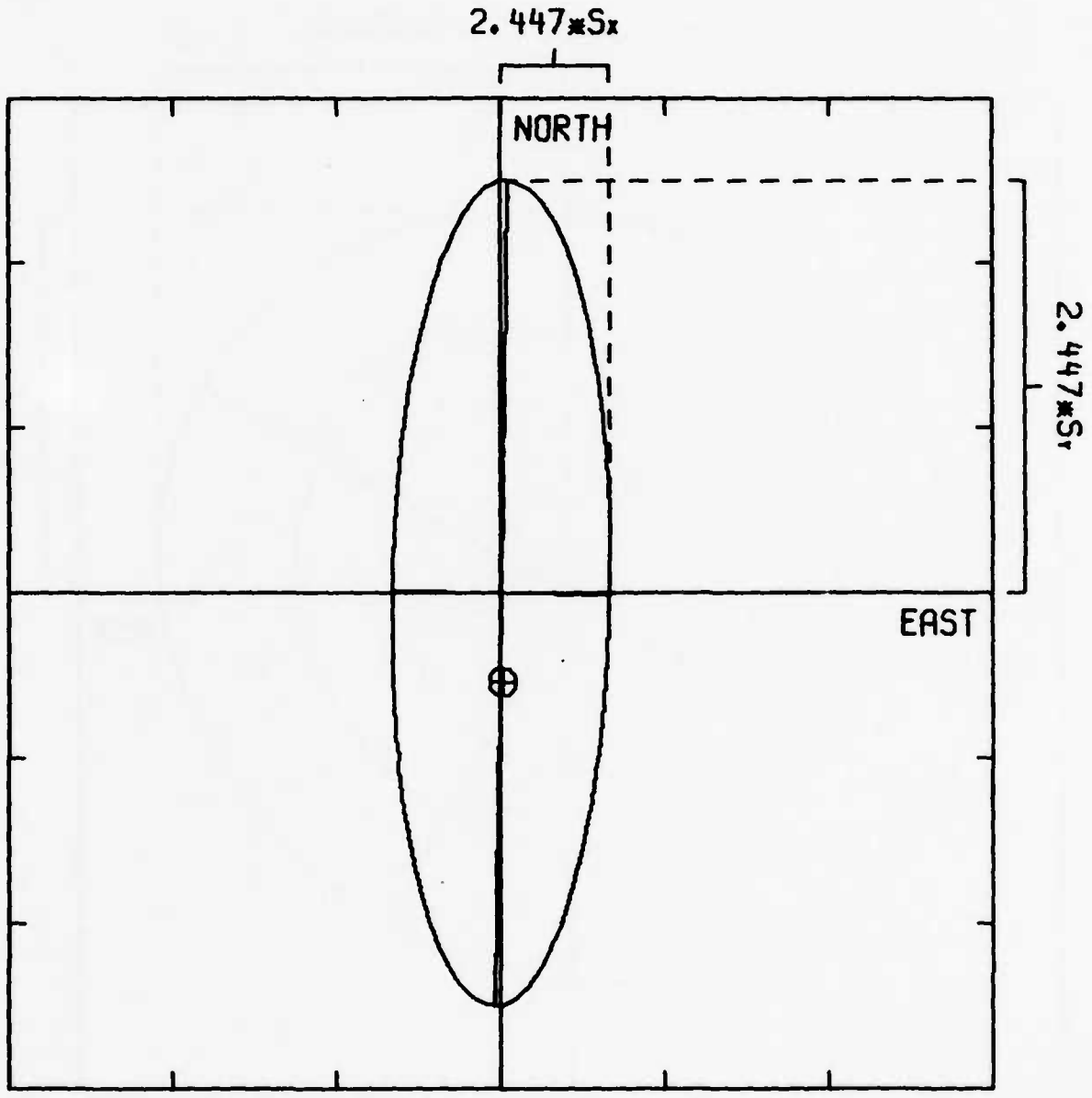

Sx : STANDARD ERROR (EAST)
Sr : STANDARD ERROR (NORTH)

⊕ TRUE EPICENTER
16.151 KM

ELLIPSE IS FOR CHI-SQUARED STATISTIC

Figure 8g - Error Ellipses for BANDICOOT

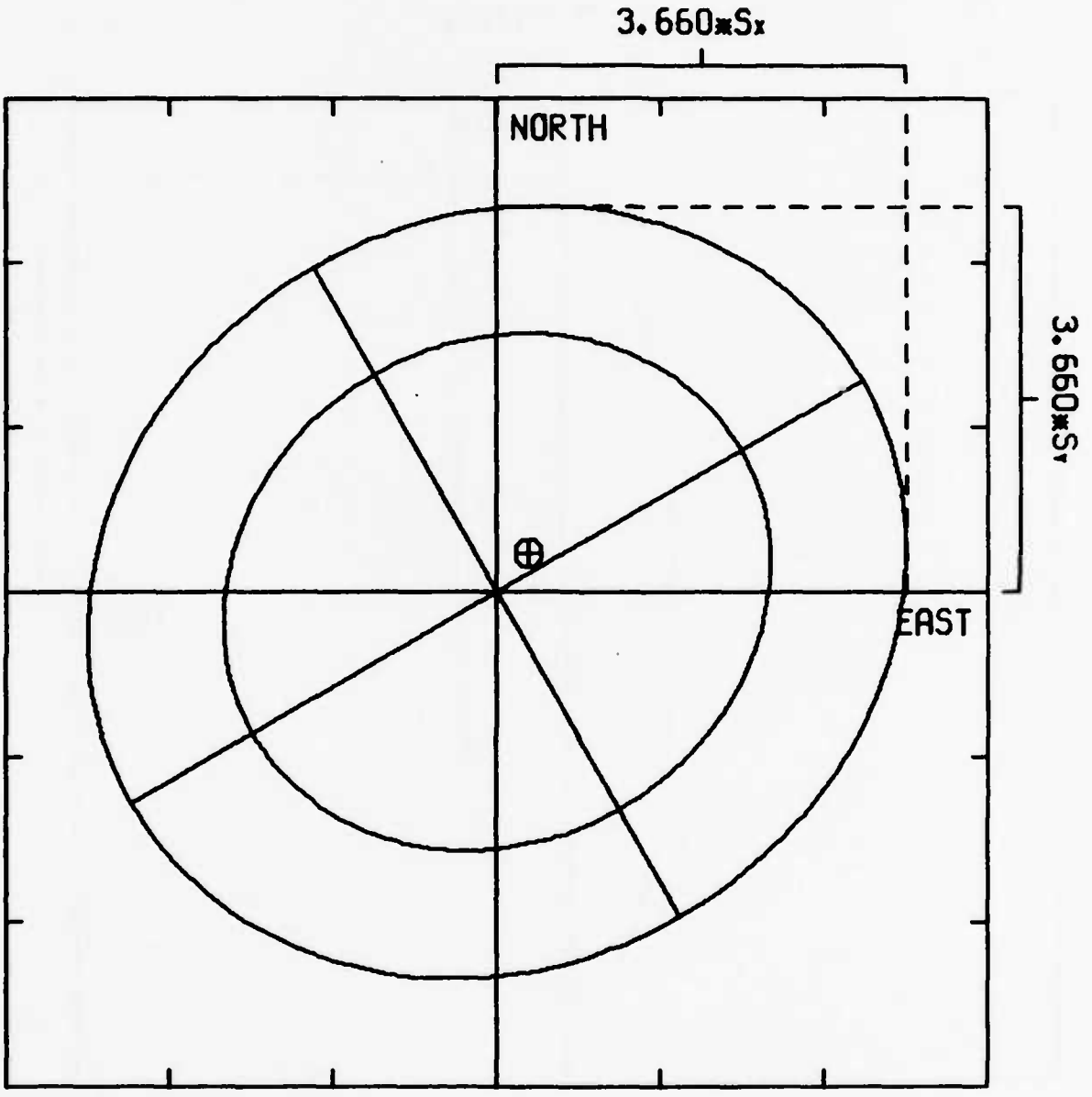

Sx : STANDARD ERROR (EAST)
Sy : STANDARD ERROR (NORTH)

⊕ TRUE EPICENTER
6.309 KM

OUTER ELLIPSE : F-STATISTIC
INNER ELLIPSE : CHI-SQUARED STATISTIC

Figure 8h - Error Ellipses for SHOAL

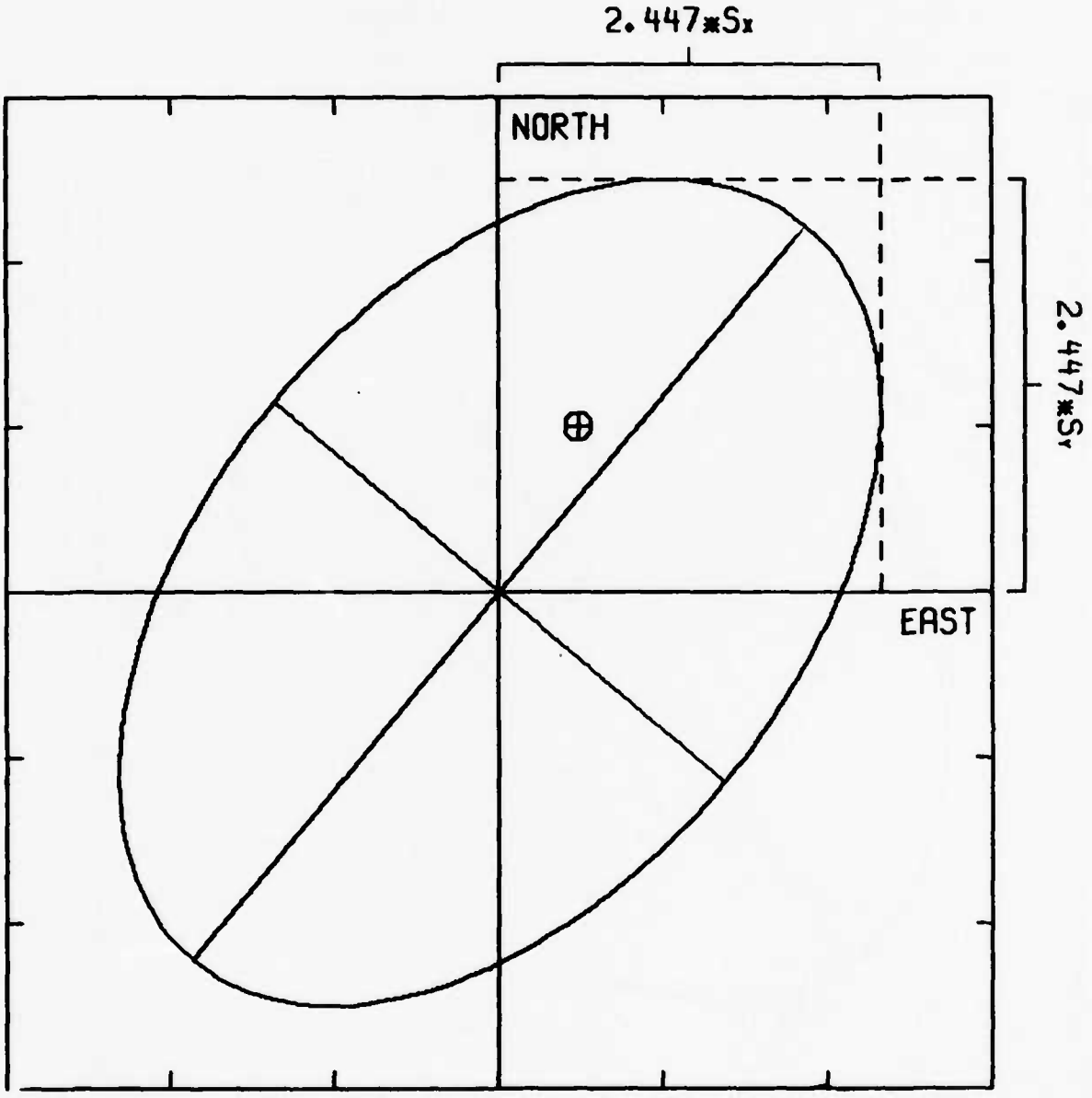

Figure 8i - Error Ellipses for MERRIMAC

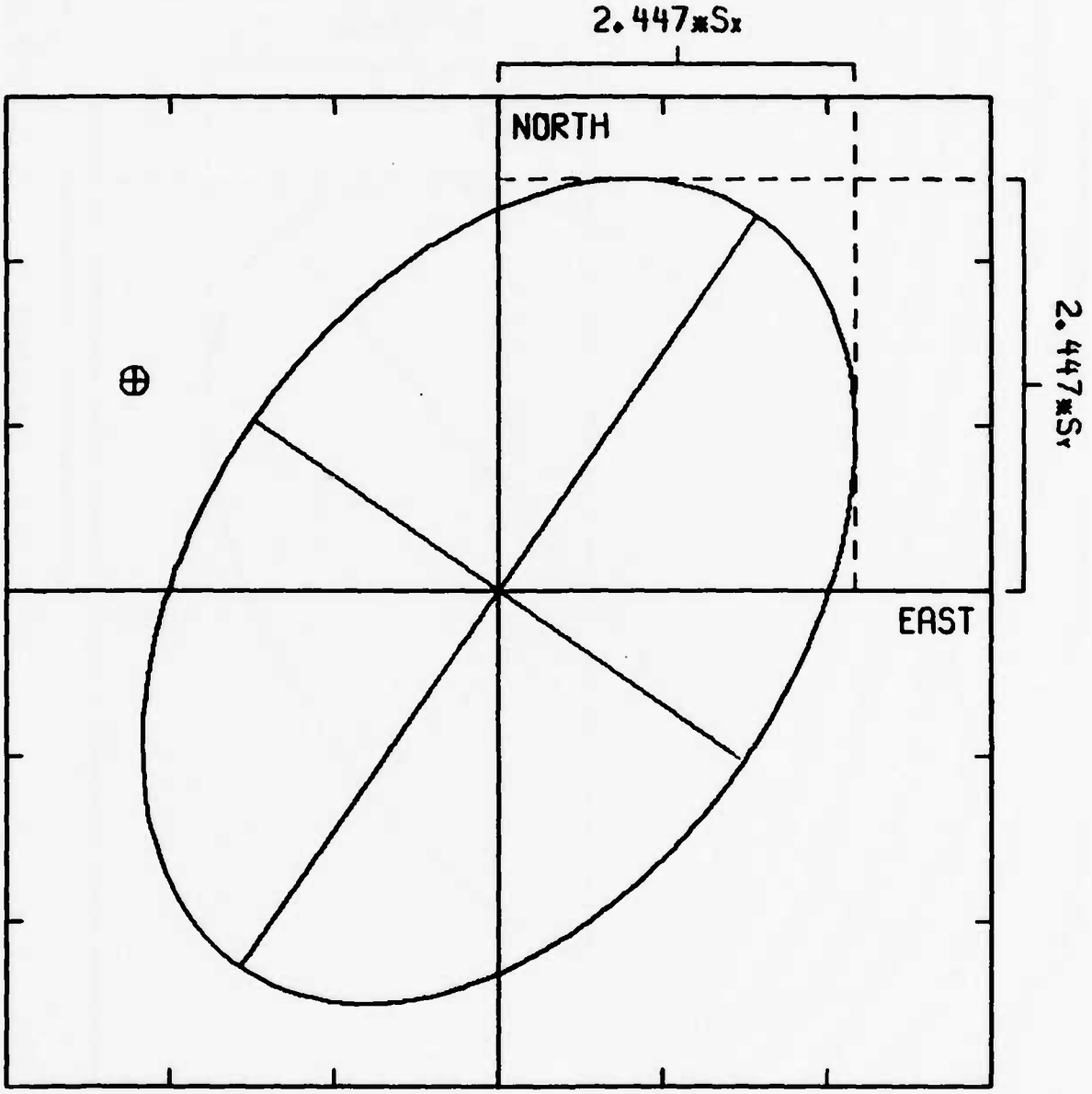

S_x : STANDARD ERROR (EAST)
S_y : STANDARD ERROR (NORTH)

⊕ TRUE EPICENTER
3.944 KM

ELLIPSE IS FOR CHI-SQUARED STATISTIC

Figure 8j - Error Ellipses for GASBUGGY

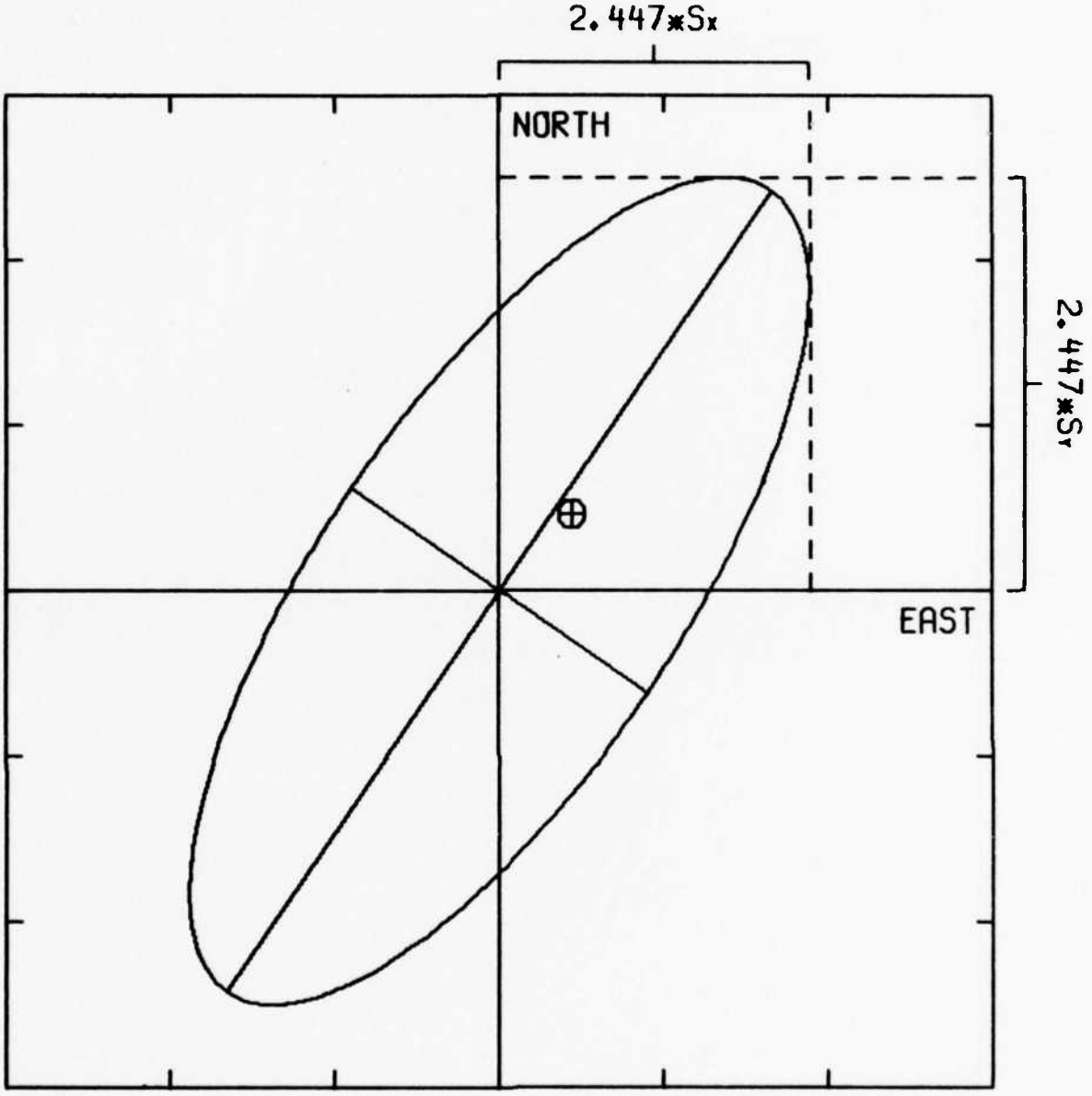

Sx : STANDARD ERROR (EAST)
Sy : STANDARD ERROR (NORTH)

⊕ TRUE EPICENTER
8.924 KM

ELLIPSE IS FOR CHI-SQUARED STATISTIC

Figure 8k - Error Ellipses for PILEDRIVER

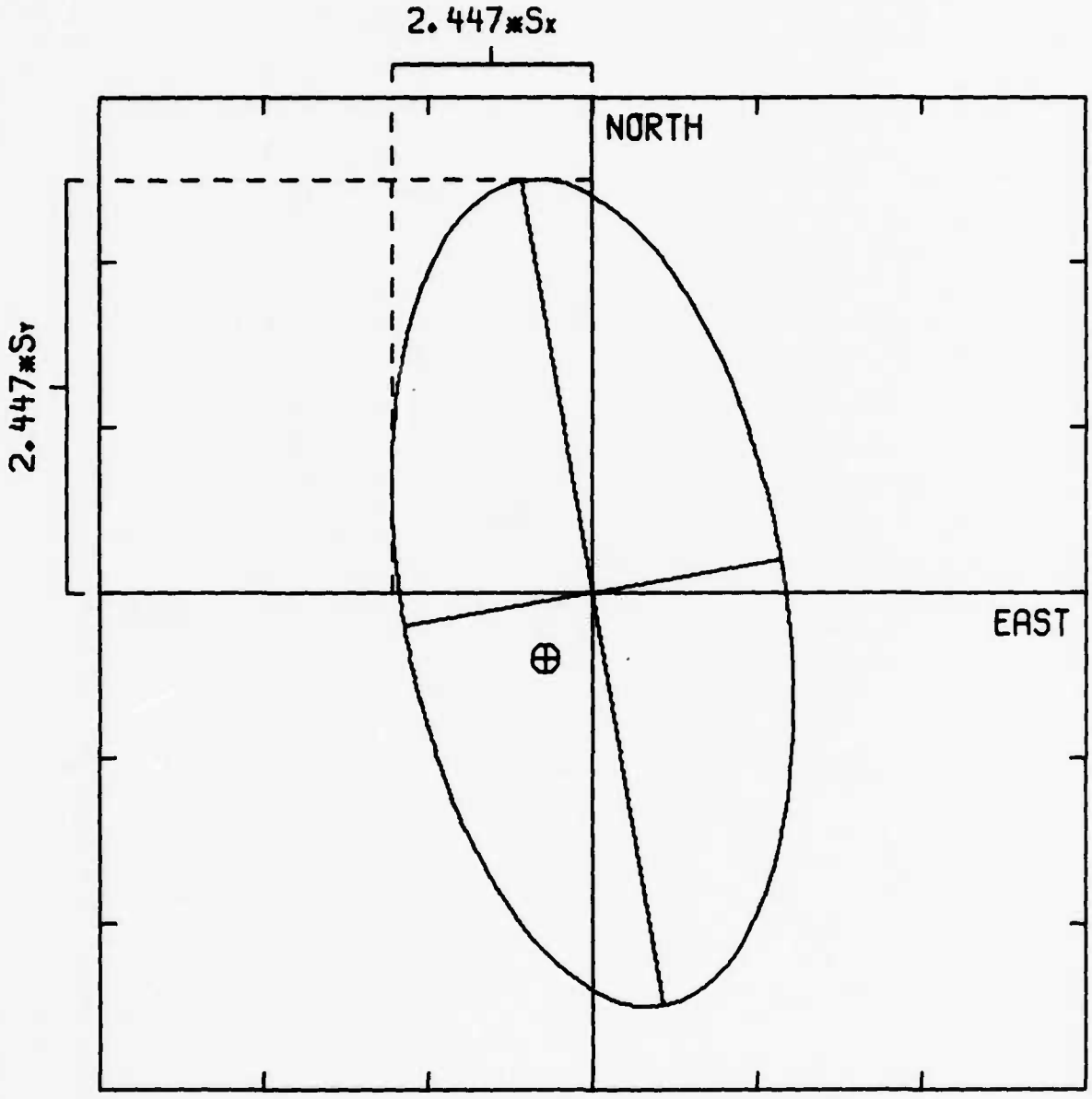

Figure 81 - Error Ellipses for ROANOKE

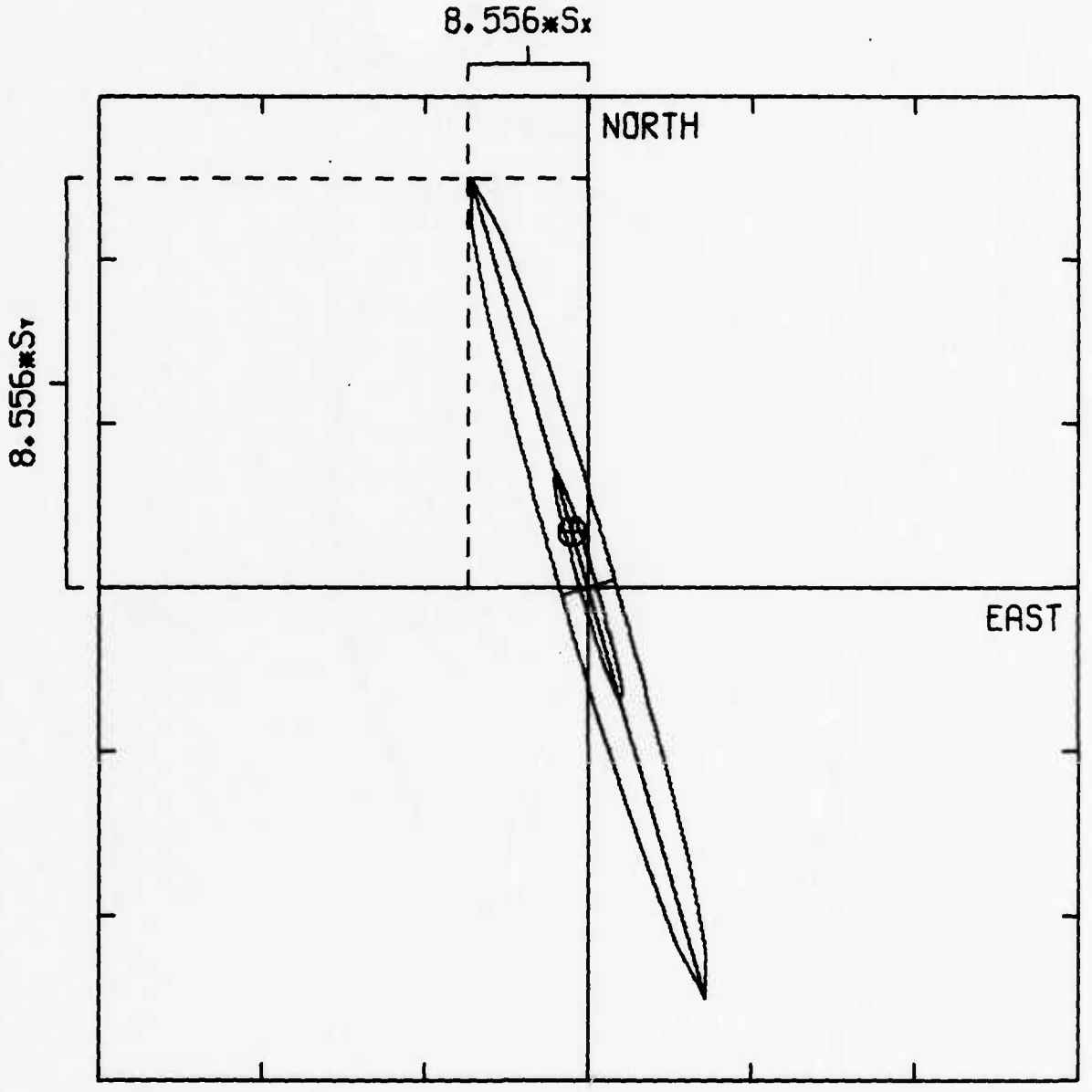

Sx : STANDARD ERROR (EAST)
Sy : STANDARD ERROR (NORTH)

⊕ TRUE EPICENTER
305.883 KM

OUTER ELLIPSE : F-STATISTIC
INNER ELLIPSE : CHI-SQUARED STATISTIC

Figure 8m - Error Ellipses for SALMON

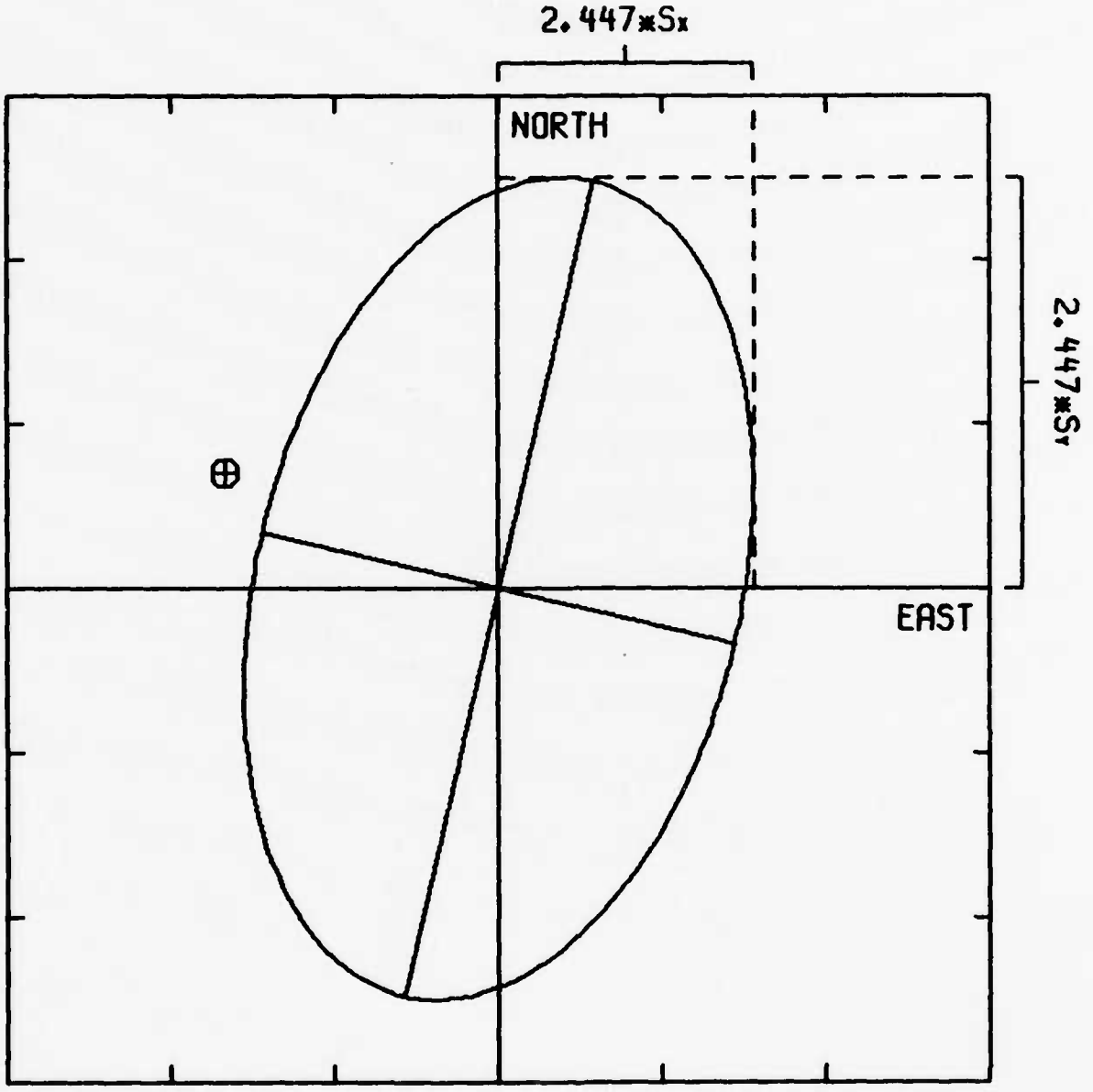

S_x : STANDARD ERROR (EAST)
S_y : STANDARD ERROR (NORTH)

⊕ TRUE EPICENTER
3.949 KM

ELLIPSE IS FOR CHI-SQUARED STATISTIC

Figure 8n - Error Ellipses for GNOME

TABLE XI

Standard Errors - Method of Simultaneous Inversions

Event	δx (km)	δy (km)	δap_n (sec)	δbp_n (sec/deg)	δap_g (sec)	δbp_g (sec/deg)	δV_{P_n} (km/sec)	δV_{P_g} (km/sec)
FAULTLESS	5.36	8.43	1.0	0.198	2.8	0.496	0.104	0.152
RULISON	4.14	3.42	1.1	0.148	3.2	0.457	0.089	0.154
PASSAIC	7.69	7.88	1.6	0.599	5.8	1.864	0.337	0.737
ROCKVILLE DAM	5.52	4.54	2.0	0.302	7.4	1.074	0.182	0.326
DORMOUSE'	8.82	17.85	3.0	0.922	4.3	1.519	0.530	0.518
KLICKITAT	4.33	2.89	0.7	0.144	2.1	0.391	0.078	0.130
BANDICOOT	4.39	16.50	3.5	1.161	6.8	2.125	0.746	0.684
SHOAL	4.31	4.04	0.8	0.142			0.078	
MERRIMAC	4.41	4.76	1.1	0.248			0.133	
GASBUGGY	3.50	4.03	1.2	0.167	3.2	0.441	0.101	0.150
PILEDRIVER	4.15	8.49	2.5	0.785	6.8	2.180	0.400	0.663
SALMON	26.54	89.38	8.8	0.223			0.138	
GNOME	2.52	4.03	0.7	0.133			0.076	

If we assume that the *a priori* assignation of standard deviations for P_g and P_n arrival time measurements are correct (which, as we have shown, they are not), then equation (31) should be replaced by:

$$(\vec{x} - \hat{\vec{x}})^T \underset{\sim}{F}^{-1} (\vec{x} - \hat{\vec{x}}) \leq \chi^2_{2:0.05}. \qquad (32)$$

In this equation we have assumed that the weighted standard deviations, σ_i/w_i, are equal to unity. On each error ellipse we show the effect of changing the length of the axes in this way. If the number of degrees of freedom of the solution is small, then $\hat{\sigma}_0^2$ may be an underestimate of the true variance of σ_0^2, and the right-hand side of equation (31) would be spuriously low. In those cases in which such an underestimate results in a smaller value for the right-hand side of equation (31) than is found for the right-hand side of equation (32), we have ignored the anomalously small F-statistic ellipse and have plotted only the ellipse for the chi-squared statistic.

5. CONCLUSIONS AND RECOMMENDATIONS FOR FURTHER RESEARCH

Significant improvements have been made in locating seismic event hypocenters with the successive determinations method and also simultaneous inversions method. We have learned that the earth is typically heterogeneous and that no simple 'model' of an area is adequate for use in each single case. Location experiments of Chang and Racine (1979) showed no improvements in location errors, probably because the regional models they used were not adequate. Experiments with local models resulted in small improvements, but with no significant difference from using one simple (Herrin) model. This is because local models adequate for the source area may not be adequate for the receiver area, and vice versa.

We found that the HYLO method, which uses average P_n velocity through the source to station path, made no significant improvements, possibly because the earth is so heterogeneous that the contour map of P_n velocity which we have used in the experiments is not suitable for each case.

The best result can be obtained by modifying P_g and P_n velocities for each event, whether successively or simultaneously. This means that even for two events a few tens of kilometers apart, P_g and P_n velocities may be significantly different, perhaps due to regional and local heterogeneities and their influence on the characters of the radiated waves.

Note that in these two methods we are not trying to obtain local crustal structures by inversions. The residual data from the successive and simultaneous methods may however contain information regarding the dip of the Moho. Thus, it may be possible to extract crustal models using these methods. In addition, the successive and simultaneous methods should be extended to include more regional phases, including L_g, which is generally the highest amplitude regional phase on the record. The two methods should be merged with the program which utilizes teleseismic data, and used to evaluate location accuracies for various combinations of regional and teleseismic data. Tests should be carried out on data other than from the WUS. The methods should be tested on AI data. Since the methods will utilize the phases P_g and L_g, whose start times are often unclear, an investigation of the precision with which analysts and automatic detectors can pick the onset of the various phases should be evaluated. Finally, the program should be incorporated into the Regional Event Location System (RELS).

ACKNOWLEDGEMENT

Robert Wagner assisted in several stages of the data analysis.

REFERENCES

Ahner, R. O., R. R. Blandford and R. Shumway (1971). Applications of the joint epicenter determination method, SDL 275, Teledyne Geotech, Alexandria, Virginia.

Chang, A. and D. P. J. Racine (1979). Evaluation of location accuracy using P_n and P_g arrivals, SDAC-TR-79-4, Teledyne Geotech, Alexandria, Virginia, (in preparation).

Douglas, A. (1967). Joint epicenter determination, Nature, 215, 47.

Evernden, J. F. (1969). Precision of epicenters obtained by small numbers of world-wide stations, Bull. Seism. Soc. Am., 59, 1365-1398.

Flinn, E. A. (1965). Confidence regions and error determinations for seismic event location, Rev. Geophys., 3, 157-185.

Herrin. E. (1968a). Regional variations of P-wave velocity in the upper mantle beneath North America, The Earth's Crust and Upper Mantle, Pembroke J. Hart, editor.

Herrin, E. (1968b). Near earthquake P phases, Bull. Seism. Soc. Am., 58 1226-1228.

Herrin, E. and J. Taggart (1962). Regional variations in P_n velocity and their effect on the location of epicenters, Bull. Seism. Soc. Am., 52, 1037-1045.

Herrin, E. and J. Taggart (1966). Epicenter determination for the SALMON event, J. Geophys. Res., 71, 3503-3507.

Julian, B. (1973). Extension of standard event location procedures, Seismic Discrimination SATS, Lincoln Laboratory, MIT, 30 June 1978, 4-9.

McCowan, D. W., and R. E. Needham (1978). The use of crustal phases in locating explosion epicenters, Seismic Discrimination SATS, Lincoln Laboratory, M.I.T., 9 June 1978, 1-2.

Pakiser, L. C. and R. Robinson (1966). Composition of the continental crust as estimated from seismic observations, The Earth Beneath the Continents, American Geophysical Union, Geophysical Monograph #10, 620-626.

Schilt, S., J. Oliver, L. Brown, S. Kaufman, D. Albaugh, J. Brewer, F. Cook, L. Jensen, P. Krumhausl, G. Long, D. Steiner (1979). The heterogeneity of the continental crust: Results from deep crustal seismic reflection profiling using the Vibroseis technique, Rev. Geophys. and Sp. Phys., 17, 354-368.

APPENDIX I

Least-Squares Fit to Figure 4

APPENDIX I

Least-Squares Fit to Figure 4
a: intercept of least-squares line
b: slope of least-squares line (reciprocal of velocity)
JED: 8 NTS events used together in Figure 4o.

FAULTLESS P_n TT-Linear Fit

Station	Δ°	TT (sec)	resid (sec)	JED resid
MN-NV	1.528	28.4	0.14	0.62
KN-UT	3.128	50.6	-0.71	-0.15
UBO	5.412	86.1	1.89	2.56
TFO	5.905	90.1	-1.21	-0.51
LC-NM	10.000	150.2	-0.11	0.80

a_{P_n} = 6.249 sec
b_{P_n} = 14.406 sec/deg → $\hat{V}$ = 7.719 km/sec

FAULTLESS P_g

Station	Δ°	TT (sec)	resid (sec)	JED resid
MN-NV	1.528	29.1	0.31	0.50
KN-UT	3.128	58.2	-0.83	0.13
UBO	5.412	102.1	-0.11	1.95
TFO	5.905	112.4	0.87	3.17
LC-NM	10.000	188.7	-0.24	4.04

a_{P_n} = -0.100 sec
b_{P_g} = 18.904 sec/deg → V = 5.882 km/sec

RULISON P_n

Station	Δ°	TT (sec)	resid
UBO	1.546	29.4	-0.86
KN-UT	4.519	71.2	0.59
ALQ	4.612	72.9	1.03
TFO	5.778	88.2	0.50
LC-NM	7.074	106.4	1.11
LAO	7.388	108.6	-0.95
TUC	7.445	108.6	-1.72
CR2NB	8.607	125.4	-0.70
BP-CL	8.679	125.9	-1.17
BMO	8.823	131.2	2.17

a_{P_n} = 9.279 sec
b_{P_n} = 13.572 sec/deg → V = 8.192 km/sec

RULISON P_g

Station	Δ°	TT	resid
UBO	1.546	31.3	2.22
KN-UT	4.519	80.7	-2.47
TFO	5.778	103.4	-2.68
LC-NM	7.074	130.9	1.24
CR2NB	8.607	159.1	1.55
BP-CL	8.679	159.9	1.04
BMO	8.823	160.6	-0.89

a_{P_g} = 0.950 sec
b_{P_g} = 18.195 sec/deg → V = 6.11 km/sec

PASSAIC P_n

Station	Δ°	TT	resid	JED resid
DV-CL	1.274	24.5	0.04	0.37
MN-NV	2.125	36.3	-0.27	-0.05
KN-UT	2.571	43.2	0.28	0.45
FS-AZ	4.343	68.1	-0.04	-0.09

a_{P_n} = 6.330 sec
b_{P_n} = 14.232 sec/deg → V = 7.812 km/sec

PASSAIC P_g

Station	Δ°	TT	resid	JED resid
MN-NV	2.125	39.7	-0.36	0.10
KN-UT	2.571	48.1	0.45	0.29
FS-AZ	4.343	77.7	-0.09	-2.76

a_{P_g} = 3.913 sec
b_{P_g} = 17.011 sec/deg → V = 6.536 km/sec

ROCKVILLE DAM P_n

Station	Δ°	TT	resid	Δ^2	TT^2
UBO	2.579	46.0	0.41	6.651	2116.0
KN-UT	5.531	85.7	0.14	30.591	7344.5
WN-SD	6.112	92.7	-0.72	37.356	8593.3
RG-SD	6.241	95.2	0.03	38.950	9063.0
TFO	6.380	97.5	0.45	40.704	9506.3
LAO	7.327	109.2	-0.67	53.685	11924.6
CR-NB	7.488	111.9	-0.15	56.070	12521.6
WMO	7.814	115.8	-0.67	61.058	13409.6
KC-MO	9.133	135.5	1.18	83.412	18360.3

a_{P_n} = 10.676 sec
b_{P_n} = 13.538 sec/deg → V = 8.213 km/sec

ROCKVILLE DAM P_g

Station	Δ°	TT	resid
KN-UT	5.531	101.3	-1.81
WN-SD	6.112	114.2	0.14
RG-SD	6.241	116.9	0.41
TFO	6.380	117.1	-2.01
LAO	7.327	143.5	6.55
CR-NB	7.488	140.0	0.01
WMO	7.814	145.0	-1.13
KC-MO	9.133	168.8	-2.19

a_{P_g} = -1.129 sec
b_{P_g} = 18.846 sec/deg → V = 5.900 km/sec

DORMOUSE ' P_n

Station	Δ°	TT	resid	JED resid
MN-NV	2.188	37.4	-0.13	0.15
KN-UT	2.555	42.9	0.16	0.38
FS-AZ	4.293	67.4	-0.03	-0.07

a_{P_n} = 6.454 sec
b_{P_n} = 14.203 sec/deg → V = 7.829 km/sec

KLICKITAT P_n

Station	Δ°	TT	resid	JED resid
CU-NV	1.592	28.6	0.09	-0.10
EK-NV	2.071	35.9	0.53	0.33
MN-NV	2.106	36.2	0.32	0.12
KM-CL	2.470	41.3	0.21	0.00
KN-UT	2.572	42.8	0.25	0.03
CP-CL	4.420	68.2	-0.82	-1.10
TFO	4.831	74.8	-0.11	-0.40
BX-UT	5.279	80.2	-1.13	-1.43
UBO	5.968	93.3	2.10	1.78
DR-CO	6.580	97.9	-2.07	-2.40
HL-ID	6.631	99.5	-1.20	-1.54
PI-WY	7.279	110.3	0.32	-0.04
LC-NM	9.095	137.5	1.51	1.09

a_{P_n} = 5.708 sec
b_{P_n} = 14.325 sec/deg → V = 7.762 km/sec

KLICKITAT P_g

Station	Δ°	TT	resid	JED resid
CU-NV	1.592	30.5	0.80	0.72
EK-NV	2.071	38.4	-0.04	-0.20
KM-CL	2.470	46.6	0.88	0.65
KN-UT	2.572	47.0	-0.59	-0.83
CP-CL	4.420	79.7	-1.62	-2.17
TFO	4.831	89.7	0.88	0.26
BX-UT	5.279	96.7	-0.30	-1.00
UBO	5.968	110.7	1.12	0.31
DR-CO	6.580	119.7	-1.05	-1.96
HL-ID	6.631	120.7	-0.99	-1.90
PI-WY	7.279	132.9	1.54	0.21

a_{P_g} = 0.635 sec
b_{P_g} = 18.255 sec/deg → V = 6.091 km/sec

BANDICOOT P_n

Station	Δ°	TT	resid	JED resid
MN-NV	2.188	37.4	-0.29	0.15
KN-UT	2.555	43.0	0.28	0.48
TF-CL	3.704	58.7	0.21	-0.32
FS-AZ	4.293	66.2	-0.38	-1.27
CP-CL	4.311	67.0	0.18	-0.73

a_{P_n} = 7.656 sec
b_{P_n} = 13.725 sec/deg → V = 8.101 km/sec

BANDICOOT P_g

Station	Δ°	TT	resid	JED resid
MN-UT	2.188	40.5	-0.04	-0.26
KN-UT	2.55	48.0	0.38	0.48
TF-CL	3.704	68.8	-0.99	0.12
FS-AZ	4.293	81.8	0.65	2.27

a_{P_g} = -1.680 sec
b_{P_g} = 19.295 sec/deg → V = 5.763 km/sec

SHOAL P_n

Station	Δ°	TT	resid
EK-NV	2.074	35.6	0.25
WI-NV	2.261	37.8	-0.21
MV-CL	2.263	37.7	-0.34
CU-NV	2.340	39.3	0.17
KN-UT	4.889	75.2	-0.13
HL-ID	5.420	81.5	-1.37
BMO	5.701	87.8	0.95
CP-CL	6.659	100.2	-0.26
UBO	6.881	106.3	2.69
BX-UT	7.215	107.5	-0.85
TFO	7.536	113.0	0.09
DR-CO	8.498	125.6	-0.97

a_{P_n} = 5.906 sec
b_{P_n} = 14.199 sec/deg → 7.831 km/sec

MERRIMAC P_n

Station	Δ°	TT	resid	JED resid
MN-NV	2.170	37.2	0.56	0.21
KN-UT	2.565	42.6	0.25	-0.07
FS-AZ	4.309	67.8	0.23	0.10
CP-CL	4.325	66.8	-1.01	-1.13
WI-NV	4.430	68.8	-0.52	-0.64
MV-CL	4.673	72.6	-0.24	-0.33
DR-CO	6.584	100.3	-0.17	-0.06
HL-ID	6.724	103.4	0.90	1.03

a_{P_n} = 5.261 sec
b_{P_n} = 14.461 sec/deg → 7.689 km/sec

GASBUGGY P_n

Station	Δ°	TT	resid
TFO	4.029	65.6	0.30
UBO	4.047	66.1	0.56
LC-NM	4.305	67.4	-1.61
KN-UT	4.440	71.7	0.87
PQ-ID	6.507	98.4	-0.26
WMO	7.359	108.6	-1.52
WZ-NV	7.402	111.9	1.20
WN-SD	8.537	125.4	-0.58
HL2ID	8.768	130.7	1.61
MN-NV	8.786	129.7	0.37
BS-MA	9.124	134.6	0.72
GV-TX	9.285	134.4	-1.65

a_{P_n} = 11.064 sec
b_{P_n} = 13.461 sec/deg → V = 8.260 km/sec

(Continued)

GASBUGGY P_g

Station	Δ°	TT	resid
TFO	4.029	75.2	-0.77
UBO	4.047	76.1	-0.20
LC-NM	4.305	79.1	-1.85
KN-UT	4.440	86.9	3.51
PQ-ID	6.507	121.2	0.54
WMO	7.359	132.6	-3.42
WZ-NV	7.402	138.4	1.61
WN-SD	8.537	157.4	0.14
HL2ID	8.768	159.6	-1.83
MN-NV	8.786	161.1	-0.65
BS-MA	9.124	170.9	3.06
GV-TX	9.285	170.6	-0.15

a_P = 3.324 sec
$b_{P_g}^{g}$ = 18.032 sec/deg → V = 6.166 km/sec

PILEDRIVER P_n

Station	Δ°	TT	resid	JED resid
MN-NV	2.049	35.2	-0.10	-0.06
KN-UT	2.589	43.1	0.03	0.09
TFO	4.885	75.7	-0.40	-0.27
UBO	5.936	92.1	0.88	1.04
BMO	7.673	115.8	-0.41	-0.20

a_{P_n} = 5.823 sec
b_{P_n} = 14.386 sec/deg → V = 7.729 km/sec

PILEDRIVER P_g

Station	Δ°	TT	resid	JED resid
MN-NV	2.049	37.6	-0.14	-0.60
KN-UT	2.589	47.0	-0.53	-1.15
TFO	4.885	90.6	1.41	0.16
UBO	5.936	108.0	-0.26	-1.80
BMO	7.673	139.3	-0.48	-2.49

a_P = 0.558 sec
$b_{P_g}^{g}$ = 18.144 sec/deg → V = 6.128 km/sec

ROANOKE P_n

Station	Δ°	TT	resid	JED resid
MN-NV	2.116	36.1	0.04	-0.12
KN-UT	2.580	42.9	-0.04	0.02
FM-UT	3.681	58.9	-0.38	0.12
TF-CL	3.724	60.3	0.38	1.00

a_P = 4.662 sec
$b_{P_n}^{n}$ = 14.838 sec/deg → V = 7.494 km/sec

(Continued)

ROANOKE P_g

Station	Δ°	TT	resid	JED resid
MN-NV	2.116	40.7	0.77	1.27
KN-UT	2.580	47.8	-1.05	-0.18
FM-UT	3.681	69.1	-0.90	0.84
TF-CL	3.724	72.0	1.18	2.95

a_{P_g} = -0.720 sec
b_{P_g} = 19.212 sec deg → 5.788 km/sec

SALMON P_n

Station	Δ°	TT	resid
EU-AL	2.178	36.5	-0.29
JE-LA	2.185	37.4	0.52
CPO	5.560	82.4	0.11
GV-TX	6.544	94.6	-0.94
WMO	8.377	120.8	0.60

a_{P_n} = 7.482 sec
b_{P_n} = 13.456 sec/deg → V = 8.263 km/sec

GNOME P_n

Station	Δ°	TT	resid
LC-NM	2.319	40.6	0.70
PO-TX	2.429	42.1	0.65
SS-TX	2.594	43.8	0.03
SM-TX	4.177	65.6	-0.39
ML-NM	4.339	68.2	-0.06
RT-NM	4.474	70.2	0.04
LP-TX	4.738	73.0	-0.87
SV-AZ	4.820	75.5	0.48
HB-OK	5.049	78.1	-0.13
AM-OK	5.698	85.7	-1.64
SF-AZ	5.972	91.5	0.31
DR-CO	6.112	94.6	1.45
TO-OK	6.456	95.6	-2.38
SJ-TX	6.685	99.7	-1.50
FS-AZ	6.808	103.7	0.77
MW-AZ	7.625	116.6	2.20
KN-UT	8.777	131.2	0.63
PM-WY	9.007	133.5	-0.30

a_{P_n} = 7.348 sec
b_{P_n} 14.039 sec/deg → V = 7.920 km/sec

GNOME P_g

Station	Δ°	TT
LC-NM	2.319	44.0

JED: FAULTLESS, PASSAIC, DORMOUSE PRIME, KLICKITAT, BANDICOOT, MERRIMAC, PILEDRIVER, and ROANOKE combined

P_n (47 data points)

a_{P_n} = 5.842 sec

b_{P_n} = 14.356 sec/deg → V = 7.745 km/sec

σ_{P_n} = 0.835 sec

P_g (37 data points)

a_{P_g} = 0.455 sec

b_{P_g} = 18.420 sec/deg → V = 6.036 km/sec

σ_{P_g} = 1.575 sec